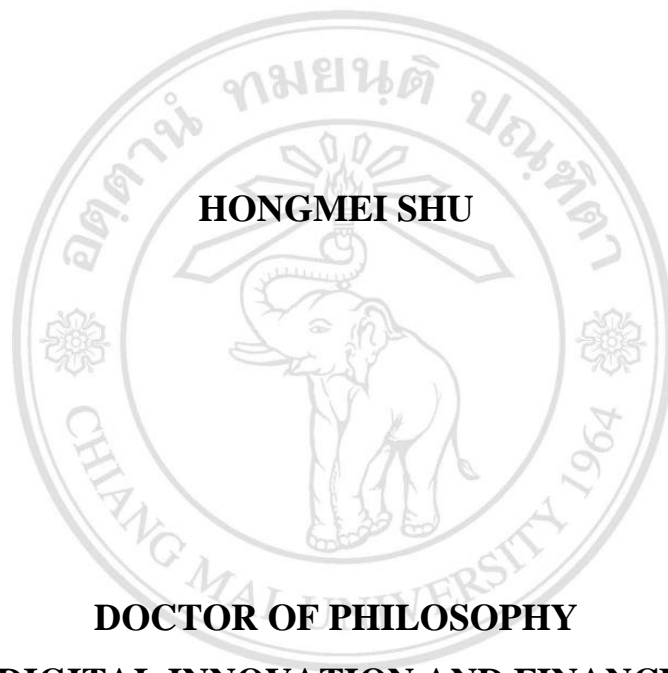


**INTELLIGENT RECOGNITION AND CLASSIFICATION
OF MICROSEISMIC EVENTS BASED ON MACHINE
LEARNING TECHNIQUES**



HONGMEI SHU

DOCTOR OF PHILOSOPHY

**IN DIGITAL INNOVATION AND FINANCIAL
TECHNOLOGY**

ลิขสิทธิ์มหาวิทยาลัยเชียงใหม่
Copyright© by Chiang Mai University
All rights reserved

CHIANG MAI UNIVERSITY

JULY 2024

**INTELLIGENT RECOGNITION AND CLASSIFICATION OF
MICROSEISMIC EVENTS BASED ON MACHINE
LEARNING TECHNIQUES**

HONGMEI SHU

**A THESIS SUBMITTED TO CHIANG MAI UNIVERSITY IN PARTIAL
FULFILLMENT OF THE REQUIREMENTS FOR THE DEGREE OF
DOCTOR OF PHILOSOPHY
IN DIGITAL INNOVATION AND FINANCIAL TECHNOLOGY**

CHIANG MAI UNIVERSITY

JULY 2024

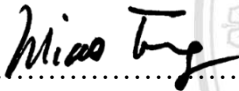
**INTELLIGENT RECOGNITION AND CLASSIFICATION OF
MICROSEISMIC EVENTS BASED ON MACHINE
LEARNING TECHNIQUES**


HONGMEI SHU


THIS THESIS HAS BEEN APPROVED TO BE A PARTIAL FULFILLMENT OF
THE REQUIREMENTS FOR THE DEGREE OF
DOCTOR OF PHILOSOPHY
IN DIGITAL INNOVATION AND FINANCIAL TECHNOLOGY

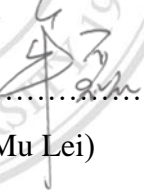
Examination Committee:

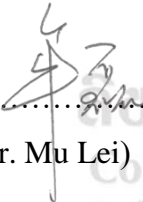
Advisory Committee:


 Chairman
(Prof. Dr. Miao Fang)


 Advisor
(Asst. Prof. Dr. Ahmad Yahya Dawod)

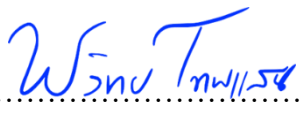
 Member
(Asst. Prof. Dr. Ahmad Yahya Dawod)

 Co-advisor
(Lect. Dr. Mu Lei)

 Member
(Lect. Dr. Mu Lei)

 Co-advisor
(Lect. Dr. Naret Suyaroj)

 Member
(Lect. Dr. Naret Suyaroj)

 Member
(Lect. Dr. Worawit Tepsan)

24 July 2024

Copyright © by Chiang Mai University

ACKNOWLEDGEMENT

During the process of completing this doctoral dissertation, I have received the meticulous support and assistance of many individuals, and I would like to express my sincerest gratitude to each of them.

First and foremost, I would like to thank my principal advisor, Asst. Prof. Dr. Ahmad Yahya Dawod, for his dedicated guidance and invaluable advice throughout the entire research process. His academic mentorship, insights into research methodologies, experimental design, and thesis writing have been instrumental in shaping my work. His commitment to rigorous scholarship and pursuit of academic excellence has been a constant source of inspiration for me. I am deeply grateful for his well-timed supervision and guidance on the progress of the research. I also appreciate the support and guidance my co-advisors, Dr. Mu Lei and Dr. Naret Suyaroj, provided during the thesis writing process. I am especially thankful to Dr. Mu for his tutoring and answers in the English language, and to Dr. Worawit for his help and support in thesis revision and graduation requirements. I sincerely appreciate your dedicated mentorship.

Furthermore, I would like to extend my appreciation to Professor Longjun Dong and members of his research group at Central South University for their generous support and assistance in this study. They have provided valuable resources, expertise, technical support, and advice that have significantly contributed to the success of my research. In particular, I would like to thank Professor Longjun Dong for our fruitful discussions, knowledge sharing, and the provision of invaluable data and experimental support. The collaboration and discussions within our laboratory have enriched my research experience. I am also thankful to Dr. Zheng Tang, Dr. Xianhang Yan, and Dr. Longbin Yang, among other doctoral students in the research group, for their shared experiences and assistance in data collection and analysis.

Additionally, I want to express my gratitude to my family and friends for their understanding, support, and encouragement throughout my entire doctoral journey. Their unwavering support and encouragement have been my driving force. I also thank my doctoral classmates and senior fellow students for their enthusiastic assistance and support, making me feel warmth and stability during my study abroad in a foreign country. Special thanks to my classmates Xiaoying Li, Li Zhao, and Lin Wu for their support and help.

I would also like to sincerely thank Chiang Mai University for the support and assistance provided during my doctoral research. They have provided an excellent academic environment and research resources, which have been crucial to my academic career. Special thanks to the staffs and teachers at the International College of Digital Innovation (ICDI) for their hard work, professional services, and care, which have made my research journey smoother. I am especially thankful to Ruchanee Mahanin for her careful assistance and support during my study abroad.

Finally, I extend my sincerest thanks to all those who have supported and helped me during my doctoral research. I am grateful to the defense committee and thesis reviewers for your recognition and valuable opinions, which have allowed my thesis to be perfected and approved.

Once again, I express my sincere gratitude to all those mentioned above!

ลิขสิทธิ์มหาวิทยาลัยเชียงใหม่
Copyright© by Chiang Mai University
All rights reserved

Hongmei Shu

หัวข้อคุณลักษณะ	การรับรู้และการจำแนกเหตุการณ์แผ่นดินไหวระดับไมโครอย่างชาญฉลาดโดยอาศัยเทคนิคการเรียนรู้ของเครื่อง	
ผู้เขียน	นางสาวชู หงเมย์	
ปริญญา	ปรัชญาดุษฎีบัณฑิต (นวัตกรรมดิจิทัลและเทคโนโลยีการเงิน)	
คณะกรรมการที่ปรึกษา	ผู้ช่วยศาสตราจารย์ ดร.อาหมัด ยาห์ยา ดาวัล อาจารย์ ดร.มู่เล่ย์ อาจารย์ ดร.นเรศ สุยะโรจน์	อาจารย์ที่ปรึกษาหลัก อาจารย์ที่ปรึกษาร่วม อาจารย์ที่ปรึกษาร่วม

บทคัดย่อ

การประยุกต์ใช้วิธีการเรียนรู้ของเครื่องและเทคโนโลยีคอมพิวเตอร์วิทัศน์ช่วยให้เกิดการจดจำและจำแนกเหตุการณ์แผ่นดินไหวขนาดเล็กในระบบตรวจสอบการสั่นสะเทือนแบบไมโครของเหมืองอย่างชาญฉลาด สิ่งนี้ช่วยให้สามารถสร้างผลการจำแนกประเภทได้อย่างรวดเร็วและแม่นยำลดภาระงานและอัตราการตัดสินใจผิดพลาดในการระบุเหตุการณ์แผ่นดินไหวขนาดเล็กด้วยตนเอง ในขณะที่เดียวกันสามารถใช้เป็นหลักฐานในการตีความสำหรับระบบเตือนภัยพิบัติของทุ่นระเบิดและการแจ้งเตือนอย่างทันท่วงทีสำหรับกิจกรรมแผ่นดินไหวที่อาจเกิดขึ้น

ระบบตรวจวัดแผ่นดินไหวขนาดเล็กมีบทบาทสำคัญในการตรวจสอบ การเตือนภัยล่วงหน้า และการป้องกันภัยพิบัติจากการระเบิดของหินในเหมือง อย่างไรก็ตาม เมื่อมีการสร้างข้อมูลการตรวจสอบจำนวนมาก การระบุประเภทของเหตุการณ์แผ่นดินไหวขนาดเล็กที่แตกต่างกันอย่างรวดเร็วและแม่นยำแบบเรียลไทม์ได้กลายเป็นข้อกำหนดพื้นฐานสำหรับการป้องกันภัยพิบัติและการทำเหมืองอัจฉริยะ บทความนี้นำเสนอวิธีการที่ใช้การเรียนรู้ของเครื่องเพื่อจำแนกและระบุเหตุการณ์แผ่นดินไหวขนาดเล็กโดยอัตโนมัติโดยใช้เทคโนโลยีทางด้านข้อมูลมหัด

ขั้นแรก ข้อมูลแผ่นดินไหวขนาดเล็กที่รวบรวมโดยระบบตรวจสอบจะถูกแปลงเป็นกราฟรูปคลื่นดิบ โดยแต่ละเหตุการณ์จะแสดงด้วยชุดของกราฟย่อย 6 กราฟเป็นภาพตัวอย่าง ชุดข้อมูลตัวอย่างของเหตุการณ์สี่ประเภท ได้แก่ เหตุการณ์แผ่นดินไหวขนาดเล็กที่เกิดจากเหมือง การระเบิด การเจาะหิน และเสียงรบกวน จะถูกสร้างขึ้นผ่านการระบุด้วยตนเอง จากนั้น Histogram of Oriented

Gradients (HOG) พร้อมด้วยอัลกอริทึมการเรียนรู้แบบต้น (เช่น ตัวจำแนกเชิงเส้น การแยกแยะของพีชเชอร์) โมเดลเครือข่ายประสาทเทียมแบบคอนโวลูชัน (CNN) และโมเดลการเรียนรู้เชิงลึกที่อิงตามการเรียนรู้การถ่ายโอน (เช่น MobileNet-V2, Inception-V3) จะถูกเลือก โมเดลเหล่านี้จะสกัดคุณลักษณะจากภาพรูปคลื่นที่แตกต่างกันโดยอัตโนมัติและสร้างโมเดลการจำแนกประเภทภาพสำหรับการจดจำเหตุการณ์แผ่นดินไหวขนาดเล็กอย่างชาญฉลาด

การทดลองดำเนินการบนชุดข้อมูลเดียวกันเพื่อเปรียบเทียบประสิทธิภาพการจำแนกประเภทและความแม่นยำในการจดจำของโมเดลทั้งสี่ ผลการทดลองแสดงให้เห็นว่าความแม่นยำโดยรวมของ HOG-SVM, MS-CNN, ResNet-18, MobileNet-V2 และ Inception-V3 บนชุดทดสอบอยู่ที่ 0.971, 0.974, 0.981, 0.982 และ 0.987 ตามลำดับ เมื่อเทียบกับวิธีการวิจัยที่มีอยู่ บทความนี้ไม่เพียงแต่รวมถึงการจดจำเหตุการณ์แผ่นดินไหวขนาดเล็กและการระเบิดเท่านั้น แต่ยังระบุเหตุการณ์การเจาะหินและเสียงรบกวนอื่น ๆ ได้อย่างมีประสิทธิภาพ ซึ่งให้การระบุรูปคลื่นแผ่นดินไหวขนาดเล็กที่ชัดเจนและแม่นยำยิ่งขึ้น

การประยุกต์ใช้วิธีการเรียนรู้ของเครื่องและเทคโนโลยีคอมพิวเตอร์วิทัศน์ช่วยให้บรรลุการจดจำและการจำแนกประเภทเหตุการณ์แผ่นดินไหวขนาดเล็กอย่างชาญฉลาดในระบบตรวจวัดแผ่นดินไหวขนาดเล็กของเหมือง ซึ่งช่วยให้สามารถสร้างผลลัพธ์การจำแนกประเภทได้อย่างรวดเร็วและแม่นยำ ลดภาระงานและอัตราการตัดสินใจผิดพลาดของการระบุเหตุการณ์แผ่นดินไหวขนาดเล็กด้วยตนเองได้อย่างมีประสิทธิภาพ ในขณะเดียวกัน ยังให้หลักฐานที่สามารถตีความได้สำหรับระบบเตือนภัยพิบัติในเหมืองและการแจ้งเตือนอย่างทันท่วงทีสำหรับกิจกรรมแผ่นดินไหวที่อาจเกิดขึ้น

Dissertation Title	Intelligent Recognition and Classification of Microseismic Events Based on Machine Learning Techniques	
Author	Ms. Hongmei Shu	
Degree	Doctor of Philosophy (Digital Innovation and Financial Technology)	
Advisory Committee	Asst. Prof. Dr. Ahmad Yahya Dawod	Advisor
	Lect. Dr. Mu Lei	Co-advisor
	Lect. Dr. Naret Suyaraj	Co-advisor

ABSTRACT

Microseismic monitoring system plays an important role in the monitoring, early warning, and prevention of mining-induced ground pressure disasters. These systems integrate functions such as collecting, locating, analyzing, and interpreting seismic activities induced by microcracks within rock masses. However, with the generation of a large amount of monitoring data, the rapid, accurate, and real-time identification of different types of microseismic events has become a fundamental requirement for disaster prevention and control, as well as for the construction of smart mines.

This paper proposed different automatic identification and classification models for microseismic events using machine learning technology, based on data mining and analysis. The aim is to improve the efficiency and accuracy of microseismic data analysis, thereby providing a solid foundation for geostress disaster management and the advancement of smart mining systems.

Firstly, microseismic data collected by monitoring systems from three different mines in Shaanxi Province, China, were processed into raw waveform images, with each event consisting of six sub-graphs forming a sample graph. Based on expert experience

and manual identification, three sample databases including four types of events—mining microseisms, blasting, drilling, and noise—were established, resulting in diverse datasets.

Subsequently, this paper employed various advanced algorithms and models to automatically extract features from different waveform images and construct an intelligent identification system for microseismic events. Specifically, methods combining Histogram of Oriented Gradients (HOG) features with Shallow Machine Learning (SML), Convolutional Neural Networks (CNN), and transfer learning-based deep learning models such as ResNet-18, MobileNet-V2, and Inception-V3 were selected.

Experiments were conducted using the three sample databases, and the classification performance and recognition accuracy of different models were compared. The results showed that on the test dataset A, the overall accuracy of the HOG-SVM, MS-CNN, ResNet-18, MobileNet-V2, and Inception-V3 models reached 0.971, 0.974, 0.981, 0.982, and 0.987, respectively. Comparative analysis of the models revealed that deep learning models, especially Inception-V3, outperformed others in terms of accuracy, demonstrating the potential of deep learning in classifying microseismic events. The HOG-SVM method demonstrated the fastest processing efficiency. The MS-CNN model achieved an effective balance between recognition efficiency and classification accuracy.

This study introduces an innovative, efficient, and precise approach for intelligently identifying microseismic events. It offers a comparative analysis of machine learning methods, aiding users in choosing the right algorithms for their tasks. The research expands beyond microseismic and blasting event identification to include drilling and noise events, enhancing the intuitive and precise recognition of waveforms. The models' adaptability across various mining data showcases their potential to boost mine safety and operational intelligence in real-world scenarios.

The application of machine learning methods and computer vision technology helps achieve intelligent recognition and classification of microseismic events in the microseismic monitoring system of mines. This enables the rapid and accurate generation of classification results, effectively reducing the workload and misjudgment rate of manual identification of microseismic events. At the same time, it provides interpretable

evidence for the mine disaster warning system and timely alerts for potential seismic activities.



ลิขสิทธิ์มหาวิทยาลัยเชียงใหม่
Copyright© by Chiang Mai University
All rights reserved

CONTENTS

	Page
Acknowledgement	c
Abstract in Thai	e
Abstract in English	g
List of Tables	n
List of Figures	o
List of Abbreviations	q
Statement of Originality in Thai	s
Statement of Originality in English	t
Chapter 1 Introduction	1
1.1 Research Background	1
1.2 Problem Statements	3
1.3 Research Questions	6
1.4 Objectives of the Study	7
1.5 Contributions of the Study	8
1.6 Scope of the Study	9
1.7 Conceptual Framework	9
1.8 Thesis Outline	12
Chater 2 Literature Review	15
2.1 Introduction	15
2.2 Theoretical Concepts	18
2.2.1 Machine Learning	18
2.2.2 Shallow Learning	21
2.2.3 Deep Learning	23

2.2.4 Transfer Learning	24
2.2.5 Image Recognition and Classification	25
2.3 Literature Review and Related Research	28
2.3.1 Traditional Identification Methods	33
2.3.2 Statistical Methods	34
2.3.3 Machine Learning Classification Methods	35
2.3.4 Hybrid Optimization Methods	38
2.4 Summary	40
Chapter 3 Data and Methodology	42
3.1 Introduction	42
3.2 Data	43
3.2.1 Data Collection	43
3.2.2 Data Preprocessing	46
3.3 Methods	49
3.3.1 HOG-SML Method	50
3.3.2 CNN Method	60
3.3.3 Transfer Learning Method	65
3.4 MS-CNN Model	68
3.5 Transfer Learning Models	73
3.5.1 MS-MobileNet-V2	74
3.5.2 MS-ResNet-18	76
3.5.3 MS-Inception-V3	78
3.6 Evaluation Metrics	81
3.7 Summary	86
Chapter 4 Results	88
4.1 Introduction	88
4.2 Experimental Environment	88
4.3 Results of the HOG-SML Method	89
4.3.1 K-fold Cross-Validation	89
4.3.2 Testing Results	92

4.4 Results of MS-CNN Model	99
4.4.1 The Impact of Hyperparameters on Model Performance	99
4.4.2 Hyperparameter Optimization	102
4.4.3 Training Process	103
4.4.4 Testing Results	107
4.5 Results of the Transfer Learning method	109
4.5.1 Hyperparameter Settings	109
4.5.2 Training Process	110
4.5.3 Testing Results	114
4.6 Summary	119
Chapter 5 Discussion	121
5.1 Introduction	121
5.2 Analysis of Results	121
5.2.1 Analysis of Training Time Differences	122
5.2.2 Analysis of Testing Time Differences	123
5.2.3 Analysis of Model Performance Differences	124
5.3 Comparison with Existing Work	128
5.4 Analysis of the Advantages of This Study	129
5.4.1 Advantages of HOG-Shallow Machine Learning Method	129
5.4.2 Advantages of CNN Method	131
5.4.3 Advantages of Transfer Learning Method	132
5.5 Summary	133
Chapter 6 Conclusion and Future Research	134
6.1 Summary of the Study	134
6.2 Implications	136
6.3 Limitations	137
6.4 Future Research	138
6.5 Summary	139
REFERENCES	141
APPENDIX A	167



ลิขสิทธิ์มหาวิทยาลัยเชียงใหม่
Copyright© by Chiang Mai University
All rights reserved

LIST OF TABLES

	Page
Table 2.1 Relevant studies in recent years (2018 - 2023).	29
Table 3.1 Microseismic monitoring event waveforms datasets from three mines	48
Table 3.2 Characteristics and advantages of the five classifiers	59
Table 3.3 Parameters of the MS-CNN network structure	72
Table 3.4 Key architectural parameters of transfer learning models	81
Table 3.5 The basic structure of a four-class confusion matrix	84
Table 4.1 The results of five-fold cross-validation of shallow machine learning models on three datasets	91
Table 4.2 Performance of shallow machine learning models on three mine test datasets	93
Table 4.3 Performance comparison of the MS-CNN model on dataset A under different hyperparameter settings	101
Table 4.4 Hyperparameter settings of the MS-CNN model during training	102
Table 4.5 MS-CNN model training results with five-fold cross-validation	106
Table 4.6 Performance of the MS-CNN model on different test sets	107
Table 4.7 Performance of transfer learning models on different datasets	114
Table 5.1 Comparative experimental results of existing research methods and the 1method of this study	128

LIST OF FIGURES

	Page
Figure 1.1 Composition of microseismic monitoring system	2
Figure 1.2 Frequency range of earthquakes, rock bursts, microseismic events, and acoustic emission	3
Figure 1.3 Conceptual framework of intelligent identification and classification of microseismic events based on machine learning techniques	12
Figure 2.1 Relationship among artificial intelligence, machine learning, supervised learning, unsupervised learning, deep learning, and transfer learning	17
Figure 2.2 Three stages of machine learning development	21
Figure 2.3 Image detection and classification using various machine learning models	37
Figure 3.1 Geographical locations of the microseismic monitoring data sources.	43
Figure 3.2 Software and hardware infrastructure of the microseismic monitoring at system Central South University.	45
Figure 3.3 Examples of 6-channel waveform images for four-type microseismic monitoring events.	47
Figure 3.4 The architecture of the microseismic monitoring event waveform recognition and classification model using the HOG-SML method.	52
Figure 3.5 CNN image classification architectures. (a) General architecture for CNN. (b) Architecture CNN-based for microseismic event waveform images.	61
Figure 3.6 The transfer learning workflow.	67
Figure 3.7 Model for microseismic event waveform recognition and classification based on convolutional neural networks (MS-CNN).	69
Figure 3.8 Feature extraction process in convolutional layers for microseismic waveforms.	70
Figure 3.9 Working principle of the Dropout layer.	71
Figure 3.10 Transfer learning model for microseismic event waveform identification and classification based on MobileNet-V2 (MS-MobileNet-V2).	75
Figure 3.11 Transfer learning model for microseismic event waveform identification and classification based on ResNet-18 (MS-ResNet-18).	77

Figure 3.12 Transfer learning model for microseismic event waveform identification and classification based on Inception-V3 (MS-Inception-V3).	79
Figure 3.13 Detailed structure of five inception models (a~e) in MS-Inception-V3.	80
Figure 4.1 Training time of shallow learning models on three training sets.	92
Figure 4.2 The testing time of shallow learning models on three testing sets.	93
Figure 4.3 The confusion matrices of shallow machine learning models on test set A.	96
Figure 4.4 The confusion matrices of shallow machine learning models on test set B.	97
Figure 4.4 The confusion matrices of shallow machine learning models on test set B.	97
Figure 4.5 The confusion matrices of shallow machine learning models on test set C.	98
Figure 4.6 Training process of the MS-CNN model on different mine datasets.	104
Figure 4.7 Confusion matrices of the MS-CNN model on three test datasets.	108
Figure 4.8 Training process of the MS-MobileNet-V2 model on three datasets.	111
Figure 4.9 Training process of the MS-ResNet-18 model on three datasets.	112
Figure 4.10 Training process of the MS-Inception-V3 model on three datasets.	113
Figure 4.11 Confusion matrix of the MS-MobileNet-V2 model on various test datasets.	116
Figure 4.12 Confusion matrix of the MS-ResNet-18 model on various test datasets.	117
Figure 4.13 Confusion matrix of the MS-Inception-V3 model on various test datasets.	118

LIST OF ABBREVIATIONS

CNN	Convolutional Neural Network
IoT	Internet of Things
AI	Artificial Intelligence
MS	Microseismic Signal
MMS	Microseismic Monitoring System
GPS	Global Position System
SML	Shallow Machine Learning
DT	Decision Tree
SVM	Support Vector Machine
DCNN	Deep Convolutional Neural Network
SPP	Spatial Pyramid Pooling
DAS	Distributed Acoustic Sensing
STA/LTA	Short-Term Average/Long-Term Average
RF	Random Forests
KNN	K-Nearest Neighbors
EEMD	Ensemble Empirical Mode Decomposition
SVD	Singular Value Decomposition
ELM	Extreme Learning Machine
DBN	Deep Belief Network
CapsNet	Capsule Network
PCA	Principal Component Analysis
CEEMDAN_SE	Complete Ensemble Empirical Mode Decomposition with Adaptive Noise Sample Entropy
XTF-CNN	Time-Frequency Convolutional Neural Network
LSTM	Long Short-Term Memory

RNN	Recurrent Neural Network
FCN	Fully Convolutional Neural Networks
ResNet	Residual Network
PSO	Particle Swarm Optimization
SSA	Singular Spectrum Analysis
BP	Back Propagation
LDA	Linear Discriminant Analysis
WSD	Wavelet Scattering Decomposition
VGG	Visual Geometry Group
ECNN	Enhanced Convolutional Natural Network
GAN	Generative Adversarial Networks
ACGAN	Auxiliary Classifier Gan
WPD	Wavelet Packet Decomposition
STFT	Short-Time Fourier Transform
NB	Naive Bayes
ANN	Artificial Neural Networks
DBSCAN	Density-Based Spatial Clustering of Applications with Noise
GRU	Gated Recurrent Unit
GPU	Graphics Processing Unit
SSD	Solid-State Drive
HDD	Hard Disk Drive
HOG	Histogram of Oriented Gradients
MS-CNN	Microseismic CNN Model
SGDM	Stochastic Gradient Descent with Momentum
RMSprop	Root Mean Square Propagation
MS-MobileNet-V2	Microseismic MobileNet-V2 Model
MS-ResNet-18	Microseismic ResNet-18 Model
MS-Inception-V3	Microseismic Inception-V3 Model
MS	Microseismic
HOG-SVM	Histogram of Oriented Gradients & Support Vector Machine
DNN	Deep Neural Networks

ข้อความแห่งการริเริ่ม

ผู้วิจัยขอรับรองว่าวิทยานิพนธ์เล่มนี้มิได้ละเมิดลิขสิทธิ์ของผู้ใดรวมถึงมิได้ขัดต่อสิทธิในการเป็นเจ้าของทรัพย์สินใดๆ และขอรับรองด้วยว่า แนวคิด เทคนิค คำกล่าวหรือเนื้อหาอื่นใดจากงานของผู้อื่นที่ได้รวมอยู่ในวิทยานิพนธ์เล่มนี้ ได้รับการยอมรับอย่างครบถ้วนโดยทั่วกันตามหลักมาตรฐานการอ้างอิงแล้ว

ผู้วิจัยขอแจ้งว่า เอกสารเล่มนี้เป็นส่วนสำคัญของวิทยานิพนธ์ของผู้วิจัย ซึ่งรวมไปถึงการแก้ไขปรับปรุงล่าสุดตามที่ถูกรับรองจากคณะกรรมการสอบวิทยานิพนธ์และบัณฑิตวิทยาลัย และขอแจ้งด้วยว่า วิทยานิพนธ์นี้มีเคยถูกนำเสนอเพื่อการสำเร็จการศึกษาจากมหาวิทยาลัยหรือสถาบันใดๆ มาก่อน

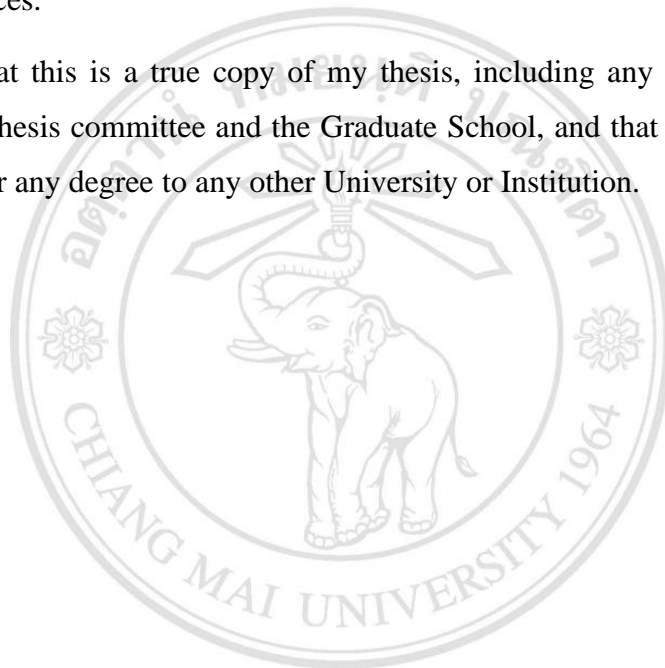


ลิขสิทธิ์มหาวิทยาลัยเชียงใหม่
Copyright© by Chiang Mai University
All rights reserved

STATEMENTS OF ORIGINALITY

I certify that, to the best of my knowledge, my thesis does not infringe upon anyone's copyright nor violate any proprietary rights and that any ideas, techniques, quotations, or any other material from the work of other people included in my thesis, published or otherwise, are fully acknowledged in accordance with the standard referencing practices.

I declare that this is a true copy of my thesis, including any final revisions, as approved by my thesis committee and the Graduate School, and that this thesis has not been submitted for any degree to any other University or Institution.



ลิขสิทธิ์มหาวิทยาลัยเชียงใหม่
Copyright© by Chiang Mai University
All rights reserved

CHAPTER 1

INTRODUCTION

1.1 Research Background

With the profound integration of information technologies like the Internet of Things (IoT) (Abdalzaher et al., 2022), big data (Arrowsmith et al., 2022), and artificial intelligence (AI) (Anikiev et al., 2023), smart mining is gradually becoming a reality (Barnewold et al., 2020). Notably, the microseismic monitoring technique, which relies on acoustic emission and seismology (Dong & Li, 2023), plays an increasingly pivotal role in monitoring mine safety (Di et al., 2023). It continues to address a growing range of issues with improving effectiveness. Its main applications encompass monitoring and providing early warnings for coal mining-induced rock bursts (Zhang et al., 2021), mine seismicity (Wang et al., 2023), metal mine goaf (Dong et al., 2022), deep mining, and slope stability studies (Iannucci et al., 2020; Li et al., 2021).

The microseismic monitoring system (MMS) in smart mining integrates microseismic signal acquisition, multi-channel clock synchronization, noise suppression, automated picking of arrival times, source localization, and analysis and interpretation of stress-induced micro-cracks within the rock mass (Dong et al., 2016; He et al., 2023). By employing quantitative seismological methods, it becomes feasible to calculate source parameters such as origin time, location (Dong et al., 2020), and magnitude, as well as frequency-domain characteristics and source mechanisms. Based on these calculations, the spatiotemporal evolution process of microseismic events can be described, enabling monitoring and early warning of potential disasters (Du et al., 2021; Feng et al., 2015; Li et al., 2023).

MMS generally consists of sensors, data acquirers, communication units, data control center, GPS timing devices, signal cables, optical fibers, and monitoring stations, as shown in Figure 1.1. Compared to traditional rock mass monitoring methods, the microseismic monitoring system has four major advantages: (1) Real-time monitoring:

continuous collection of on-site microseismic signals for 24 hours; (2) Comprehensive three-dimensional monitoring: fully digitalized data acquisition, storage, and processing; (3) Automated spatial localization and display: automatic collection, localization, and display of microseismic signals; (4) Remote transmission and monitoring of information: remote collaboration and monitoring through internet connectivity, enabling visualization and analysis on multiple user computers.

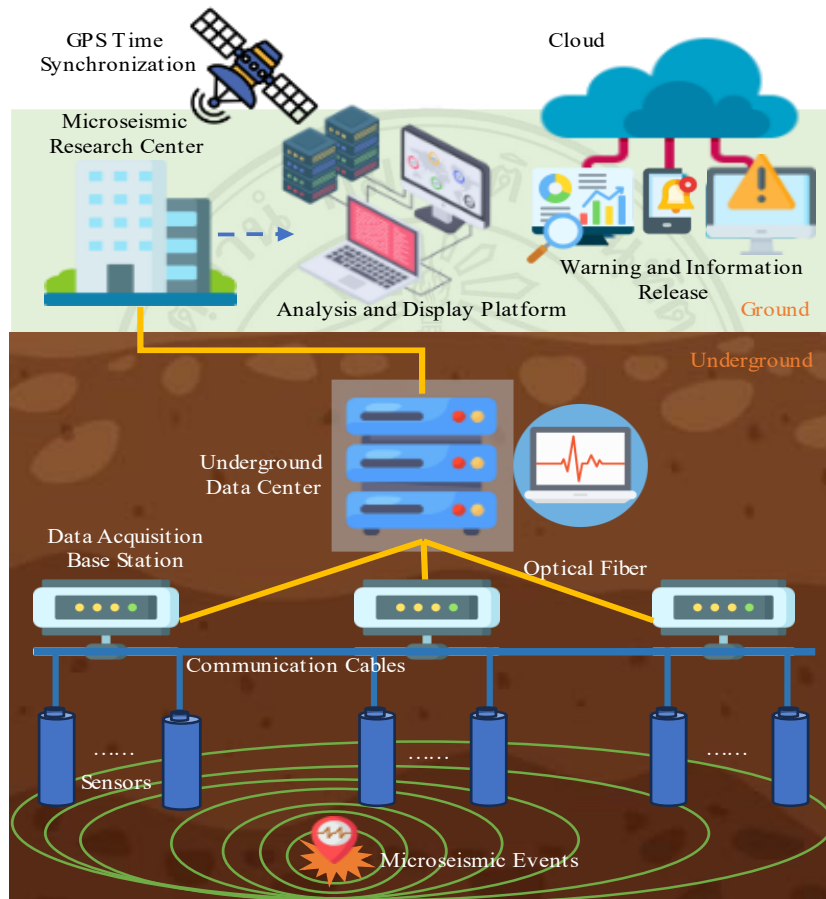


Figure 1.1 Composition of microseismic monitoring system

The signals collected by existing microseismic monitoring systems are diverse and vary in nature. Previous research has mostly focused on two categories: microseismic events and blasting events. However, in practical mining environments, signals are not limited to these two categories but also include rock drilling, fan noise, power interference, and other sources of noise. In this work, the research objects in mining are divided into four main categories: (1) blasting events, (2) microseismic events, (3) rock drilling events, and (4) other noise events. Blasting events refer to signals directly caused by shock waves generated from explosive detonations resulting in rock fragmentation

(Dong et al., 2016). Microseismic events are seismic phenomena resulting from structural instability caused by rock deformation (Cui et al., 2023) and internal crack propagation. Rock drilling events involve engineering operations where holes are drilled into rocks (or ore bodies), resulting in event signals. Noise events primarily include background noise, ore chute discharge, shovel operation, fan vibration, power interference, and other signals that cannot be attributed to blasting, microseismic, or rock drilling.

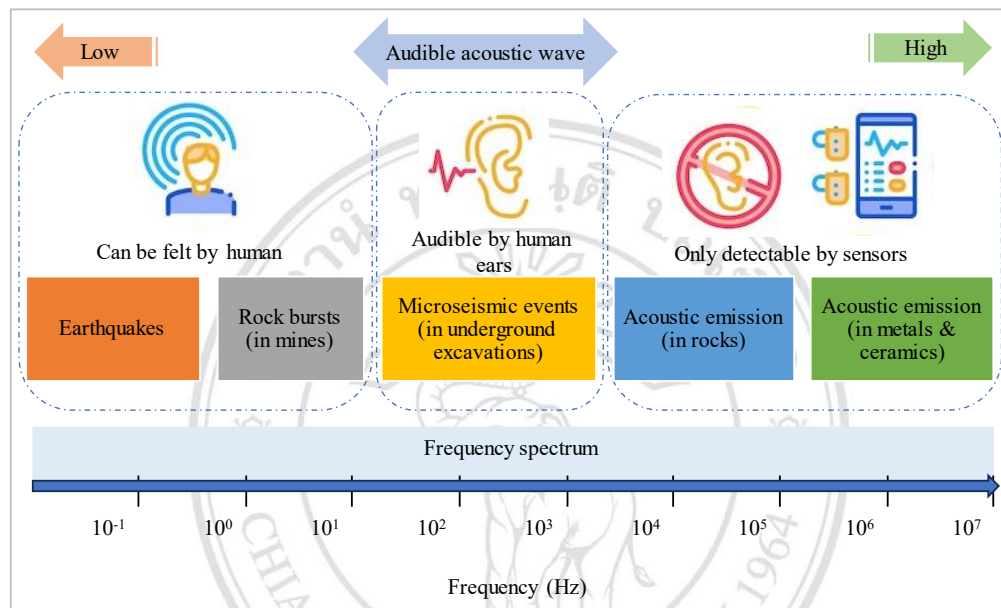


Figure 1.2 Frequency range of earthquakes, rock bursts, microseismic events, and acoustic emission

The analysis of microseismic events is based on accurate and clean microseismic monitoring signals, requiring the exclusion of interference signals from blasting, rock drilling, and noise before analysis. Although microseismic monitoring systems have been successfully applied in rock stability analysis, it remains challenging to extract precise microseismic events in complex environments, especially amidst various interferences such as noise and explosions. Due to the significant overlap in frequency distribution between blasting signals and microseismic events (Figure 1.2), relying solely on spectral analysis makes it challenging to accurately distinguish between these two types of events.

1.2 Problem Statements

Microseismic events are small-scale seismic activities that occur in mines due to rock fracturing or mining operations. They are essential indicators of the structural stability within a mine. Monitoring and accurately identifying these events can help

predict and prevent potential hazards, such as mine collapses or rock bursts, ensuring the safety of mine workers and equipment. There are various challenges and issues in the current identification and classification of microseismic events, including:

1. Data quality and quantity issues: The current recognition and classification of microseismic events face multiple challenges in terms of data quality and quantity, including low data quality, imbalanced event quantities, high workload for data preprocessing, low efficiency in manual identification, and difficulties in data sharing (Dong et al., 2016).

- Low data quality: Microseismic event data is often affected by noise and interference, resulting in lower clarity and accuracy of the signals (Othman et al., 2022). This can pose challenges for feature extraction and model training of microseismic events.
- Imbalanced event quantities: The distribution of microseismic events among different categories may be imbalanced, with some categories having a larger number of events while others have fewer (Li et al., 2021). This can impact the training and classification performance of models, leading to lower recognition capabilities for minority classes.
- High workload for data preprocessing: Due to the large-scale nature of microseismic event data, significant effort is required for data preprocessing tasks such as denoising and data alignment (Zhu et al., 2019). Complex algorithms and computational resources are needed, resulting in considerable time and energy consumption.
- Low efficiency in manual identification: Traditional manual identification methods rely on domain experts for manual annotation and classification, but these methods are inefficient and prone to human errors (Ma et al., 2021).
- Difficulties in data sharing: The sensitivity and commercial confidentiality of microseismic event data make data sharing and communication challenging, affecting collaboration among researchers and the transferability of models (Arrowsmith et al., 2022).

2. Challenges in feature extraction: Microseismic events typically exhibit small, complex, and variable features, which pose limitations to traditional feature extraction methods in capturing effective features. Additionally, due to the diversity of microseismic monitoring events (Ge, 2005), different types of events possess distinct features, making it challenging to effectively capture and characterize the features of microseismic events (Dong et al., 2020). Specifically, the challenges are as follows:

- Manual selection of feature parameters by experts: Traditional methods often rely on domain experts' experience and knowledge to manually select feature parameters (Zhang et al., 2021). This approach is time-consuming, susceptible to subjective factors, and lacks scalability and generalizability.
- Selection of source parameter features: The source parameters of microseismic events are crucial features (Yu et al., 2022). However, selecting appropriate source parameters for feature extraction remains challenging. Different types of microseismic events may correspond to different source parameters, necessitating the exploration of methods that consider multiple parameters comprehensively.
- Selection of waveform parameter features: Waveform parameters of microseismic events contain rich information. Extracting effective features from complex waveform data remains a difficult task. Existing feature extraction methods may not fully capture the details and variations in microseismic event waveforms (Kan et al., 2022), leading to inaccuracies and missing feature representations.
- Waveform image recognition and classification: In recent years, image processing and machine learning techniques (Yang et al., 2021) have been widely applied in the identification and classification of microseismic signals. Transforming microseismic waveform data into images and leveraging image recognition and classification technologies can provide more comprehensive and accurate feature representations. However, further research is needed to explore suitable image representation methods and effective training and optimization of image recognition models.

3. Challenges in classification model: Building accurate and reliable classification models for microseismic event data is a challenging task due to its complexity. Traditional machine learning algorithms may face issues such as high computational complexity and

poor generalization ability when dealing with high-dimensional, non-linear, and large-scale data (Li et al., 2022). In the process of designing classification models, the following issues and challenges exist:

- **Accuracy:** Ensuring that the classification model accurately categorizes microseismic events is a key objective (Wilkins et al., 2020). The model should have high accuracy to correctly identify various types of microseismic events, including minority classes.
- **Efficiency:** In practical applications, the efficiency of the classification model is an important consideration (Wamriew et al., 2022). The model should be able to classify large-scale microseismic event data quickly and accurately within a reasonable time frame.
- **Resource requirements:** Designing efficient classification models for large-scale microseismic event data requires effective utilization of computational resources. The model should consider computational complexity and storage requirements while being able to operate effectively on existing hardware infrastructure.
- **Interpretability:** Interpretability of the model is also an important requirement for the recognition and classification of microseismic events (Basnet et al., 2024). The model should provide explanations and reasoning for classification decisions, enabling users to understand the working principles and results of the model.
- **Generalization and robustness:** The classification model should possess good generalization ability, exhibiting stable and reliable performance across different datasets (Pham et al., 2021). Additionally, the model should demonstrate robustness against noise, interference, and data variations to ensure its effectiveness and reliability in real-world applications.

1.3 Research Questions

Based on a comprehensive review and analysis of relevant literature, our research aims to address the following three questions:

1. How to utilize machine learning methods for automatic microseismic signal identification, addressing the issue of high workload and low efficiency in manual identification?

2. How to improve the recognition efficiency and classification accuracy of existing microseismic signal identification and classification models?

3. How to enhance the generalization and robustness of models in the identification and classification of microseismic event waveforms?

By focusing on these research questions, we aim to advance the automation of microseismic signal processing, improve the accuracy of classification algorithms, and provide insights and references for the performance of different classification models in microseismic signal recognition.

1.4 Objectives of the Study

Based on the above research gaps, the objective of this work is to develop a machine learning model with high accuracy and timeliness, which can automatically identify and classify microseismic signals into different categories of events (such as microseismic events, blasts, drilling and noises). In addition, the proposed model is compared and evaluated with existing research methods and classical image classification models. Specifically, the purpose of this study includes the following three aspects:

1. To develop a classification model that can automatically identify microseismic event waveforms without the need for human intervention, aiming to address the issue of traditional machine learning identification methods relying on expert experience and manual feature engineering.

2. To improve and optimize existing classification models and algorithms to further enhance the efficiency and accuracy of waveform recognition for different types of microseismic events.

3. To meticulously refine and augment the model's architecture, with a focus on bolstering its adaptability and fault tolerance. This endeavor will integrate advanced machine learning techniques and rigorous testing methodologies to ensure the model maintains exceptional performance across a wide array of microseismic data.

By achieving these research objectives, this study can provide more reliable and effective technical support for the intelligent identification and classification of microseismic signals, thus playing an important role in microseismic monitoring and mine safety and other related fields.

1.5 Contributions of the Study

This study has made the following major contributions to the domain of microseismic event identification and classification:

1. Dataset construction and preprocessing: This study is dedicated to building a high-quality dataset for monitoring microseismic events in mines. By generating 6-channel waveforms of microseismic events and leveraging human expertise to label them as microseismic, blasting, rock drilling, and noise events, a reliable data foundation is provided. This dataset ensures the repeatability and comparability of research on microseismic events, offering support for subsequent research work and experiments.

2. Efficient intelligent recognition model: By constructing an intelligent recognition model based on machine learning techniques, this study aims to improve the efficiency of microseismic signal classification and reduce the workload of manual judgment. The model utilizes advanced algorithms and technologies to rapidly and accurately classify microseismic signals, thereby enhancing the level of automation in recognition. Through appropriate feature representation methods, adjustment of model parameters, and addressing issues such as overfitting and underfitting, we have successfully achieved accurate identification and classification of microseismic events.

3. Model performance evaluation and validation: To evaluate the performance of the proposed microseismic event recognition and classification model, this study conducted experiments and tests, employing suitable metrics and methods for evaluation. By comparing with existing methods, we verified the superiority of the proposed model and demonstrated its potential applications in engineering safety, geological exploration and resource development, and earthquake activity monitoring and early warning (Mousavi et al., 2023).

4. Practical application promotion: The achievements of this study can be applied in various fields, including not only mining engineering safety but also earthquake activity monitoring and early warning, geological exploration, and oil and gas resource development. By applying the research outcomes to practical scenarios, valuable references and support are provided for research and applications in related fields, promoting further development and application of intelligent microseismic event recognition and classification technologies (Kang et al., 2023).

In summary, this study has made significant contributions by improving the efficiency of microseismic signal recognition, enhancing the accuracy of recognition models, and providing effective data for mine disaster monitoring. These contributions advance the field of mine safety monitoring and offer new insights and methodologies for related research.

1.6 Scope of the Study

The scope of this study is to achieve rapid and accurate identification and classification of microseismic signals in mining environments. The research covers the fields of computer vision techniques and machine learning algorithms, with data primarily sourced from metal mines (Feng et al., 2017).

Firstly, microseismic signals will be transformed into event waveform images. Utilizing computer vision techniques such as image processing, recognition, and classification, different datasets of event waveform images will be established. Subsequently, machine learning algorithms such as Shallow Machine Learning (SML), Convolutional Neural Networks (CNN) (Chen et al., 2019), and Deep Neural Networks (DNN) will be employed. These algorithms will be trained using sample databases from different mining areas to obtain optimal models, thereby improving the accuracy and timeliness of microseismic signal identification and classification.

To ensure the reliability and effectiveness of the research, a large amount of real microseismic signal data will be utilized for testing, and comparisons will be made with existing research methods and image classification models. The performance of the models will be comprehensively evaluated based on accuracy, identification duration, precision, recall, and F1 score, leading to the selection of the best-performing model. The ultimate goal is to provide more reliable and intelligent technological support for microseismic monitoring and mining safety research (Choi et al., 2024). This will facilitate the intelligent transformation and safe development of mining operations.

1.7 Conceptual Framework

This study aims to achieve rapid and accurate identification and classification of microseismic signals in mining environments by combining computer vision techniques and machine learning algorithms. The conceptual framework of this study is illustrated below (Figure 1.3):

1. Data collection and preprocessing: Firstly, a microseismic monitoring system will be deployed in metal mines to collect microseismic signal data, encompassing various locations and time periods. The collected data will undergo preprocessing operations such as denoising, filtering, and data cleaning to enhance signal quality and reduce interference. The preprocessed microseismic signals will be transformed into event waveform plots suitable for processing by machine learning algorithms.

2. Establishment of event waveform databases: Corresponding datasets of event waveform images will be constructed for different types of microseismic events. Expert engineers will employ manual identification and classification methods to annotate and categorize the event waveform plots. This will establish datasets of event waveform images for different categories, providing the foundation for subsequent model training and recognition.

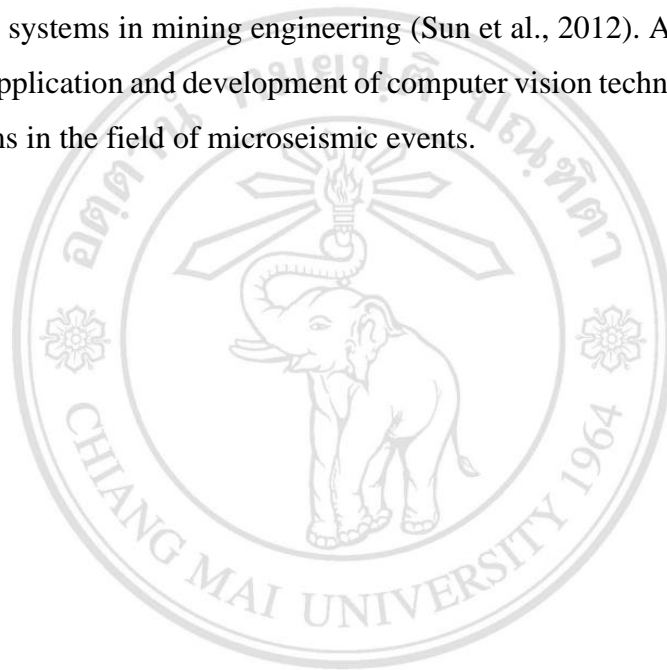
3. HOG and Shallow machine learning methods (SML): First, we use the Histogram of Oriented Gradients (HOG) algorithm to extract features from microseismic event waveform images. These features will serve as inputs for subsequent classifiers. Drawing on previous research, we will select five commonly used shallow machine learning algorithms to build classifiers: SVM classifier, Linear classifier, Decision tree classifier, K-Nearest Neighbors (KNN) classifier, and Fisher discriminant classifier. By selecting appropriate feature representation methods and optimizing model parameters, automated recognition and efficient classification of microseismic events will be achieved.

4. Convolutional neural network models: CNN models will be introduced, leveraging their powerful representation capabilities in image processing, to perform end-to-end learning and feature extraction on event waveform plots. Through designing suitable network architectures, tuning hyperparameters, and employing appropriate loss functions, the classification performance of microseismic events will be enhanced.

5. Deep learning and transfer learning models: To further improve recognition and classification performance, deep learning methods such as MobileNet-V2, Inception-V3 and ResNet-18 will be employed. Additionally, transfer learning techniques will be utilized to transfer pre-trained models from other domains to the microseismic event recognition and classification task, accelerating model training and improving performance.

6. Performance evaluation and comparison: The proposed methods and models will be tested using extensive real microseismic signal datasets. Performance evaluation will be conducted using metrics such as accuracy, precision, recall, and F1 score. Furthermore, comparisons with existing research approaches and image classification models will be performed to validate the superiority and feasibility of the proposed methods.

Through this conceptual framework, this study aims to achieve intelligent identification and classification of microseismic signals in mining environments. This research will provide more reliable and efficient technical support for safety monitoring and early warning systems in mining engineering (Sun et al., 2012). Additionally, it will contribute to the application and development of computer vision techniques and machine learning algorithms in the field of microseismic events.



ลิขสิทธิ์มหาวิทยาลัยเชียงใหม่
Copyright© by Chiang Mai University
All rights reserved

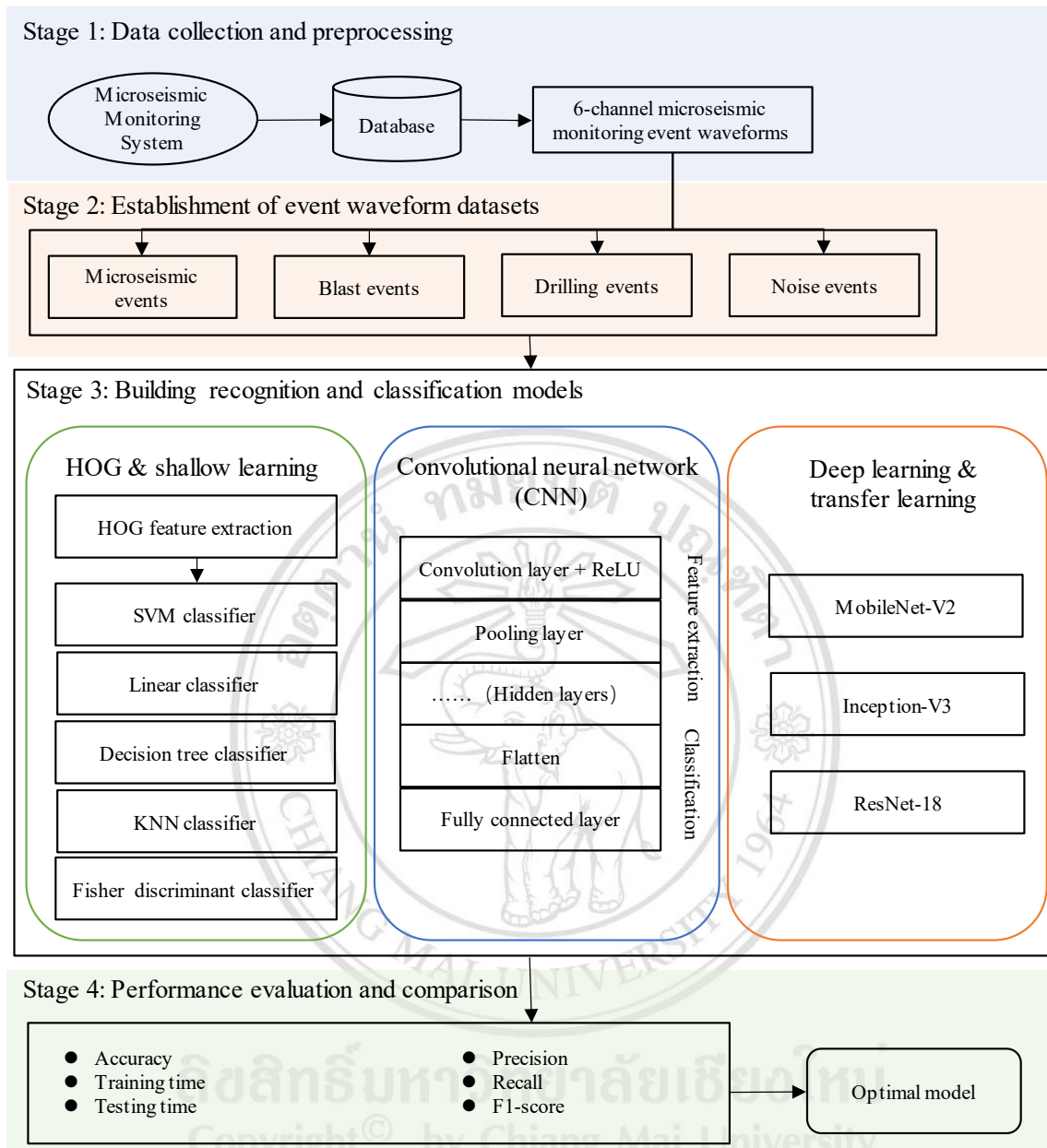


Figure 1.3 Conceptual framework of intelligent identification and classification of microseismic events based on machine learning techniques

1.8 Thesis Outline

Through the introduction section, readers will gain an understanding of the research background and the significance of microseismic event recognition and classification. We identify the existing problems and challenges in the research field and state the research problems, objectives, and contributions of this study. The following is a detailed outline of the relevant content to be presented in this thesis:

Chapter 2: Literature Review. This chapter will review the relevant research achievements in the domain of microseismic event identification and classification. A comprehensive analysis and comparison will be conducted, exploring the application of computer vision techniques and machine learning algorithms in microseismic events, highlighting the strengths and limitations of existing methods.

Chapter 3: Data and Methodology. This chapter will provide a detailed description of the methods and data used in the research. It will cover data collection, sample selection, and data preprocessing methods. Additionally, it will explain the machine learning algorithms and models employed, including shallow machine learning methods, convolutional neural networks, and deep learning methods such as MobileNet and Inception-V3. This chapter aims to ensure accurate and clear descriptions of the data and methods.

Chapter 4: Results. This chapter will introduce the experimental design, including dataset selection, feature extraction methods, and model configurations. It will provide a detailed description of the training and optimization processes of the models, as well as parameter adjustments and model evaluation methods. Experimental results will be presented, followed by performance evaluations and comparisons using metrics such as accuracy, recall, and F1 score. Detailed analysis and discussions of the experimental results will be conducted to explore the strengths and limitations of the methods.

Chapter 5: Discussion. This chapter will comprehensively analyze and discuss the results and findings of the research, summarizing the performance of different methods and models in microseismic event recognition and classification. Current challenges and issues will be discussed, and future research directions and prospects will be proposed to further improve and expand the field of study.

Chapter 6: Conclusion. This chapter will provide a summary of the main research findings and contributions, emphasizing the innovation and practical value of the research. Limitations of the study will be acknowledged, and possible avenues for improvement will be suggested.

Through this thesis structure overview, this research will comprehensively introduce the relevant work in microseismic event recognition and classification, provide detailed explanations of data collection and preprocessing, the application of machine

learning models, and analysis of experimental design and results. Additionally, the discussion and future directions section will explore current challenges and propose future research directions. Finally, the conclusion section will summarize the main research findings and discuss their potential practical applications.



ลิขสิทธิ์มหาวิทยาลัยเชียงใหม่
Copyright© by Chiang Mai University
All rights reserved

CHAPTER 2

LITERATURE REVIEW

2.1 Introduction

Microseismic monitoring technology has been proven to be an effective method for predicting underground engineering disasters (Li et al., 2022). Correctly identifying microseismic events during underground excavation is the basis for subsequent geophysical analysis such as ground pressure warning and tunnel deformation monitoring (Ma et al., 2020). Rapid identification of microseismic source types within the monitoring area and accurate extraction of valid events are fundamental to the application research of microseismic monitoring technology (Zhang et al., 2021). However, due to various noise and explosion interferences during mining operations, accurately identifying microseismic signals from complex environments and operating conditions still poses certain challenges (Shu & Dawod, 2023).

Traditional identification methods, such as manual waveform analysis (Zhao et al., 2015), require operators to have strong knowledge of physics and signal processing, and pre-determine artificial identification criteria. However, this method is prone to individual experience differences and it is difficult to achieve satisfactory results due to the variability of collected signals. At the same time, with the increasing amount of monitoring data, this method is labor-intensive, time-consuming, and inefficient. Therefore, researchers have extensively explored effective methods for accurately identifying microseismic signals.

Based on the principles of different identification methods, we categorize existing microseismic signal identification methods into three main classes: (1) spectral analysis or frequency spectrum analysis (Li et al., 2012), (2) statistical analysis (Dong et al., 2019), and (3) machine learning methods.

Spectral analysis (Fagan et al., 2013) refers to the analysis of signals in the frequency domain. It transforms time-domain signals into frequency-domain signals to display the energy distribution of different frequency components. Common methods used in spectral analysis include Fourier Transform (FT) (Ma et al., 2023) and Power Spectral Density Estimation. Spectral analysis can be used to determine the presence and strength of specific frequency components in a signal and is widely applied in fields such as communication, audio processing, and image processing (Wei et al., 2020). On the other hand, frequency spectrum analysis focuses more on describing and analyzing the frequency characteristics of signals, including the number of frequency components, frequency range, and frequency intervals. Frequency spectrum analysis typically involves discretizing the signal and then using algorithms such as Discrete Fourier Transform (DFT) or Fast Fourier Transform (FFT) (Jiang et al., 2015; Li et al., 2021) to calculate the signal's spectrum. Analyzing the energy distribution of the signal in the frequency domain helps us understand its characteristics at different frequencies. However, spectral and frequency spectrum analysis requires a certain level of expertise, which presents challenges in practical engineering applications (Yin et al., 2021).

In the early 21st century, statistical analysis methods were introduced and experienced significant growth (Dong et al., 2016). Statistical analysis methods primarily rely on the statistical properties of signals and use manually designed waveform features for identification and classification (Chakraborty et al., 2022). By performing statistical analysis on microseismic signals, statistical parameters, correlation, and other features can be extracted and further used for event identification and classification. However, statistical analysis methods still rely on the subjective experience of researchers in feature extraction and model selection, which may affect the accuracy of the classification model. Additionally, this method is time-consuming and may not produce satisfactory results.

In recent years, with advancements in hardware and software technology, machine learning methods have been widely applied in the field of microseismic signal identification (Anikiev et al., 2023). Machine learning-based methods can efficiently and accurately identify microseismic events without the need for explicit identification instructions. In particular, deep learning-based neural network models (Huang et al., 2021), by combining the power of machine learning and computer vision (Zhao et al., 2024), can automatically extract unique features from different waveforms and establish

an image classification framework for intelligent recognition of microseismic events. This technological approach surpasses traditional statistical methods and improves the efficiency of microseismic event identification. As a result, microseismic monitoring systems can acquire valuable microseismic data, laying the foundation for subsequent earthquake source localization, magnitude prediction, and timely warning of potential induced seismic activities (He et al., 2017).

Figure 2.1 illustrates the relationship among artificial intelligence, machine learning, supervised learning (Choi et al., 2019), unsupervised learning (Cano et al., 2021), deep learning, and transfer learning (Umeaduma, 2024). Shallow learning, deep learning, and transfer learning are subclasses of machine learning, which in turn is a subset of artificial intelligence. Supervised learning and unsupervised learning are two distinct approaches within machine learning, with supervised learning utilizing labeled data for training, while unsupervised learning does not require pre-labeled data. Transfer learning (Bahri et al., 2020) involves leveraging knowledge gained from one task to improve performance on another related task.

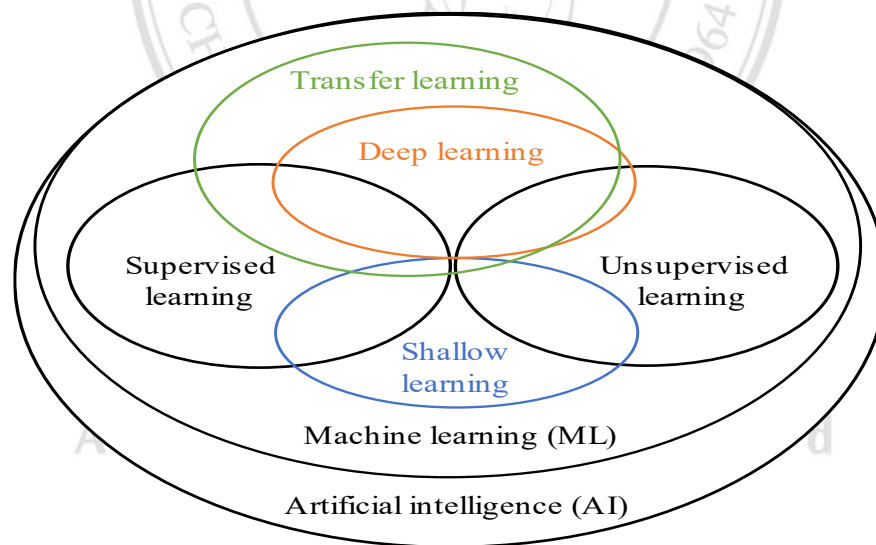


Figure 2.1 Relationship among artificial intelligence, machine learning, supervised learning, unsupervised learning, deep learning, and transfer learning

This chapter will introduce the current research status of machine learning in the domain of microseismic signal identification. First, we provide a brief overview of the evolution of traditional identification methods and machine learning methods, and briefly analyze the advantages and limitations of different methods. Then, based on the

characteristics of machine learning methods, we classify and introduce them, and discuss the latest research developments in microseismic event identification methods. Lastly, we investigate the prospects and obstacles that machine learning encounters in microseismic event classification.

2.2 Theoretical Concepts

2.2.1 Machine Learning

Machine learning (Bergen et al., 2019) is a subfield of artificial intelligence that focuses on developing algorithms and models to enable computers to learn and make predictions or decisions without explicit programming. It utilizes statistical techniques to automatically analyze and interpret data, improving performance based on experience. In the realm of microseismic signal detection, machine learning models can be trained on annotated datasets to identify patterns and features that distinguish various types of events. These algorithms can then be used to classify new, unlabeled microseismic signals into different event categories.

Supervised learning (Zhao et al., 2017) is a commonly used branch of machine learning for microseismic signal recognition. In supervised learning, algorithms are provided with a training dataset that includes input features (such as waveform features and statistical parameters) and corresponding output labels (such as event types). The algorithm learns from these labeled data and builds a model capable of predicting the correct labels for new, unseen inputs. Common supervised learning algorithms include SVM (Cervantes et al., 2020), decision tree (Zhao et al., 2021), random forests, and neural networks. These algorithms can handle complex relationships between input features and output labels, capturing intricate patterns in the data.

In addition to supervised learning, there is also research based on unsupervised learning methods. Unsupervised learning (Yang et al., 2023) is another important branch of machine learning that does not require pre-labeled training datasets. Instead, it learns and infers by discovering intrinsic structures, patterns, and associations within the data. In the field of microseismic signal recognition, unsupervised learning can be applied to tasks such as clustering analysis (Duan et al., 2021), anomaly detection, and dimensionality reduction.

Clustering analysis (Fagan et al., 2013) is a commonly used technique in unsupervised learning, which groups data into clusters with similar features. In microseismic signal recognition, clustering analysis can help identify microseismic events with similar waveform characteristics, enabling automatic classification of event types. Common clustering algorithms (Feng et al., 2023) include k-means clustering, hierarchical clustering, and density-based spatial clustering of applications with noise (DBSCAN) (Yin et al., 2023).

Anomaly detection (Li et al., 2009) aims to identify anomalies or outliers that do not conform to normal patterns. In microseismic monitoring, anomaly detection can be used to identify abnormal microseismic events that may represent potential geological changes or activities, providing deeper analysis and warning of underground conditions (Wang et al., 2021). Common anomaly detection algorithms include statistical-based outlier detection, density-based outlier detection, and isolation forest-based outlier detection.

Additionally, dimensionality reduction techniques (Mousavi et al., 2022) are also utilized in unsupervised learning. Dimensionality reduction maps high-dimensional data to a lower-dimensional space to reduce complexity and redundancy in the data. In microseismic signal analysis, dimensionality reduction techniques can help extract the most informative features and reduce computational complexity. Common dimensionality reduction algorithms include Principal Component Analysis (PCA) (Zhu et al., 2023) and Linear Discriminant Analysis (LDA) (Dong et al., 2011).

The advantage of unsupervised learning (Chen, 2018) methods is that they do not require pre-labeled data and can automatically discover patterns and structures within the data. However, due to the lack of supervision, unsupervised learning methods may be more challenging to interpret and validate, requiring further research and exploration in their application to microseismic signal recognition.

Another important concept in machine learning is feature extraction. Feature extraction involves selecting or transforming raw data into a meaningful and informative set of features that can serve as input for machine learning algorithms. In the context of microseismic signal recognition, these features may include time-domain characteristics,

frequency-domain properties, statistical indicators, or other relevant parameters used to capture unique features of different event types.

Machine learning methods offer the advantages of automatic learning and adaptability to new data, enabling them to handle the variability and complexity of microseismic signals. They can also efficiently process large amounts of data, which is particularly important as microseismic monitoring data continues to grow. However, machine learning also has limitations. It requires sufficiently large and representative labeled datasets for training, as the quality and diversity of the training data greatly impact the performance of the models. Overfitting is another challenge in machine learning, occurring when the model becomes overly focused on the training data and performs poorly on new data. Regularization techniques and careful model selection can help mitigate overfitting issues.

The evolution of machine learning in microseismic signal identification can be broadly categorized into three stages: shallow learning, deep learning, and transfer learning. Figure 2.2 shows the distinctions among these three stages.

In summary, machine learning provides a powerful framework for microseismic signal recognition by utilizing statistical techniques and the ability to learn automatically from data. It enables the development of models that accurately classify and interpret microseismic signals, driving advancements in microseismic monitoring technology.

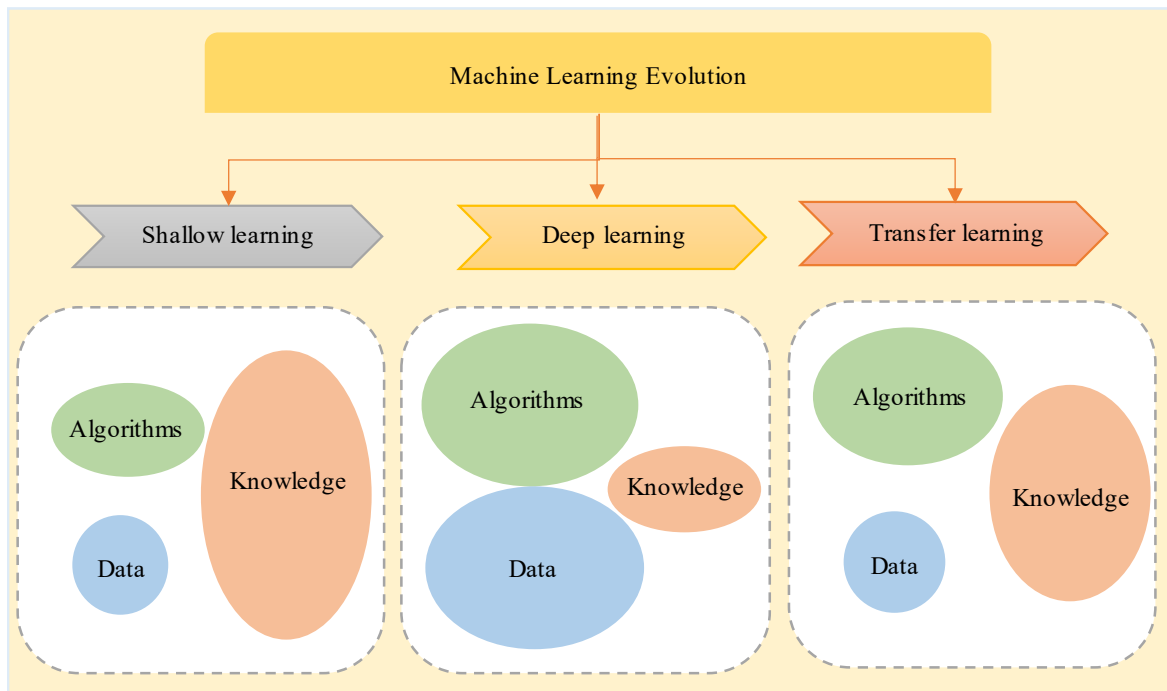


Figure 2.2 Three stages of machine learning development

2.2.2 Shallow Learning

Shallow learning (Wang et al., 2020), also known as traditional machine learning, is another commonly used approach in microseismic signal recognition. Unlike deep learning (Alarfaj et al., 2022) methods that involve complex neural network structures and large amounts of labeled data, shallow learning algorithms are simpler and have lower computational requirements. Shallow machine learning methods rely on feature engineering, which involves extracting manually designed features from input data and using them to train classification models.

In microseismic signal recognition, shallow learning algorithms can be applied to various types of features extracted from waveform data. These features can include statistical measures such as mean, variance, skewness, and kurtosis, as well as time-domain features like energy, zero-crossing rate, and peak amplitude. Additionally, frequency-domain features like spectral centroid, spectral entropy, and spectral flatness can also be used. Other commonly used features in microseismic signal recognition include wavelet coefficients, autoregressive coefficients, and cepstral coefficients (Peng et al., 2019).

After extracting these features from the waveform data, they are used as inputs to shallow learning algorithms such as SVM (Chandra et al., 2021), Random Forests, or k-Nearest Neighbors. These algorithms learn patterns and decision boundaries based on the extracted features and are trained using labeled data. Once trained, the models can classify new microseismic signals into different classes or detect specific events of interest.

Shallow learning approaches have several advantages in microseismic signal recognition. They are computationally efficient and can handle large-scale datasets, making them suitable for real-time or near-real-time applications. Shallow learning methods also require less labeled data compared to deep learning methods, which can be beneficial when labeled data is limited or expensive to obtain. Additionally, shallow learning algorithms provide interpretable results, allowing domain experts to understand and analyze the underlying features contributing to the classification or detection.

However, there are limitations to shallow learning approaches. These methods heavily rely on the quality and relevance of handcrafted features, which require domain knowledge and expertise to select and design appropriately. The performance of shallow learning algorithms highly depends on the choice and effectiveness of these features. Moreover, shallow learning methods may face difficulties in capturing the intricate patterns or relationships present in the data, which deep learning models are particularly adept at handling (Huang et al., 2018).

To overcome these limitations, a hybrid approach combining shallow learning and deep learning techniques can be employed (Mousavi et al., 2016). This involves using deep learning models for feature extraction and representation learning, followed by shallow learning algorithms for classification or detection based on the extracted features. This hybrid approach takes advantage of both the representational power of deep learning and the interpretability and efficiency of shallow learning.

In summary, shallow learning methods offer a simpler and computationally efficient alternative to deep learning for microseismic signal recognition. By extracting manually designed features from waveform data and training traditional machine learning models, automatic classification and event detection can be achieved. However, careful feature engineering and selection are crucial for the performance of shallow learning algorithms. Combining shallow learning with deep learning methodologies can

significantly improve the accuracy and efficiency of microseismic signal identification systems.

2.2.3 Deep Learning

Deep learning (Yang et al., 2015) is an important branch of machine learning that utilizes multi-layer neural networks to model and learn data representations. By stacking multiple hidden layers, deep learning can automatically extract and learn more abstract and complex features. In the domain of microseismic signal classification, deep learning methods have been widely applied and achieved significant results (Zhang et al., 2022). Deep learning models can effectively handle large-scale, high-dimensional microseismic data and directly learn task-specific feature representations from raw data. This end-to-end learning approach eliminates the need for manual feature design, allowing the models to better adapt to different types of microseismic events (Yang et al., 2015).

Common deep learning models include convolutional neural networks (Li et al., 2022), recurrent neural networks (RNN) (Di et al., 2023), and Autoencoders (Mousavi et al., 2019). CNNs (Alzubaidi et al., 2021) perform well in processing time-domain or frequency-domain microseismic waveform data, effectively capturing local features and spatial correlations. RNNs are suitable for handling time series data (Ding et al., 2022), and capturing temporal relationships in microseismic signals. Autoencoders are unsupervised learning models that can be used for unsupervised feature learning and data dimensionality reduction (Huang, 2019).

The advantages of deep learning methods in microseismic signal recognition include their ability to model complex features, automate feature extraction, and robustness against noise and interference. They can learn more discriminative feature representations from large amounts of data and handle nonlinear relationships and complex spatiotemporal structures in the signals. However, deep learning also faces challenges and limitations. Firstly, deep learning models usually require a large amount of labeled data for training, which may be limited in the microseismic field due to data scarcity. Secondly, deep learning models have high computational complexity, requiring significant computational resources and time for training and inference. Additionally, the interpretability of these models is limited, which complicates understanding and explaining their internal decision-making processes (Schmidhuber, 2015).

To overcome these challenges, researchers are constantly improving deep learning models and algorithms to enhance their performance and efficiency (Z. Xie et al., 2022). For example, transfer learning and semi-supervised learning techniques can utilize pre-trained models or a small amount of labeled data to improve the generalization ability of the models. Additionally, research on model interpretation and explainability is an important direction aimed at enhancing understanding and interpretability of the decision-making processes within deep learning models.

In summary, deep learning, as an important branch of machine learning, exhibits powerful capabilities in microseismic signal recognition. By constructing deep structures and employing end-to-end learning, deep learning models can effectively extract and learn feature representations of microseismic signals, enabling accurate event classification and recognition. However, further research and development are still needed to overcome challenges such as data scarcity, computational complexity, and model interpretability.

2.2.4 Transfer Learning

Transfer learning (Zhu et al., 2022) is also a machine learning method that aims to accelerate the learning process and improve performance in a new task by applying the knowledge and experience learned from another related task (Setiawan et al., 2020). In the field of microseismic signal recognition, transfer learning is widely used to address the challenges of data scarcity and labeling difficulties (Deepak et al., 2019). Conventional algorithms within the realm of machine learning often necessitate extensive datasets with labeled information for model training, and each new task requires training a separate model from scratch. However, in practical microseismic monitoring applications, it is often difficult to obtain a sufficient amount of labeled data, which limits the performance and applicability of models. Transfer learning overcomes this data limitation by leveraging existing large-scale, high-quality labeled datasets and transferring the knowledge and features learned from other related tasks to the microseismic signal recognition task (Pan et al., 2010).

Transfer learning can be applied in two ways: feature transfer and model transfer. Feature transfer involves directly applying the learned feature representations from the source domain to the target domain without retraining the feature extractor. This approach

is suitable when the source and target domains have similar feature representations. Model transfer, on the other hand, involves using a pre-trained model from the source domain as an initial model and fine-tuning or further training it on the target domain. This approach is applicable when there are differences between the source and target domains but still have some relevance (Dong et al., 2023).

The core idea of transfer learning is to enhance the learning effectiveness and generalization ability of the target task by sharing knowledge and feature representations. It reduces the dependency on a large amount of labeled data and leverages existing experience to accelerate the learning process of new tasks. Additionally, transfer learning can help address the challenge of labeling difficulties by assisting in labeling more challenging samples based on the knowledge learned from existing labeled data. However, transfer learning also faces challenges and limitations. Firstly, the differences between the source and target domains may lead to a decrease in the performance of transfer learning. Therefore, selecting appropriate source domains and designing effective transfer strategies are crucial. Secondly, transfer learning requires a sufficient quantity and quality of source domain data to learn good feature representations and knowledge. Lastly, the effectiveness of transfer learning is influenced by the correlation and similarity between the source and target domains, and different application scenarios may require different transfer methods and strategies.

In conclusion, transfer learning is a powerful machine learning method with broad applications in the field of microseismic signal recognition. By leveraging existing knowledge and experience, transfer learning can overcome the challenges of data scarcity and labeling difficulties, improving the performance and applicability of microseismic signal recognition. However, further research and exploration are still needed to address the challenges related to differences between source and target domains, selection of transfer strategies, and requirements for source domain data.

2.2.5 Image Recognition and Classification

Image recognition and classification is an important research direction in the fields of machine learning and computer vision (Chugh et al., 2020; Huang et al., 2021), and it has been widely applied in microseismic signal recognition. Its goal is to automatically

analyze and interpret input image data, categorizing them into different classes or performing object detection (Khayer et al., 2023).

In microseismic signal recognition, image recognition and classification methods can be used to process the visual representations of microseismic waveform data, such as time-domain graphs, spectrograms, or time-frequency spectrograms (Li et al., 2022; Wei et al., 2020). These image representations provide more intuitive, interpretable, and easily processable features that help capture spatial and frequency information of microseismic events. By training image recognition and classification models, automatic classification and recognition of microseismic signals can be achieved. The explanations of different visualization methods for microseismic waveform data are as follows:

1. Time-domain graphs: Microseismic waveforms are plotted over the time axis, where the horizontal axis represents time and the vertical axis represents the amplitude of the signal (Zhang et al., 2021). This visualization method intuitively displays the amplitude and duration of microseismic events.

2. Spectrograms: By applying the Fourier transform to microseismic waveform signals, the signals are transformed into the frequency domain, and the spectral information is presented as a heatmap or color map. Spectrograms show the energy distribution of microseismic signals at different frequencies, helping to capture the frequency characteristics of microseismic events.

3. Time-frequency spectrograms: Microseismic waveform signals are decomposed into small segments in different time periods and frequency ranges, and plotted as two-dimensional images. Common time-frequency analysis methods include Short-Time Fourier Transform (STFT), Continuous Wavelet Transform (CWT), and Wavelet Packet Transform (WPT). Time-frequency spectrograms provide local features of microseismic events in both time and frequency domains, aiding in capturing their time-frequency characteristics (Bi et al., 2021).

4. Wavelet packet spectrograms: Microseismic waveform signals are decomposed into sub-signals of different scales and frequency bands using wavelet packet transform, and plotted as two-dimensional images. Wavelet packet spectrograms display the energy distribution of microseismic events at different scales and frequency bands, helping to capture multi-scale features of microseismic events.

5. Phase diagrams: Phase information of microseismic waveform signals is displayed. Phase diagrams can help identify phase differences between microseismic events, inferring their spatial distribution and propagation paths.

Among these visualization methods, time-domain graphs and spectrograms are the most widely used in the analysis and recognition of microseismic waveform data. Common image recognition and classification methods include Convolutional Neural Networks, feature extraction, and image matching. CNNs are deep learning models suitable for image data, capable of automatically extracting feature representations from images and performing classification or object detection (Zhao et al., 2019). Feature extraction is a traditional method that selects and extracts local features of images, such as texture, shape, and edges, for classification. Image matching involves calculating the similarity or distance between images for classification or recognition.

Image recognition and classification methods offer several advantages in microseismic signal recognition. Firstly, image representations provide more intuitive and interpretable features, making the models more sensitive to spatial and frequency information of microseismic events. Secondly, image recognition and classification methods are efficient and flexible when handling large-scale image data, capable of dealing with complex spatiotemporal structures and nonlinear relationships (Wang et al., 2024). Additionally, image recognition and classification methods can be combined with other machine learning methods, such as deep learning and transfer learning, to further enhance the performance of microseismic signal recognition.

However, image recognition and classification methods also face challenges and limitations. Firstly, the image representation of microseismic waveform data requires appropriate preprocessing methods and parameter settings to retain important feature information and reduce the impact of noise. Secondly, the process of model training and fine-tuning parameters often necessitates an extensive collection of annotated data along with considerable computational power. In the domain of microseismic analysis, these requirements can be challenging due to the constraints posed by limited data availability and the intricate computational demands. Lastly, different types of microseismic events may have different image representation methods and features, requiring appropriate model design and training strategies for specific problems.

In summary, image recognition and classification methods provide an effective solution for microseismic signal recognition. By selecting suitable image representation methods and models, automatic classification and recognition of microseismic waveform data can be achieved. However, further research and exploration are still needed to overcome challenges related to data preprocessing, labeling data requirements, and model design, promoting the further development of image recognition and classification in microseismic monitoring technology.

2.3 Literature Review and Related Research

In this study, relevant literature was obtained from reputable academic databases such as Google Scholar, Web of Science, Scopus, and PubMed. Initially, a predefined set of keywords including "microseismic event," "microseismic waveform," "machine learning," "deep learning," "image recognition," and "image classification" was used to index the research information. An extensive search on Google Scholar was conducted, and studies were selected based on their significance in the field.

A thorough review of current literature is essential for comprehending the techniques used in microseismic event waveform recognition and classification. By examining current research, valuable insights can be drawn from previous studies to guide future research. Table 2.1 summarizes the research objectives, methodologies, and significant findings (or limitations) of various methods employed in this field over the past six years, arranged in chronological order. It serves as a comprehensive reference for researchers, covering statistics, spectral analysis, traditional machine learning, deep learning (Ku et al., 2021), and transfer learning methods. The table illustrates the variety of methodologies employed in microseismic event identification, ranging from traditional methods like EEMD and SSA to decision trees, support vector machines (Cortes et al., 1995), and convolutional neural networks. Such a variety of approaches equips researchers with an extensive array of options, enabling them to pick the most fitting instruments tailored to their precise demands.

Table 2.1 Relevant studies in recent years (2018 - 2023).

Scholars	Objectives	Methods	Key Findings/Gaps
Lin et al., 2018	Joint recognition and classification of multi-channel microseismic waveforms	Deep convolutional neural network with spatial pyramid pooling (DCNN-SPP)	The classification accuracy of the test set was 91.13%, but further improvement is possible with more training data.
Binder et al., 2019	Detect microseismic events in a distributed acoustic sensing (DAS) strain wavefield	Convolutional neural networks (CNNs)	Neural networks offer cost-effective and automated detection of microseismic events.
Bi et al., 2019	Identify and classify multi-channel microseismic waveforms	A hybrid technique of DCNN and support vector machine (SVM)	DCNN-SVM method outperformed random forests (RF) and k-nearest neighbors (KNN), with an accuracy rate of 98.18%.
Zhang et al., 2019	Automatic identification of microseismic data	Combining ensemble empirical mode decomposition (EEMD), singular value decomposition (SVD), and extreme learning machine (ELM)	ELM outperformed backpropagation neural networks, neural networks optimized with genetic algorithms, and SVM classification models.
Dong et al., 2020	Identification of microseismic events and explosions in seismic waveforms.	A CNN-based image recognition model	CNN demonstrated significant advantages, achieving accuracy rates of 99.46% for microseismic events and 99.33% for explosions in the test dataset.
Kang et al., 2020	Classification of microseismic events and explosions	Deep belief network (DBN)	The model outperformed the accuracy obtained with SVM and Fisher classifiers, achieving 94.4%.
Peng et al., 2020	Classification of limited sample microseismic records	Capsule network (CapsNet)	On a limited set of training examples, the method achieved a 99.2% accuracy rate. It outperformed CNN and other machine learning algorithms in terms of effectiveness.
Song et al., 2020	Identification of mining microseismic and blast signals	CNN and Stockwell transform-based color images	Utilized the strengths of CNN in image recognition by directly training on raw microseismic signal images, thus eliminating the need for extensive data preprocessing.

Table 2.1 Relevant studies in recent years (2018 - 2023) (continued)

Scholars	Objectives	Methods	Key Findings/Gaps
Wei et al., 2020	Identification of microseismic events and explosions	A waveform image discrimination method using principal component analysis (PCA) and SVM	Combining waveform image features extracted by PCA with the SVM classifier accurately identifies microseismic events, achieving a peak accuracy of 90%.
Yi et al., 2020	Identification of mining microseismic and blast signals	Complete ensemble empirical mode decomposition with adaptive noise sample entropy (CEEMDAN_SE)	Distinct differences in sample entropy values are observed between microseismic and blast signals. By integrating these values with ELM, the CEEMDAN_SE method achieves a classification accuracy of 91.5%.
Peng et al., 2021	Identification of microseismic events and explosions	Ten machine learning methods based on six source factors.	The logistic regression algorithm performs the best with an accuracy of over 95%. The quality of training samples directly affects the model's classification accuracy.
Bi et al., 2021	Microseismic waveform categorization	An understandable time-frequency convolutional neural network (XTF-CNN)	Compared with CNN, LSTM, RNN-FCN, and ResNET, XTF-CNN obtains excellent performance and outstanding interpretability.
Jiang et al., 2021	Identification of mining microseismic and blast signals	An improved Hilbert-Huang transform is adopted to reveal the time-frequency spectrum (HHS)	This approach minimized the operator's influence on classification, enhancing both the accuracy and efficiency of mass spectrometry signal data identification in spectral monitoring technology applications.
Peng et al., 2021	Identify effective microseismic signals	Deep convolutional neural network Inception (DCNN-Inception)	DCNN-Inception algorithm outperformed CNN in recognition accuracy.
Rao et al., 2021	Discriminating microseismic events and mine blasts	Particle swarm optimization (PSO) algorithm optimized ELM artificial intelligence model (PSO-ELM)	Compared to the original ELM model and other models (BPNN, NBC, and FDA), PSO-ELM showed the best discrimination performance.

Table 2.1 Relevant studies in recent years (2018 - 2023) (continued)

Scholars	Objectives	Methods	Key Findings/Gaps
Tang et al., 2021	Identification of microseismic events	CNN combined with an attention mechanism	The model refines CNN's intermediate data to increase efficiency without a significant rise in parameters or computational load. Applied to multiple channels, it achieves the best results.
Zhao et al., 2021	Identification of microseismic signals (three types: microseismic, blast, and mechanical)	A hybrid model combining singular spectrum analysis (SSA), CNN, and long short-term memory network (LSTM)	Compared with CNN, LSTM, BP, SVM, decision tree (DT), KNN, and linear discriminant analysis (LDA), this model achieved higher recognition accuracy.
Ding et al., 2022	Mine microseismic event recognition	Neural network combined with transfer learning	The enhanced T-SimCNN model, utilizing transfer learning, attained a 95% accuracy rate in identifying microseismic occurrences.
Fan et al., 2022	Discriminating microseismic events from noise.	Wavelet scattering decomposition (WSD) transform and SVM	Each signal's scattering coefficients demonstrated their aptness for serving as distinctive features in the training of specialized models.
Jia et al., 2022	Classification of three-channel seismic full-waveform time series and spectral data (three classes: earthquakes, blasting, and mine collapses)	VGGnet, ResNet, and Inception	The findings indicated that the classifier's performance metrics, both in terms of recall and precision, surpassed the 90% threshold.
Li et al., 2022	Recognition and classification of microseismic waveform images and spectrograms	Deep learning models, including VGG16, ResNet18, AlexNet and their ensemble models.	The individual models exhibited strong performance on the raw waveform image dataset, achieving 96% accuracy for AlexNet, 98% for VGG16, 96% for ResNet18, and an ensemble model reaching 98% accuracy.
Wang et al., 2022	Microseismic waveform classification	Enhanced convolutional neural network (ECNN) based on the ACGAN structure	The research examined the impact of varying training sample sizes on both ECNN and conventional CNNs. It revealed that classification accuracy for both types of models stabilizes at a count above 1024 samples and experiences a sharp decline when the sample size is reduced below 512.

Table 2.1 Relevant studies in recent years (2018 - 2023) (continued)

Scholars	Objectives	Methods	Key Findings/Gaps
Wang et al., 2022	Identifying microseismic events	A dual-channel CNN model with time-domain information and wavelet packets decomposition coefficients (T-WPD CNN).	The wavelet packet decomposition technique accentuates the intrinsic properties of signals and effectively diminishes the impact of noise. Experimental data suggests that the T-WPD CNN model outperforms standard CNN in reliability and robustness against noise interference.
Zhu et al., 2022	Discriminating earthquakes and quarry blasts.	Proposed an application strategy that combines deep learning and transfer learning	Deep learning enables accurate identification of seismic events using raw waveforms, and the utilization of transfer learning allows for effective generalization of deep learning models across various locations.
Chen et al., 2022	Microseismic signal detection.	Conv-LSTM-Unet is a deep learning model which utilizes convolutional neural networks and long short-term memory networks	The Conv-LSTM-Unet model utilizes a semantic segmentation approach to more effectively capture the spatiotemporal features of microseismic data.
Li et al., 2023	Microseismic waveform recognition	A modified LeNet5 CNN	The revised model recognized 13 forms of MS from real data with a maximum accuracy of 98%, an increase of 10% over the original model.
Ma et al., 2023	Recognition and classification of microseismic signals	Deep learning techniques and short-time Fourier transform (STFT) technologies	STFT time-frequency analysis reveals unique characteristics of noise, microseismic, and blasting signals, enabling precise temporal differentiation from noise signals that closely resemble microseismic events.
Dong et al., 2023	Recognition and classification of microseismic event waveforms	CNN-based transfer learning models (AlexNet, GoogLeNet, and ResNet50)	Four categories of microseismic event datasets were created, and transfer learning was applied to pre-trained models. GoogLeNet demonstrated the highest overall performance, achieving a recognition accuracy of 99.8%.

2.3.1 Traditional Identification Methods

In the field of microseismic signal recognition, several traditional recognition methods have been proposed and applied in practical engineering. These traditional recognition methods primarily include manual identification, correlation analysis, and spectral analysis.

- Manual Identification:

Manual identification is one of the earliest and most commonly used methods for microseismic signal recognition (Peng et al., 2021). This method relies on experts in the field who observe and analyze waveform data to determine the occurrence of microseismic events (Dong et al., 2020). Manual identification methods require experienced professionals and are time-consuming and labor-intensive, but they can still be effective in certain cases. However, due to subjectivity and individual differences, manual identification methods suffer from issues such as inconsistent recognition results and uncertainty in labeling data (Jiang et al., 2023).

- Correlation Analysis:

Correlation analysis is another commonly used traditional recognition method, which determines whether different microseismic signals have similar features or shared structures by calculating their correlations (Shang et al., 2017). Correlation analysis methods can be applied to time-domain or frequency-domain data and utilize cross-correlation or autocorrelation functions for computation (Caffagni et al., 2016; Wu et al., 2016). These methods help capture the similarity or correlation between signals for recognition and classification. However, correlation analysis methods are sensitive to signal noise and may have high computational complexity when dealing with large-scale data.

- Spectral Analysis:

Spectral analysis is a common traditional recognition method that utilizes the frequency-domain characteristics of signals for classification or identification (Li et al., 2021). Spectral analysis methods calculate the spectral information of signals using Fourier transform or other spectral estimation techniques and extract frequency features for recognition (Fagan et al., 2013). Common spectral features include spectral energy,

dominant frequency components, and spectral shape (Li et al., 2018). Spectral analysis methods effectively capture the frequency characteristics of signals but may not be as sensitive to time-domain and time-frequency domain features.

In addition to traditional identification methods, numerous research works have been dedicated to improving the recognition performance of microseismic signals. Some of these studies focus on enhancing feature engineering techniques to extract more discriminative features (Mousavi et al., 2016). For instance, methods like wavelet transform, singular value decomposition, and adaptive filtering have been employed to extract features from microseismic signals and utilize them for classification using classifiers (Shu et al., 2022). Other studies concentrate on improving machine learning algorithms such as support vector machines (Foody et al., 2004), random forests, and deep learning (Y. Fu et al., 2020) to enhance the accuracy and robustness of microseismic signal classification (Shu et al., 2023).

Overall, while traditional methods like manual identification, correlation analysis, and spectral analysis have laid the foundation for microseismic signal recognition, advancements in feature extraction techniques and machine learning algorithms are continuously improving the precision and reliability of these recognition systems.

2.3.2 Statistical Methods

During the late 20th and early 21st centuries, various statistical methods were employed to construct classification models for microseismic events (Cao et al., 2009). These methods include regression analysis (Vallejos et al., 2013), discriminant analysis (Dong et al., 2016), principal component analysis (PCA) (Shang et al., 2017), and support vector machines (SVM) (Bi et al., 2019; Ding et al., 2019). As microcrack energy is released in the form of seismic waves in rocks and blasting is an artificially induced active seismic source (Holtzman et al., 2018), these two types of signals possess distinct source parameters. However, despite this distinction, parameter extraction and model selection still heavily rely on researchers' subjective experience, which can affect the accuracy of classification models. Moreover, disregarding the correlation between parameters may result in inadequate classification. Therefore, before constructing a classification model, each parameter must be thoroughly analyzed, considering its correlation with other

variables and its applicability in specific models. This process inevitably increases computational time.

When constructing classifier models, a common approach is to extract key parameters from raw waveforms or seismic sources to create event classifiers that can differentiate between different events in microseismic data. These parameters include waveform features across the time and amplitude domains. Key parameters, such as time and frequency variation parameters (Sugondo et al., 2021), spectral ratios, maximum frequency, P-wave and S-wave (Li et al., 2023) amplitude ratios, signal duration, first peak amplitude, and maximum peak arrival time, can be obtained through waveform correlation analysis. Additionally, some feature parameters can be extracted from seismic sources, such as seismic moment, seismic energy, event occurrence time, stress drop, sensor trigger counts, and corner frequency. These feature parameters aid in distinguishing different types of microseismic events and provide crucial input information for classifier models (Dong et al., 2016).

This research (Orlic et al., 2010) employed a specially designed genetic algorithm to autonomously search for an approximately optimal set of seismic waveform features and applied this method to classify natural earthquakes and anthropogenic events (blast events). The method was validated on a collection of seismic waveforms consisting of 60 local earthquake waveforms and 60 blast waveforms, achieving an accuracy rate of 85%.

2.3.3 Machine Learning Classification Methods

In addition to traditional recognition methods, machine learning classification methods have also been widely applied to the identification and classification of microseismic signals. Machine learning utilizes a data-driven approach to automatically learn and recognize different types of microseismic signals through training models. Remarkable advancements and implementations have been observed in specific domains such as image recognition, speech recognition, signal processing, and computer vision (Wei et al., 2020). Commonly used machine learning classification methods include SVM, Random Forests, k-Nearest Neighbors (KNN), decision trees, artificial neural networks (Zhang et al., 2023), CNN, and DNN (Wamriew et al., 2021). In the context of microseismic signal recognition and classification, machine learning can be categorized

into two main branches: supervised learning (Feng et al., 2022; Qu et al., 2020) and unsupervised learning (Johnson et al., 2020; R. Liu, 2021).

Next, we will delineate the evolutionary trajectory of machine learning applications within the sphere of microseismic event detection and categorization:

1. Shallow Machine Learning Methods

Early research primarily employed shallow machine learning methods such as SVM, random forests, KNN, and decision trees. These methods extract features from microseismic signals and construct classifier models to achieve the identification and classification of microseismic events.

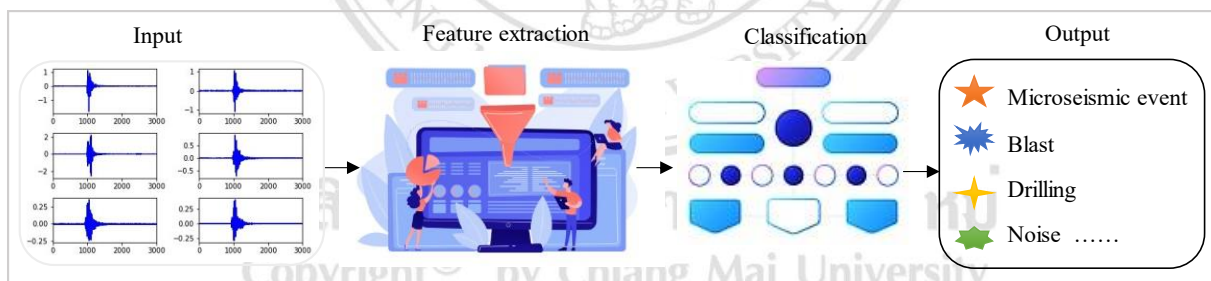
For instance, This research (Vallejos et al., 2013) used logistic regression and neural networks for the classification of seismic records, achieving accuracies exceeding 95% at their respective optimal decision thresholds. Zhao et al. (2015) conducted research to identify discriminative features for classifying mine seismic events in seismic graphs. They established a signal database based on manually identified blast and microseismic event signals. Addressing the challenge of inaccurate picking of P-wave arrivals (Chen et al., 2022; Chen, 2020; Guo et al., 2021), they proposed using the slope value of the starting trend line obtained through linear regression as a substitute for the angle. Two slope values associated with the coordinates of the first peak and the maximum peak were extracted as characteristic parameters. A statistical model, utilizing Fisher discriminant analysis, was established with an accuracy exceeding 97.1%.

This research (Dong et al., 2016) utilized random forests, support vector machines, and naive Bayes classifiers for the classification of microseismic events and blasts. The research findings showed that the random forest model not only achieved higher accuracy in automatic classification but also ranked discriminators based on computed weight values. This study (Jiang et al., 2020) introduces a novel approach that combines the improved complete ensemble empirical mode decomposition with adaptive noise (I-CEEMDAN), singular value decomposition (SVD), and the k-nearest neighbors algorithm for microseismic signal classification. The I-CEEMDAN and SVD techniques are employed to automatically extract relevant features, while the KNN algorithm is utilized for automated classification of microseismic and blasting signals.

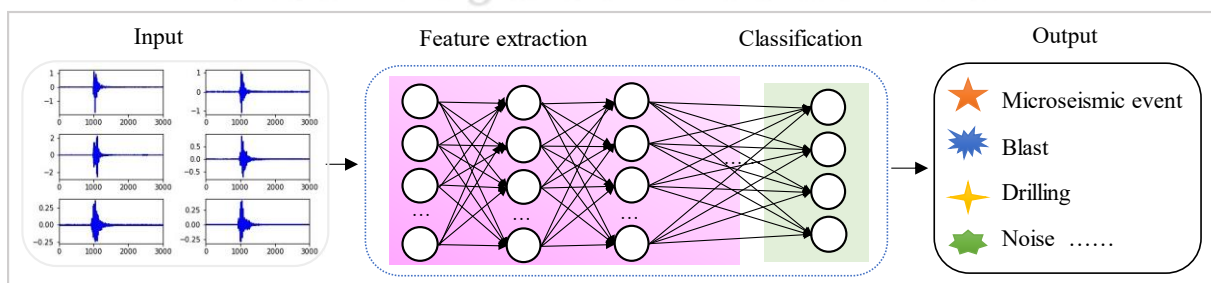
2. Deep Learning Methods

Deep learning has become a potent instrument for image recognition of microseismic event waveforms (Wang et al., 2021). The procedural diagram of image recognition, including conventional machine learning strategies and advanced deep learning algorithms is depicted in Figure 2.3. Specifically, convolutional neural networks are utilized as the deep learning model, incorporating multiple stacked convolutional layers and pooling layers to extract local and global features from waveform data. These features encompass vital information, including waveform shape, frequency, and temporal characteristics. The subsequently extracted features are then input into fully connected layers for the recognition and classification of microseismic events.

Characteristics of shallow machine learning methods include (1) the necessity for manual feature engineering, entailing the selection and design of pertinent features for the specific problem; (2) lower data requirements, making them susceptible to overfitting when working with smaller datasets; (3) quicker computation speed and relatively straightforward training processes; (4) challenges in capturing intricate nonlinear relationships when faced with limited feature expression capabilities.



(a) Traditional machine learning method



(b) Deep learning method

Figure 2.3 Image detection and classification using various machine learning models.

In comparison, deep learning methods present notable advantages in the realm of microseismic event image recognition. Primarily, they can autonomously discern intricate patterns and features from waveform data, eliminating the need for manual feature engineering. Additionally, deep learning models can systematically abstract features by extracting both low-level local characteristics and high-level global features, facilitating a more precise comprehension and representation of semantic information in microseismic event waveforms. Furthermore, deep learning leverages extensive dataset training, contributing to improved accuracy and generalization capabilities (He et al., 2022) when addressing noise and variability in microseismic event recognition tasks. However, it is important to acknowledge that deep learning methods may demand more computational resources and time due to the training process involving multiple layers of neural networks.

3. Transfer Learning Methods

Transfer learning methods have been proven effective in reducing the need for a large amount of labeled data and speeding up the training process (Ding et al., 2022; Dong et al., 2023; Wang et al., 2022). They allow us to leverage knowledge learned from rich general image datasets and apply it to the specific task of microseismic event recognition. By incorporating transfer learning techniques into our workflow, we can enhance the performance and efficiency of deep learning models in microseismic event waveform image recognition tasks.

Therefore, transfer learning methods offer a powerful solution for microseismic event waveform image recognition. By utilizing pre-trained models, performing feature extraction, and addressing domain shifts, we can enhance the performance and adaptability of deep learning models in microseismic event recognition.

2.3.4 Hybrid Optimization Methods

Hybrid optimization methods play an important role in microseismic event recognition and classification, combining different optimization techniques and algorithms to improve model performance and efficiency. For example, in this paper (Peng et al., 2020), an automatic classification method based on deep learning is proposed for identifying suspicious microseismic events in underground mines. Using a genetic algorithm-optimized correlation-based feature selection, 11 representative features are

selected from the extracted time and frequency domain features. By dividing microseismic records into frames and utilizing an 11×50 feature matrix as input, a convolutional neural network with 35 layers is trained on 20,000 samples, achieving a 98.2% accuracy in correctly determining the event type, surpassing traditional machine learning methods. GA evolves candidate solutions within a population using principles inspired by natural selection and genetic operations, gradually finding better solutions. This hybrid optimization strategy accelerates model convergence and improves optimization performance in microseismic event recognition tasks.

In another study (Rao et al., 2021), the PSO-ELM model, based on the particle swarm optimization (PSO) algorithm and extreme learning machine (ELM), was successfully applied to discriminate microseismic events and blasts in mines, demonstrating its superior performance compared to other intelligent discrimination models, thus providing a promising method for ensuring mine safety and smooth operation.

In addition, hybrid optimization approaches also integrate traditional machine learning algorithms with deep learning models (Azevedo et al., 2024). Traditional machine learning algorithms excel in feature extraction and classification tasks, while deep learning models are proficient at learning feature representations from raw data. By using traditional machine learning algorithms for feature engineering and dimensionality reduction, followed by utilizing the extracted features as input for deep learning models, the strengths of both approaches can be fully leveraged to enhance microseismic event recognition performance and efficiency.

For instance, a study (Li et al., 2021) proposed an interpretable deep learning model that utilizes three-dimensional attention maps and high-resolution spectral analysis to improve the accuracy and efficiency of seismic phase analysis, as well as reveal subtle relationships between geology and seismic spectra. The experimental results demonstrate that this trainable deep dilated convolutional neural network (ADDCNN), based on soft attention mechanisms, achieves improvements in classification accuracy, computational efficiency, and optimization performance while reducing model complexity.

In conclusion, the application of hybrid optimization methods holds significant importance in microseismic event recognition and classification. By combining

techniques such as Genetic Algorithms, gradient optimization, metaheuristic algorithms, and traditional machine learning algorithms with deep learning models, we can further improve the performance and generalization ability of models, addressing the challenges in microseismic event analysis. The development of these hybrid optimization methods continues to drive progress in the field, providing effective solutions for more accurate and reliable microseismic event recognition.

2.4 Summary

The development of microseismic signal identification and classification methods highlights three notable trends: (1) the integration of machine learning methods, (2) the emergence of deep learning models, and (3) the amalgamation of hybrid models and algorithm optimization. Each developmental stage has distinct characteristics.

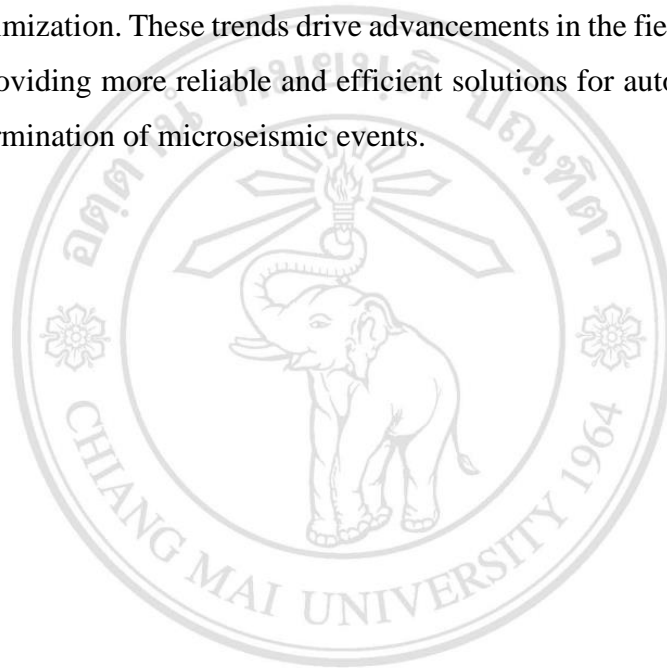
Firstly, the introduction of machine learning methods significantly alleviates the burden of traditional manual identification and classification of microseismic signals, thereby improving signal processing efficiency. By utilizing machine learning algorithms for tasks such as feature extraction, classification, and clustering, the analysis of a large volume of microseismic data can be automated, reducing human intervention and enhancing speed and accuracy. This trend makes microseismic event monitoring and analysis more feasible and efficient.

Secondly, with the advent of deep learning models, it becomes feasible to cultivate more accurate classification models by leveraging extensive collected data, significantly improving the accuracy and reliability of microseismic signal identification and classification. Deep learning models possess strong learning and representation capabilities, enabling them to automatically learn complex feature representations and train high-performance models on large-scale datasets. Through deep learning models, key features in microseismic signals can be better captured, leading to more precise identification and classification.

Lastly, the optimization of models and algorithms aims to achieve higher computational efficiency while maintaining high accuracy or shifting the focus towards improving model generalization and robustness. By employing hybrid models and algorithm optimization techniques such as genetic algorithms, metaheuristic algorithms, and ensemble learning, the strengths of different approaches are combined to enhance the

performance and efficiency of microseismic event identification and classification tasks. Furthermore, parameter tuning and algorithm optimization play a crucial role in improving system performance. These optimization methods aim to improve computational efficiency, reduce computational costs, and enable models to adapt to various data and scenarios.

In conclusion, the development of microseismic signal identification and classification methods exhibits three important trends: the integration of machine learning methods, the emergence of deep learning models, and the amalgamation of hybrid models and algorithm optimization. These trends drive advancements in the field of microseismic event analysis, providing more reliable and efficient solutions for automated processing and accurate determination of microseismic events.



ลิขสิทธิ์มหาวิทยาลัยเชียงใหม่
Copyright© by Chiang Mai University
All rights reserved

CHAPTER 3

DATA AND METHODOLOGY

3.1 Introduction

This study aims to achieve rapid and accurate identification and classification of microseismic signals in the mining environment. The research encompasses computer vision techniques and machine learning algorithms, primarily utilizing data from metal mines. Initially, microseismic signals are transformed into event waveform images. Utilizing computer vision techniques such as image processing, recognition, and classification, databases of different event waveform images are established. Subsequently, machine learning algorithms, including SML, CNN, and DNN, are employed. These algorithms are trained using sample databases from different mining areas to obtain the optimal model, thereby improving the accuracy and timeliness of microseismic signal identification and classification.

To ensure the reliability and effectiveness of the research, extensive testing will be conducted using a large dataset of real microseismic signal data. A comprehensive evaluation of the model's performance will be carried out by comparing it with existing research methods and image classification models. Performance metrics such as accuracy, recognition duration, precision, recall, and F1 score will be used to select the best-performing model. The ultimate goal is to provide more reliable and intelligent technical support for microseismic monitoring (Chen et al., 2022) and mining safety research, promoting the intelligent transformation and safe development of mining operations.

This chapter provides a comprehensive overview of the experimental dataset, methodology, and the foundational principles guiding the research. It begins with an introduction to the data collection environment, equipment used, waveform characteristics of microseismic monitoring events, and the data preprocessing process.

Subsequently, it details the commonly used machine learning methods and their principles, as well as the specific models employed in this study. Finally, the chapter concludes with an overview of the metrics used to evaluate the models.

3.2 Data

3.2.1 Data Collection

The datasets used in this study were collected from three different mines located in Baoji City, Shaanxi Province, China (as shown in Figure 3.1). These mines, namely A, B, and C, are situated in different villages within Feng County. Mine A is located in Pingkan Town, with geographical coordinates ranging from $106^{\circ}55'$ to $106^{\circ}58'$ east longitude and $33^{\circ}54'$ to $33^{\circ}57'$ north latitude. The mining area stretches from Yanjiaping in the west to Hetougou in the east, and from Yindonggounao in the north to Sihao Gounao in the south, covering an area of 16 square kilometers. It is a large-scale ductile shear-type gold deposit. Mine B is situated in Yinmusi Village, Pingkan Town, and is a lead-zinc mine. Mine C, located in Liufengguan Village, Liufengguan Town, is also a lead-zinc mine with a mining area of 0.95 square kilometers. The environmental disparities among these mines inevitably introduce variations in the characteristics of the collected microseismic monitoring data.

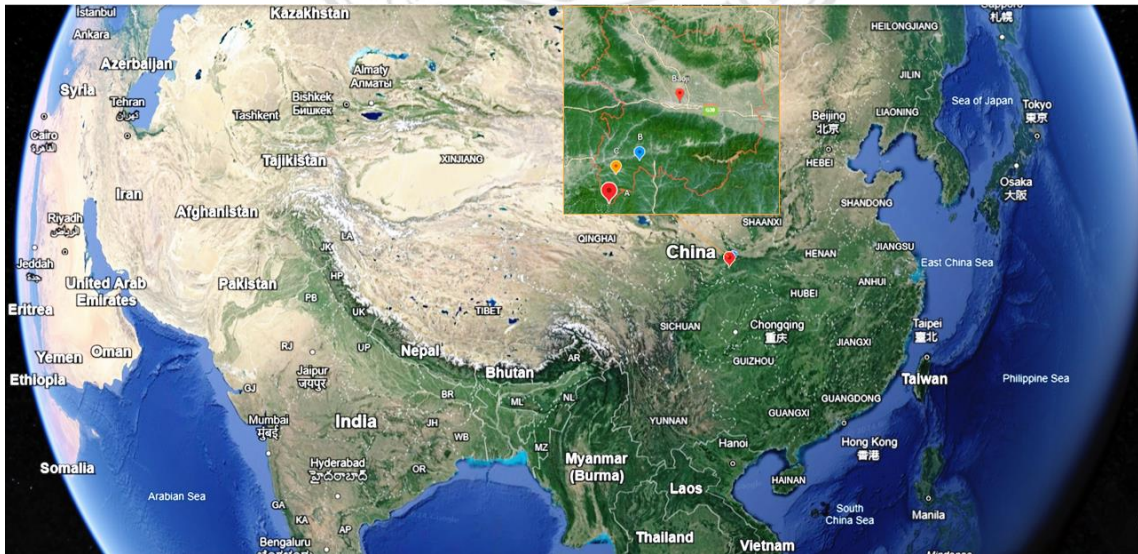


Figure 3.1 Geographical locations of the microseismic monitoring data sources.

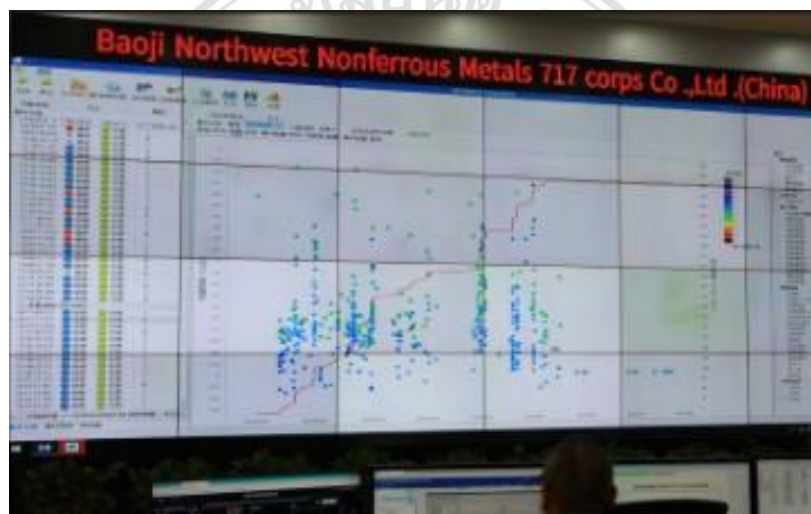
The data collection process involved the use of specialized equipment and software systems for microseismic monitoring. In terms of hardware, signal detectors (sensors) and data acquisition devices (base stations) were strategically deployed in key areas within each mine to capture microseismic signals generated during mining operations. These sensors were responsible for the real-time recording of microseismic events, with the captured signals transmitted to the base stations. The base stations, in turn, received and transmitted the signals to the central monitoring system. Taking Mine A as an example, based on the safety monitoring requirements of the mine, a total of 26 sensors were installed at different depths in five working sections. These sensors are connected to seven sub-collection systems and ultimately linked to the central processing system via optical fibers. The sampling frequency range for each sensor is from 50 Hz to 8000 Hz.

In addition to the hardware equipment, dedicated software systems were utilized for microseismic monitoring. Figure 3.2 displays the software and hardware infrastructure of the microseismic monitoring system used in the mines.



(a) Sensors

(b) Data acquisition base stations



(c) Software module

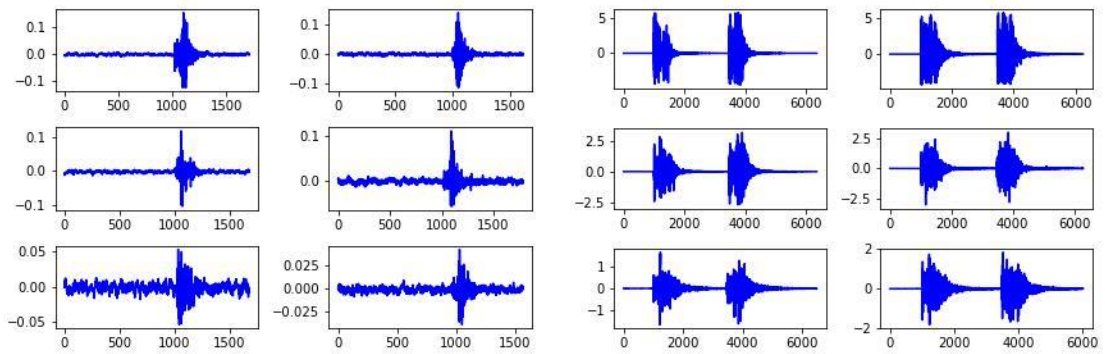
Figure 3.2 Software and hardware infrastructure of the microseismic monitoring system at Central South University.

These software systems enabled real-time acquisition, processing, and analysis of microseismic signals. They provided a comprehensive suite of tools and functionalities for visualizing and interpreting the collected data. Overall, the datasets used in this study were obtained through the integrated application of advanced hardware infrastructure and software systems. This ensured the reliability and usability of the dataset for further analysis and model development.

3.2.2 Data Preprocessing

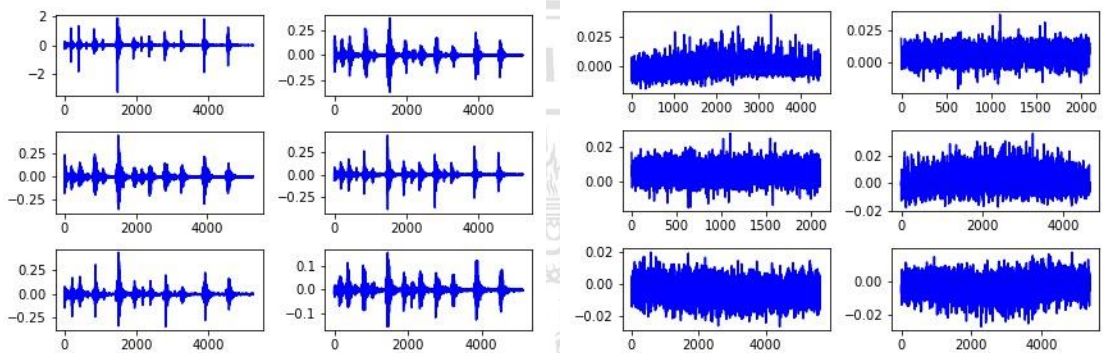
Previous studies have shown that if fewer than four sensors are triggered during event detection, there will be insufficient known parameters to accurately calculate the location of the microseismic source and other key information (Dong et al., 2011). As more sensors simultaneously detect the signal, the reliability of the microseismic events also increases when evaluating their validity. To ensure the complete validity of events, we chose events captured by at least six sensors. Therefore, during data preprocessing, we set a criterion: only when a microseismic event detected by at least six sensors is triggered, it is considered a valid event. Otherwise, the signal will be filtered out. Considering the high accuracy of image classification and the widespread application of computer vision techniques, this study uses event waveforms as inputs for classification and recognition. We input the images on an event-by-event basis, with each image containing six waveforms to differentiate individual valid events. We demonstrate the waveform data sorted by signal capture and ultimately generate the output of six-subplot event waveforms.

We use the Python plotting library (Matplotlib) to plot event waveforms from the data collected by the sensors. Based on waveform characteristics and engineering expertise, microseismic and blasting events constitute the most critical part of the raw dataset. Furthermore, noise events comprise a significant portion of the recorded data, with rock-cutting events being particularly frequent. By "converting noise into use," we combine the waveform plots of the raw dataset with engineering experience to create three databases, A, B, and C, consisting of four different categories of events: microseismic events, blasting events, rock drilling events, and noise events. Each event is treated as a separate unit. Figure 3.3 displays the typical results of these four types of event waveforms. In each subplot of the figure, the horizontal axis represents Time (ms) and the vertical axis represents Amplitude (V). These events exhibit unique waveform characteristics.



(a) Microseismic event waveforms

(b) Blast event waveforms



(c) Drilling event waveforms

(d) Noise event waveforms

Figure 3.3 Examples of 6-channel waveform images for four-type microseismic monitoring events.

- Microseismic events appear as a single continuous waveform with low amplitude, low frequency, short duration, and rapid attenuation, as shown in Figure 3.3(a).
- Blasting waveforms vary depending on the time interval between explosions and feature recurring peaks. They are typically characterized by high amplitude, high-frequency signals with long duration and significant signal variations. Blast signals usually evolve from a rapid initial decay without a developed tail wave to a slow, developed tail wave, as shown in Figure 3.3(b).
- Drilling event waveforms exhibit repetitive periodic vibrations, reflecting the operating impact frequency of drilling equipment, as shown in Figure 3.3(c).
- Noise events, due to their numerous and diverse sources, result in different waveforms: (1) chute release signals, recording small-amplitude oscillations within the main amplitude, usually detected by sensors close to the chute; (2) scraper operations,

continuous waveform events lasting two to three seconds; (3) fan vibrations, typically characterized by unordered continuous waveforms, detectable by sensors near the fan; (4) power disturbance signals, typically represented as continuous waveforms with large amplitudes, short rise times, simple oscillation patterns, and no attenuation characteristics, as shown in Figure 3.3(d). These signals are mainly received by sensors located close to the power source.

After obtaining the event waveform sample databases for each mine, we divide the samples into training sets (80%) and testing sets (20%) in a 4:1 ratio to ensure consistency between the training and testing samples for each model (Brownlee, 2016). The training set is used to train the machine learning models, while the testing set is used to evaluate the performance of the trained models on unseen data. Table 3.1 provides detailed information about the A, B, and C mine datasets used in this study.

Firstly, each dataset comes from a different mining area, so there will be some differences in geological characteristics and data features. This effectively tests the model's generalization and robustness. Secondly, datasets A and C have relatively long-time spans, covering nearly two years of data, while dataset B has a shorter time span of about five months. Lastly, the sample sizes of datasets A and B are similar, while dataset C has the largest sample size, significantly more than datasets A and B, with dataset C being approximately 2.6 times the size of dataset A.

Table 3.1 Microseismic monitoring event waveforms datasets from three mines

Mine	Date time	Dataset	Four categories			
			MS	Blast	Drilling	Noise
A	25/4/2022-8/12/2023	6422	2176	1826	1040	1380
B	28/6/2023-24/11/2023	6540	2000	348	2062	2130
C	29/4/2022-14/12/2023	16668	6446	2832	3260	4130
Total		29630	10622	5006	6362	7640

The purpose of splitting the data into training and testing sets is to avoid overfitting issues. If we evaluate the model using all the data during training, the model may overly memorize the features and noise present in the training set, resulting in poor performance

on unseen data. By dividing the data into training and testing sets, we can objectively evaluate the model's performance and validate its ability to generalize to unknown data.

In addition, cross-validation techniques can be used during model selection and parameter tuning to further optimize model performance (Schumacher et al., 1997). Cross-validation involves dividing the training set into multiple subsets and using one subset as a validation set to assess the model's performance. This allows for a more comprehensive evaluation of the model's performance and stability. Through cross-validation, we gain a better understanding of how the model performs on different subsets and can select the best model parameters and configurations.

3.3 Methods

Through the collection and processing of real microseismic signals, combined with manual expertise, image processing, and techniques for identification and classification, the aim is to improve the accuracy and efficiency of microseismic signal classification. To achieve this research goal, the study follows a seven-step approach: data preparation, construction of microseismic event waveform image databases, selection of machine learning algorithms, parameter optimization, model training, model evaluation, and model application. The specific explanations for each step are as follows:

1. Data Preparation: Before identifying and classifying microseismic signals, a large amount of real microseismic signal data needs to be collected from field sources. Subsequently, programming languages like Python are utilized to perform image processing on the collected microseismic signals, converting them into waveform images, and applying computer vision techniques (Zhang et al., 2024).

2. Construction of Microseismic Event Waveform Image Database: Based on engineering experience and expert recognition and classification, manual identification and labeling of microseismic event waveform images obtained from mining sites are conducted to establish a database comprising four categories: microseismic events, explosion events, rock-cutting events, and noise events.

3. Method Selection: This study employs machine learning algorithms suitable for image classification, such as support vector machines (Campbell et al., 2022), convolutional neural networks, and deep neural networks (Cao et al., 2022), to train the

classification model, thereby improving the recognition efficiency and classification accuracy of microseismic events.

4. **Parameter Optimization:** Model parameters are updated through algorithm optimization to enhance the performance of training data. This often involves selecting appropriate loss functions and optimization algorithms to minimize prediction errors (Fu et al., 2024).

5. **Model Training:** The selected model is trained using the training data, with continuous adjustment of model parameters to minimize the loss function.

6. **Model Evaluation:** Comprehensive evaluation and analysis are conducted to ensure the effectiveness of the proposed machine learning model (Rainio et al., 2024). A comparison with existing methods is performed to determine its advantages, limitations, and applicability.

7. **Model Application:** Finally, the trained model is applied to the identification and classification of newly generated microseismic signals to validate its practicality and reliability.

Through this process, this study achieves automatic recognition and classification of microseismic events, providing reliable and intelligent technological support for microseismic monitoring and mining safety.

3.3.1 HOG-SML Method

Based on existing research and literature review, Shallow Machine Learning (SML) algorithms exhibit various advantages in microseismic signal classification (Möller, 2023). Firstly, compared to complex models such as deep neural networks, shallow machine learning algorithms have lower computational complexity and resource requirements. This enables them to perform rapid inference and classification in real-time applications, such as real-time event recognition in microseismic monitoring systems. Secondly, the model structure of shallow machine learning algorithms is relatively simple, making their decision processes easy to understand and explain. This facilitates a better understanding of the model's predictions by researchers and domain experts, providing valuable insights for interpreting and analyzing microseismic signals. Additionally, despite not having the same complex representation capabilities as deep neural networks,

shallow machine learning algorithms demonstrate good performance in small sample situations, showing good generalization ability. Even with limited training data, they can still learn effective patterns.

Moreover, shallow machine learning algorithms typically have only a few adjustable hyperparameters, making their adjustment and optimization relatively simple. Through appropriate parameter selection and optimization strategies, their performance in microseismic signal classification tasks can be further improved. In summary, these advantages make shallow machine learning algorithms crucial tools in the field of microseismic monitoring and mining safety, providing reliable and efficient technical support. Therefore, to construct a model with high accuracy and fast recognition efficiency, we employed the combination of HOG (Histogram of Oriented Gradients) (Dalal et al., 2005) feature extraction algorithm and shallow machine learning algorithms to develop a recognition and classification model based on microseismic waveform images.

Regarding the choice of feature extraction algorithm, we selected the HOG algorithm to perform feature extraction on microseismic waveform images. This decision was based on several reasons. Firstly, the HOG algorithm (Cheng et al., 2023) is capable of effectively describing local texture and shape features in images, particularly suitable for images with distinct edges and textures. Secondly, HOG features are insensitive to changes in lighting conditions and colors, maintaining a certain level of stability. Additionally, the HOG algorithm has fast computational speed, making it suitable for applications with high real-time requirements. Considering the advantages of the HOG algorithm in feature description, stability, and computational speed (Chapelle et al., 1999), we chose it as the method for extracting features from microseismic waveform images.

In terms of selecting shallow machine learning algorithms, we utilized SVM due to its superior overall performance (Ji et al., 2020). Furthermore, for comparison purposes, we also included four other classification algorithms, namely linear classifiers, decision trees, KNN, and Fisher discriminant. By comparing these algorithms, we can comprehensively evaluate their effectiveness and performance in microseismic signal classification.

Figure 3.4 illustrates the architecture of the microseismic monitoring event waveform recognition and classification model that utilizes the HOG-SML method. This model consists of two key components: HOG feature extraction and shallow machine learning classifiers. The subsequent sections will provide a detailed explanation of the principles, methodologies, and fundamental computational formulas employed in these components.

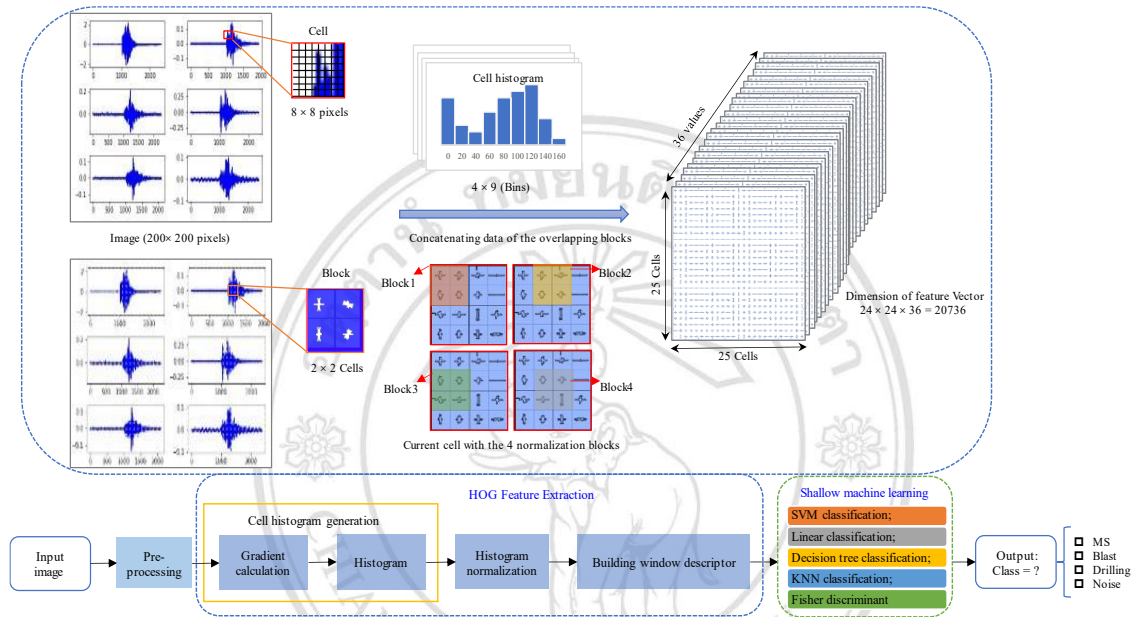


Figure 3.4 The architecture of the microseismic monitoring event waveform recognition and classification model using the HOG-SML method.

1. HOG feature extraction

The principle of Histogram of Oriented Gradients (HOG) feature extraction is based on the gradient distribution of local textures and shapes in an image. By calculating the gradient values and directions of each pixel, it becomes possible to capture texture and edge information from different regions of the image.

In the process of HOG feature extraction, the original image (432×288 pixels) is first resized to 200×200 pixels. Then, the image is divided into small cells of size 8×8 , forming a grid of 25×25 cells. Each cell contains 128 values representing gradient and angle information, organized into a 9-length array called the gradient histogram. The 9 values in the histogram correspond to angles $0, 20, 40, 60 \dots 160$, collectively forming 9 bins in each histogram.

Next, for each cell, the gradient magnitude (G) and gradient direction (θ) are calculated based on the horizontal and vertical gradient values (G_x , G_y) of each pixel, using Equations (3.1) and (3.2). The image is then further divided into smaller local blocks, with each block consisting of 2×2 cells, resulting in a total of 36 values per block. Within each local block, the gradient histograms are computed and normalized. In the entire image, there are 24 positions horizontally and 24 positions vertically, giving a total of $24 \times 24 = 576$ blocks.

$$G = \sqrt{G_x^2 + G_y^2} \quad (3.1)$$

$$\theta = \arctan \left(\frac{G_y}{G_x} \right) \quad (3.2)$$

Finally, the gradient histograms obtained from all local blocks are concatenated to form the final feature vector representation. Therefore, all the feature vectors from these blocks are merged into a one-dimensional vector with a size of 20736.

The HOG feature extraction method, which is based on gradient computation, is widely used in the field of image processing due to its excellent performance and stability. In this study, we employed the HOG algorithm to extract features from the six-channel waveform graphs of microseismic monitoring events. Following the aforementioned steps, we obtained a suitable feature representation for subsequent classification models.

2. SVM classifier

Support Vector Machine (SVM) is a widely used machine learning algorithm for pattern recognition and classification tasks (Cervantes et al., 2020). In this study, we employed an SVM classifier to categorize feature vectors extracted by HOG. The principle of the SVM classifier is based on finding an optimal hyperplane to effectively separate data samples from different categories. For four-class event classification, a multi-class problem is addressed, where each category represents a specific event type. SVM handles multi-class problems by constructing multiple binary classifiers, commonly using strategies such as “one-vs-all” and “one-vs-one” (Krawczyk et al., 2015).

- “One-vs-all” strategy: Construct a binary classifier for each category, labeling samples from the i -th class as positive ($y = 1$) and all other classes as negative

($y = -1$). For four-class events, we obtain four binary classifiers, each corresponding to one event category.

•“One-vs-one” strategy: Construct a binary classifier for each pair of category combinations. For example, with four categories, six binary classifiers are built (C_1 vs C_2 , C_1 vs C_3 , C_1 vs C_4 , C_2 vs C_3 , C_2 vs C_4 , C_3 vs C_4). The final category is determined through voting or other ensemble methods.

During the training phase, SVM learns how to partition samples from different categories using labeled training data. In the testing phase, inputting a sample for classification, SVM predicts and assigns it to the most likely category based on the learned model. The following outlines the core formulas used in the SVM classification of four categories:

(1) The SVM model can be represented as Equation (3.3):

$$y = f(x) = \text{sign}(w \cdot x + b) = \text{sign}(w^T x + b) \quad (3.3)$$

where y is the label vector; $f(x)$ is the decision function used to predict the class of input sample x . w is the weight vector that represents the importance of different features in classification. x is the feature vector of the input sample. b is the bias term used to adjust the threshold of the decision function.

The decision function $f(x)$ determines which class x belongs to the result of $w^T x + b$. If $w^T x + b > 0$, x is predicted as a positive class; if it is less than zero, x is predicted as a negative class (Equation (3.4)):

$$\begin{cases} w^T x + b > 0, & y = 1 \\ w^T x + b \leq 0, & y = -1 \end{cases} \quad (3.4)$$

(2) SVM optimization problem: The training process of the SVM model involves finding the optimal weight vector w and bias term b , in order to minimize the classification error on the training samples and separate samples from different classes. To maximize the margin between classes, it is required to satisfy the following Equation (3.5):

$$\begin{aligned}
\min w(b) &= \frac{1}{2} \|w\|^2 + C \sum (1, n) \delta_i \\
s. t. y^{(i)}(w^T x^{(i)} + b) &\geq 1 - \delta_i \\
\delta_i &\geq 0, i = 1, \dots, n
\end{aligned} \tag{3.5}$$

where C is the regularization parameter that balances the size of the margin and the penalty for misclassification. δ_i is a slack variable that allows some data points to be on the wrong side of the margin. $x^{(i)}$ is the feature vector of the training sample, and $y^{(i)}$ is the label of the training sample, taking values of 1 or -1, representing positive class and negative class, respectively.

(3) Testing phase: For a new sample x to be classified, input it into the trained binary classifiers, and calculate its distance to each hyperplane. The distance formula is given by Equation (3.6):

$$distance = \frac{|w^T x + b|}{\|w\|} \tag{3.6}$$

For the “one-vs-all” strategy, assign the sample to the category with the maximum distance as the prediction. In other words, select the category represented by the hyperplane with the farthest distance as the final classification result. For the “one-vs-one” strategy, use voting or other ensemble methods to determine the final category. Each binary classifier outputs a category result, and the final classification label is determined based on these results. In this study, we choose “one-vs-one” strategy.

3. Linear classifier

Secondly, we employed the linear classifier to categorize feature vectors extracted by HOG. The principle of a linear classifier for four-class classification is based on defining a decision boundary in the feature space using a linear equation. The general form of a linear classifier is given by Equation (3.7):

$$f(x) = w^T x + b \tag{3.7}$$

where x is the feature vector of the input sample. b is the bias term used to adjust the threshold of the decision function. w is the weight vector that represents the importance

of different features in classification. $f(x)$ is the decision function used to predict the class of input sample x .

When the output of the decision function $f(x)$ is greater than zero, the sample is classified into the positive class; when it's less than zero, the sample is classified into the negative class. For four-class classification, different thresholds can be set to determine the specific class for a given sample (Equation (3.8)):

$$y = \begin{cases} 1, & \text{if } \omega^T x + b > 0 \\ -1, & \text{otherwise} \end{cases} \quad (3.8)$$

4. Fisher Discriminant

Fisher Discriminant analysis is typically designed for binary classification problems. However, it can be extended for multiclass classification, including cases with four classes (Rozza et al., 2012). Here is a simplified formulation for a Fisher Discriminant classifier with four classes:

(1) Calculate the mean vectors m_i for each class (for four classes, there are m_1, m_2, m_3, m_4).

(2) Compute the within-class scatter matrix S_W and the between-class scatter matrix S_B . The formula is given by Equation (3.9):

$$\begin{cases} S_W = \sum_{i=1}^4 \sum_{x \in C_i} (x - m_i)(x - m_i)^T \\ S_B = \sum_{i=1}^4 n_i (m_i - m)(m_i - m)^T \end{cases} \quad (3.9)$$

where n_i is the number of samples in class C_i , and m is the overall mean vector.

(3) Solve the generalized eigenvalue problem $S_W^{-1} S_B$ to obtain eigenvalues and corresponding eigenvectors.

(4) Select the top $c - 1$ eigenvectors with the largest eigenvalues, where c is the number of classes, to form a projection matrix W .

(5) Fisher discriminant classifier aims to find a projection direction to maximize the separation between different categories in the projected space. Specifically,

it determines the optimal projection direction by computing the ratio of between-class scatter and within-class scatter, as expressed in Equation (3.10):

$$J(\omega) = \frac{\omega^T \cdot S_B \cdot \omega}{\omega^T \cdot S_W \cdot \omega} \quad (3.10)$$

where ω is the projection direction, S_B is the between-class scatter matrix, and S_W is the within-class scatter matrix. Solving this optimization problem yields the optimal projection direction ω . Classify based on the projected values, typically using thresholds or other rules.

5. Decision tree

The decision tree is a classification algorithm based on a tree-like structure that classifies samples by continuously partitioning the feature space. Each node in a decision tree represents a feature test, and samples are allocated to different branches based on the values of that feature. By recursively constructing the decision tree, accurate classification of samples can be achieved (Chen et al., 2020). The classification process of the decision tree is based on a series of feature tests and partitioning rules. For each node, the optimal feature is selected for testing, and samples are allocated to different branches based on the values of that feature.

When constructing a decision tree model, the core computational formulas involved primarily include entropy, information gain, and the Gini index. Below is a detailed explanation of these mathematical formulas.

(1) Entropy

Entropy is used to measure the impurity of a dataset, defined as Equation (3.11):

$$H(D) = - \sum_{i=1}^m p_i \log_2 p_i \quad (3.11)$$

where $H(D)$ is the entropy of dataset D , m is the number of classes, and p_i is the probability of class i .

(2) Information Gain

Information gain is used to select the optimal splitting feature, defined as Equation (3.12):

$$IG(D, A) = H(D) - \sum_{v \in \text{values}(A)} \frac{|D_v|}{|D|} H(D_v) \quad (3.12)$$

where $IG(D, A)$ is the information gain of feature A for dataset D , and D_v is the subset of D where feature A has value v .

(3) Gini Index

The Gini index is used to measure the impurity of a dataset, defined as Equation (3.13):

$$Gini(D) = 1 - \sum_{i=1}^m p_i^2 \quad (3.13)$$

where $Gini(D)$ is the Gini index of dataset D , m is the number of classes, and p_i is the probability of class i .

For the Gini index of feature A , it is defined as Equation (3.14):

$$Gini(D, A) = \sum_{v \in \text{values}(A)} \frac{|D_v|}{|D|} Gini(D_v) \quad (3.14)$$

(4) Selecting Features using Information Gain

When using information gain to select the optimal splitting feature, the feature with the highest information gain is chosen (Equation (3.15)):

$$A^* = \arg \max_A IG(D, A) \quad (3.15)$$

(5) Selecting Features using the Gini Index

When using the Gini index to select the optimal splitting feature, the feature with the lowest Gini index is chosen (Equation (3.16)):

$$A^* = \arg \min_A Gini(D, A) \quad (3.16)$$

The process of constructing a decision tree is a recursive partitioning process. Using the above core computational formulas, the optimal splitting feature is selected, and the dataset is recursively divided into subsets until the stopping criteria are met.

6. KNN classifier

The k-nearest neighbors algorithm determines the category of a sample by comparing its distance to samples in the training set (Chugh et al., 2020). Specifically, in KNN, we first select a distance metric (such as Euclidean distance), then sort the samples in the training set based on distance from smallest to largest. Finally, we choose the k nearest neighbors and determine the category of the sample based on the categories of these neighbors.

In the task of intelligent recognition and classification of microseismic event waveforms, the choice of classifiers such as SVM, linear classifier, Fisher discriminant, decision tree, and KNN is due to their distinct characteristics and advantages that cater to different classification needs. The characteristics and advantages of each model are summarized in Table 3.2 below.

Table 3.2 Characteristics and advantages of the five classifiers

Model	Characteristics	Advantages
SVM	Finds the optimal hyperplane to separate data by maximizing the margin between classes. Can handle data in high-dimensional spaces, suitable for complex classification problems.	Can address non-linearly separable cases using kernel functions. Effectively prevents overfitting, especially in high-dimensional spaces. Performs well with small sample sizes.
Linear Classifier	Assumes data is linearly separable and uses linear equations to classify data into different categories.	Low computational complexity, with fast training and prediction speeds. Suitable for datasets with a clear linear relationship between features and classes. High interpretability and easy to understand and implement.
Fisher Discriminant	Based on Linear Discriminant Analysis (LDA), it classifies by maximizing the ratio of between-class variance to within-class variance.	Performs well when the distribution of sample classes is Gaussian. Can reduce dimensionality while retaining maximum classification information, improving accuracy. Suitable for multi-class classification problems.
Decision Tree	Recursively selects the best features to split data, forming a tree structure.	Intuitive and easy to interpret, with clear visualization of classification decisions. Can handle categorical and numerical features. Does not require data normalization.

Table 3.2 Characteristics and advantages of the five classifiers (continued)

Model	Characteristics	Advantages
KNN	Instance-based learning method that classifies by calculating the distance between the sample to be classified and the training samples.	Simple implementation with no training process, classification is done by calculating distances. Performs well on complex decision boundaries. Classification performance improves as training data increases.

The classifiers were chosen for their unique strengths, which cater to different needs in the intelligent recognition and classification of microseismic event waveforms. SVM and Fisher discriminant classifiers are suitable for handling high-dimensional and multiclass problems, while linear classifiers are computationally efficient. Decision trees are easy to interpret and can handle nonlinear relationships, and KNN performs well in complex boundary situations. Comparing these classifiers provides a comprehensive classification approach, ensuring good performance across various data characteristics and classification requirements.

3.3.2 CNN Method

Convolutional neural networks (CNNs) are an important form of deep learning, known for their powerful feature extraction capabilities and effectiveness in handling complex data such as images and audio. In this study, a CNN-based image classification model is adopted. Figure 3.5 shows the architecture of CNN. It includes an input layer, an output layer, and several hidden layers. The hidden layers are comprised of convolutional layers, pooling layers, ReLU (Rectified Linear Unit) layers, and fully connected layers. The model leverages components such as convolutional layers, pooling layers, and fully connected layers to extract features and make predictions. The optimization objective is achieved by using the cross-entropy loss function (Zhang et al., 2018).

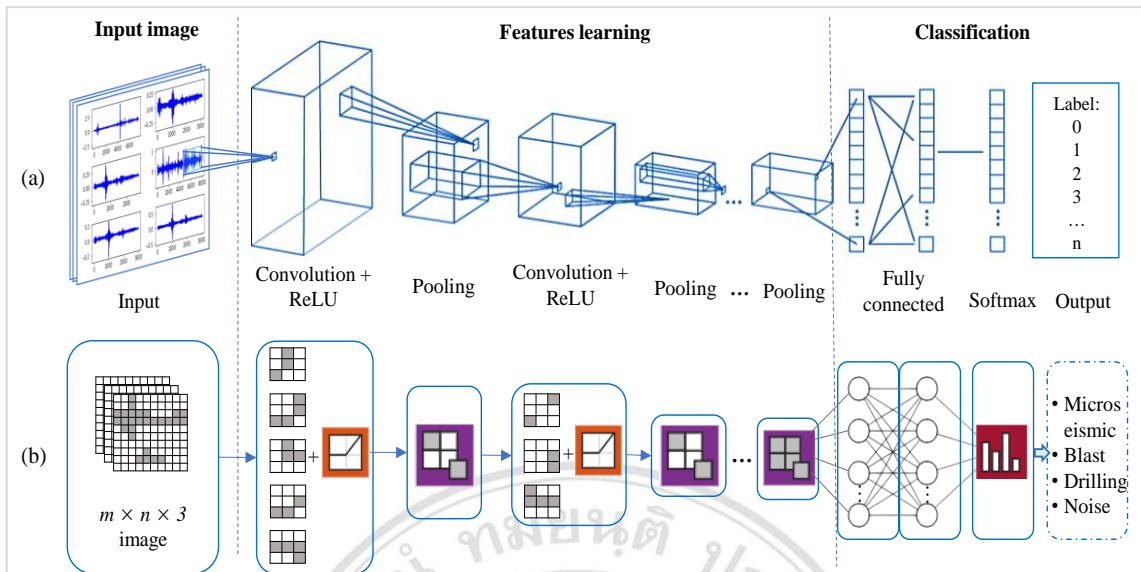


Figure 3.5 CNN image classification architectures. (a) General architecture for CNN.

(b) Architecture CNN-based for microseismic event waveform images.

CNN is a type of deep learning model specifically designed for processing image data. The training process typically includes the following major steps:

1) Data Preparation:

- Data Collection: Gather a large amount of annotated image data. The dataset is usually divided into training, validation, and test sets.
- Data Preprocessing: Normalize the images and apply data augmentation techniques (such as rotation, cropping, flipping, etc.) to enhance the model's generalization ability.

2) Model Construction:

- Convolutional Layers: Extract spatial features from the images. Through convolution operations (using filters/kernels), extract features from edges and textures to more complex features in a hierarchical manner.
- Pooling Layers: Reduce the size of the feature maps, retain the main features, decrease computational complexity, and prevent overfitting. Common pooling operations include Max Pooling and Average Pooling.

- Fully Connected Layers: Flatten the extracted features and pass them to fully connected layers for classification tasks. The output of fully connected layers is usually the probability distribution of image categories.
- Activation Functions: Such as ReLU, introduce non-linearity to enable the model to learn complex patterns.
- Loss Functions: Such as Cross-Entropy Loss, measure the discrepancy between the model predictions and the true labels.

3) Model Training:

- Forward Propagation: The input images pass through the convolutional, pooling, and fully connected layers to produce the prediction results.
- Loss Calculation: Compute the loss value based on the prediction results and the true labels.
- Backward Propagation: Calculate the gradient of the loss with respect to each parameter using the Chain Rule.
- Parameter Updates: Adjust the model parameters according to the gradients using optimization algorithms such as Stochastic Gradient Descent (SGD) or Adam to minimize the loss function.

4) Hyperparameter Tuning:

- Adjust learning rate, batch size, kernel size, number of layers, etc., and select the best combination of hyperparameters through Cross-Validation.

5) Model Evaluation:

- Evaluate model performance using the validation set, and calculate metrics such as accuracy, precision, recall, and F1 score to ensure the model performs well on unseen data.

6) Model Testing:

- Test the final model performance on the test set to assess its performance in real-world scenarios.

The key points in training a CNN model are as follows:

1. Convolution Operation

The computation of the convolutional layer is a crucial component of the model. Features are extracted by applying a sliding window with filters over the image, enabling local perception. For an input feature map X and convolutional kernel weights W , the convolution operation can be represented by Equation (3.17):

$$Y = f(\text{conv}(X, W) + b) \quad (3.17)$$

where conv denotes the convolution operation and f represents the activation function. Through the convolution operation, local information in the feature map X is convolved with the convolutional kernel weights W , and the bias term b is added. The activation function f introduces nonlinearity to enhance the expressive power of the model.

2. Pooling Operation

The pooling layer is used to reduce the size of the feature map while retaining important information. The size of feature maps is reduced by taking the maximum or average value of local regions. For an input feature map X , the pooling operation can be represented by Equation (3.18):

$$Y = \text{pool}(X, k, \text{stride}) \quad (3.18)$$

where pool represents the pooling operation, k denotes the pooling kernel size, and stride represents the stride. Common pooling operations include max pooling and average pooling, which perform pooling on local regions of the input feature map to obtain the output feature map Y .

3. Activation Functions

Activation functions introduce non-linearity, allowing the neural network to learn and model more complex functions and decision boundaries. This is crucial for tasks like image recognition, where data relationships are non-linear. They enable the neural

network to learn diverse features, with different layers capturing varying levels of complexity, such as edges and textures. Additionally, activation functions facilitate the efficient flow of gradients during backpropagation, mitigating issues like vanishing or exploding gradients common in deep networks.

Common activation functions include Sigmoid, Tanh, and ReLU (Apicella et al., 2021). Among these, ReLU is the most widely used in CNNs due to its simplicity and effectiveness. The ReLU function can be represented by Equation (3.19):

$$ReLU(x) = \max(0, x) \quad (3.19)$$

The input (x) to the ReLU function is a real-valued number, which could be the output from a neuron in the previous layer of the neural network. The ReLU function applies the maximum function between 0 and the input value (x). This operation results in: If x is positive ($x \geq 0$), the output is x , while if x is negative ($x < 0$), the output is 0.

This means any negative input is set to zero, while positive inputs remain unchanged. The reasons for choosing ReLU as the activation function in this study are threefold: (1) ReLU is computationally efficient because it involves only a simple threshold operation. (2) ReLU activates only a portion of the neurons, promoting model sparsity, which improves computational efficiency and reduces the risk of overfitting. (3) ReLU helps mitigate the vanishing gradient problem, allowing gradients to flow more effectively through deeper networks.

4. Fully connected layer

The fully connected layer multiplies the feature vector X obtained from the pooling layer with the weight matrix W and adds the bias term b . The computation of the fully connected layer can be represented by the Equation (3.20):

$$Y = f(W \cdot X + b) \quad (3.20)$$

where f represents the activation function. Through the fully connected layer, the model is able to combine and abstract the extracted features for better classification predictions.

5. Loss Function and Optimization

Model parameters are gradually adjusted by calculating loss and applying backpropagation. To train the model, we utilize the cross-entropy loss function to measure the difference between the model's predicted results and the true labels. The cross-entropy loss function can be represented by the Equation (3.21):

$$L = - \sum (y \log(y_{\hat{}})) \quad (3.21)$$

where y represents the probability distribution of the true labels, and $y_{\hat{}}$ represents the probability distribution of the predicted labels. By minimizing the cross-entropy loss function, the model gradually optimizes and reduces prediction errors.

To update the model parameters, we employ the backpropagation algorithm (Yang et al., 1989) to compute the gradients of the parameters with respect to the loss function. Through the chain rule, the gradients are propagated from the output layer to the input layer, and optimization methods such as gradient descent (Yann et al., 1998) are used to update the parameters. In this way, the model is gradually optimized and its accuracy in image classification is improved.

6. Regularization

Techniques such as Dropout and L2 regularization are used to prevent overfitting. These methods improve the model's generalization ability, allowing it to perform better on unseen data.

3.3.3 Transfer Learning Method

Using transfer learning techniques, we employ three well-known DNN models (MobileNet-V2, Inception-V3, and ResNet-18) to accurately classify microseismic event images. Due to differences in network structures with sequential and residual connections, as well as variations in depth and convolutional kernel sizes in sequential architectures, neural networks exhibit variations in waveform recognition for different types of events. Building upon these classic models, we explore deep learning models with expert-designed and mature architectures. Furthermore, fine-tuning pre-trained networks through transfer learning is faster and easier compared to training from scratch. The transferred DNN models require less data and computational resources.

Despite the diverse landscape of transfer learning architectures and applications, the majority follow a standardized workflow. Figure 3.6 outlines the transfer learning workflow for image classification. (1) Pre-trained model selection: Taking the pre-trained Inception-V3 model as an example, a widely adopted 48-layer deep network trained for classifying a dataset containing 1000 object categories. (2) Replacement of final layers: To adapt the network for new image sets and categories, the last learnable layer and classification layer of Inception-V3 are replaced. The final fully connected layer is adjusted to match the new category count (e.g., 4 in this study), and the new classification layer generates output based on softmax-calculated probabilities. (3) Post-layer modification, the final fully connected layer determines the network's new category count, while the classification layer defines output in the new categories of interest (e.g., four categories). (4) Optional weight freezing: By setting the learning rate of earlier layers to zero, weights in these layers are selectively frozen, significantly expediting training. Weight freezing can prevent overfitting to small new datasets. (5) Model retraining: Retraining updates the network to recognize features relevant to new images and categories, typically requiring less data compared to training from scratch. (6) Prediction and accuracy evaluation: Post-retraining, the model classifies new images, and network performance is assessed.

The calculation formulas of the transfer learning image classification model mainly involve the feature extraction part and the fully connected layer. By using a pre-trained model for feature extraction and performing classification prediction on a custom fully connected layer, an effective transfer learning model can be built to utilize the knowledge and features of the existing model to solve new image classification tasks.

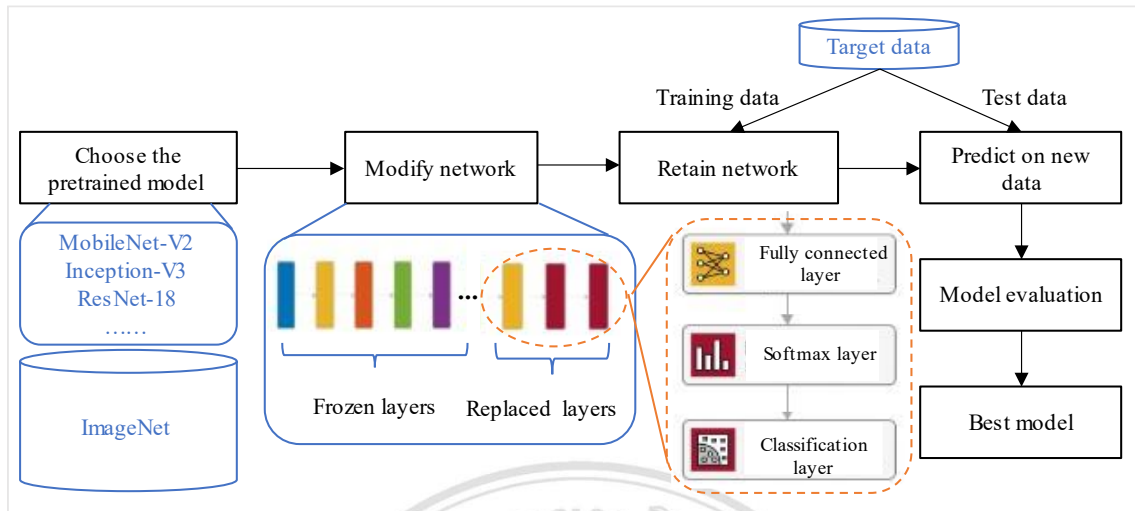


Figure 3.6 The transfer learning workflow.

1. Feature extraction in transfer learning

In transfer learning, we will use a pre-trained convolutional neural network (pre-trained model) trained on a large-scale image dataset as a feature extractor. For a given input image x , the feature vector $f(x)$ is obtained through forward propagation, which can be represented as: $f(x)=\text{CNN}(x)$.

2. Computation of the fully connected layer

In transfer learning, we can choose to add a custom fully connected layer after the pre-trained model for classification prediction. Assuming the weight matrix of the fully connected layer is W and the bias term is b , and the feature vector is $f(x)$, the classification prediction result can be calculated using Equation (3.22). The softmax function converts the output values into a probability distribution.

$$y_hat = \text{softmax}(W \cdot f(x) + b) \quad (3.22)$$

Furthermore, regarding the calculation of the loss function, as well as the backpropagation algorithm and parameter updates, they are the same as in CNN and will not be further elaborated here.

In conclusion, through the above methods, we can build intelligent recognition models for microseismic events based on the HOG-SML method, CNN, and

deep learning with transfer learning methods, enabling accurate classification and recognition of microseismic events.

3.4 MS-CNN Model

Inspired by the literature [55], we integrated existing convolutional neural network (CNN) optimization techniques to construct the MS-CNN model (Figure 3.7) for the identification and classification of microseismic events. Our goal was to achieve a balance between recognition accuracy and classification efficiency, highlighting the advantages of this model. Compared to the original network structure presented in [55], which comprises 4 convolutional layers, 2 pooling layers, 1 fully connected layer, and 1 dropout layer, our network structure consists of 3 convolutional layers, 2 max-pooling layers, 2 fully connected layers, and 1 dropout layer. The specific modifications include reducing the number of convolutional layers, adjusting the kernel size, introducing batch normalization layers after the convolutional and fully connected layers, and increasing the dropout rate (from 0.25 to 0.5).

The settings of our model parameters adhere to general principles of CNN design, including gradually reducing spatial dimensions, increasing the number of channels, and employing batch normalization and ReLU activation functions to enhance performance and stability. Secondly, our model starts with smaller convolutional kernels and transitions to larger ones, which helps capture features at different scales. Thirdly, the fully connected layers have a large number of parameters, necessitating a sufficient amount of training data to fully leverage these parameters and prevent overfitting. Additionally, the use of a dropout layer is a rational choice to improve the model's generalization capability.

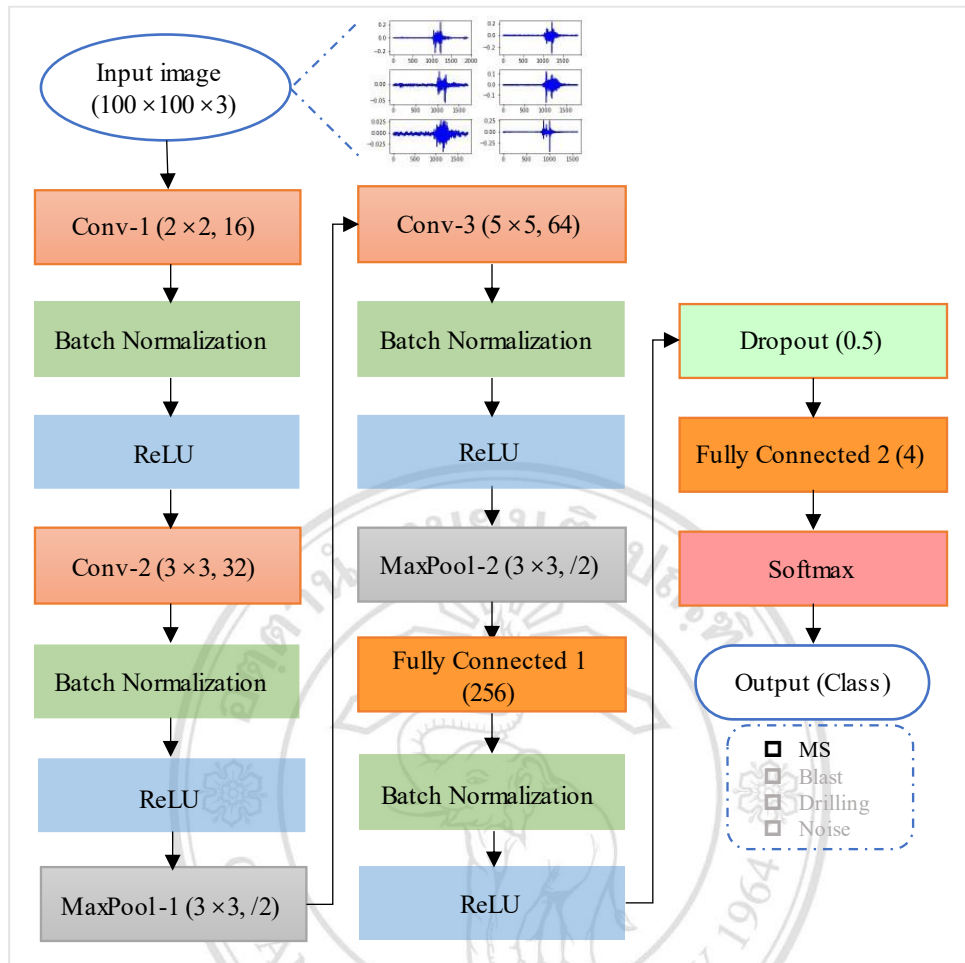


Figure 3.7 Model for microseismic event waveform recognition and classification based on convolutional neural networks (MS-CNN).

We trained and tested the original and modified MS-CNN models on the same dataset. The final experimental results indicate that the MS-CNN model can achieve a higher classification accuracy within nearly the same amount of time, with an approximate improvement of about 5% in accuracy compared to the original model.

The convolutional layers play a pivotal role in extracting feature values from microseismic waveform images by utilizing a set of learnable convolutional kernels (or filters). These kernels slide over the input waveform images to identify local patterns and features. Each kernel is responsible for extracting a specific feature, such as particular frequency components of the waveform or the arrival times of waves. As the convolutional kernel moves across the waveform image, it computes the weighted sum of local areas, generating feature maps. These feature maps are then used as higher-level feature representations to identify different categories of microseismic events. By

stacking multiple convolutional layers, the network can progressively build more complex and abstract feature representations from simple waveform characteristics, enabling efficient classification and identification of microseismic waveform images. The process of feature extraction in the convolutional layers is illustrated in Figure 3.8.

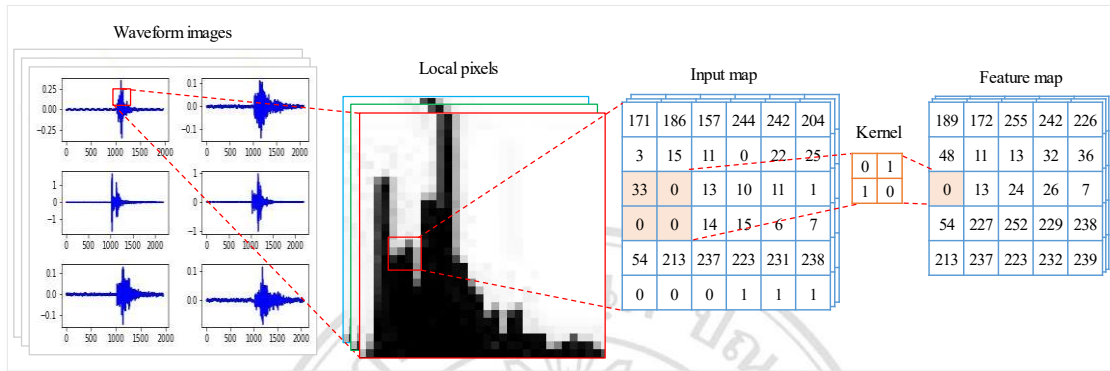


Figure 3.8 Feature extraction process in convolutional layers for microseismic waveforms.

Dropout is an efficient regularization technique that significantly enhances the generalization capability of CNNs (Poernomo et al., 2018). Its core mechanism involves randomly "dropping out" a certain proportion of neurons and their connections during the training process, preventing the network from overfitting to the training data. Specifically, each neuron is independently dropped with a certain probability, meaning that during each iteration, these neurons' outputs are set to zero and do not participate in the forward and backward propagation processes. This randomness encourages the network to learn more robust feature representations, as it cannot rely on any single neuron. The implementation principle of this process is clearly demonstrated in Figure 3.9.

The role and benefits of Dropout layers are manifold. It reduces the risk of overfitting, achieves model regularization, and improves computational efficiency by sparsifying network representation. Additionally, Dropout aids in automatic feature selection and enhances the stability of the training process. During the testing phase, to prevent inconsistencies with the training phase outputs, the outputs of all neurons are typically multiplied by the complement of the dropout probability (for example, 0.5) to adjust the network's response. This adjustment ensures the model's performance on new data while maintaining the consistency of the learned feature representations from the training phase. In summary, by its unique randomness, Dropout not only enhances the

model's generalization ability but also simplifies the search for hyperparameters, providing a powerful tool for building efficient CNN models.

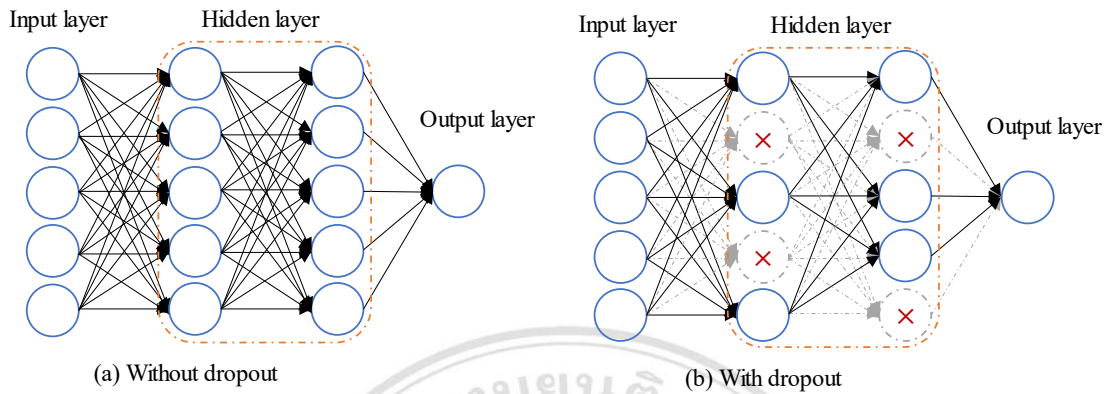


Figure 3.9 Working principle of the Dropout layer. (a) is a standard neural network architecture featuring two hidden layers. (b) is depicted a streamlined version of the network, achieved by implementing dropout, where the crossed-out units represent those that have been randomly omitted during the training process.

Our MS-CNN network is meticulously designed with multiple layers, comprising convolutional layers, batch normalization layers, ReLU activation layers, max pooling layers, fully connected layers, and a Softmax classification layer. The key parameter settings for each layer of its network structure are shown in Table 3.3. The network accepts input images of 100×100 pixels in color with three channels. The initial convolutional layer (Conv-1) employs a 2×2 kernel size with 16 kernels, a stride of 1, and padding of 1, yielding an output feature map of $101 \times 101 \times 16$ pixels. This is immediately followed by a batch normalization layer (BatchNorm-1) and a ReLU activation layer (ReLU-1). The subsequent convolutional layer (Conv-2) utilizes a 3×3 kernel, increasing the number of kernels to 32, maintaining the same stride, resulting in a feature map of $101 \times 101 \times 32$ pixels. After passing through the max pooling layer (MaxPooling-1), the feature map size is halved to $50 \times 50 \times 32$.

The third convolutional layer (Conv-3) employs a 5×5 kernel, further increasing the kernel count to 64 to capture broader image features, with the output feature map size being $48 \times 48 \times 64$ pixels. Another max pooling layer (MaxPooling-2) reduces the spatial dimensions, shrinking the feature map to $23 \times 23 \times 64$ pixels. The fully connected layer (FullyConnected-1) then flattens the feature map and projects it into a 256-dimensional

space, followed by a batch normalization layer (BatchNorm-4) and a ReLU activation layer (ReLU-4). A Dropout layer with a probability of 0.5 randomly eliminates neurons to mitigate overfitting. The second fully connected layer (FullyConnected-2) maps the features to a four-dimensional space corresponding to the four categories of the classification problem.

Table 3.3 Parameters of the MS-CNN network structure

Layer	Input	Filter	Stride	Padding	Output	Learnable	Parameters
ImageInput	100×100×3	-	-	-	100×100×3	-	0
Conv-1	100×100×3	2×2	1	1	101×101×16	Weights 2×2×3×16 Bias 1×1×16	208
BatchNorm-1	-	-	-	-	101×101×16	Offset 1×1×16 Scale 1×1×16	32
ReLU-1	-	-	-	-	101×101×16	-	0
Conv-2	101×101×16	3×3	1	1	101×101×32	Weights 3×3×16×32 Bias 1×1×32	4640
BatchNorm-2	-	-	-	-	101×101×32	Offset 1×1×32 Scale 1×1×32	64
ReLU-2	-	-	-	-	101×101×32	-	0
MaxPooling-1	101×101×32	3×3	2	0	50×50×32	-	0
Conv-3	50×50×32	5×5	1	1	48×48×64	Weights 5×5×32×64 Bias 1×1×64	51264
BatchNorm-3	-	-	-	-	48×48×64	Offset 1×1×64 Scale 1×1×64	128
ReLU-3	-	-	-	-	48×48×64	-	0
MaxPooling-2	48×48×64	3×3	2	0	23×23×64	-	0
FullyConnected-1	23×23×64	-	-	-	1×1×256	Weights 256×33856 Bias 256×1	8667392
BatchNorm-4	-	-	-	-	1×1×256	Offset 1×1×256 Scale 1×1×256	512
ReLU-4	-	-	-	-	1×1×256	-	0
Dropout	1×1×256	-	-	-	1×1×256	-	0
FullyConnected-2	1×1×256	-	-	-	1×1×4	Weights 4×256 Bias 4×1	1028
Softmax	1×1×4	-	-	-	1×1×4	-	0
Classification	-	-	-	-	4	-	0
Total							8,725,268

Finally, the Softmax layer normalizes the output such that the values for each category represent a probability distribution, and the classification layer produces the final classification outcome. The entire network encompasses a substantial number of

learnable parameters, with approximately 8.67 million parameters in the FullyConnected-1 layer and over 50,000 parameters in the Conv-3 layer. These parameters are optimized through backpropagation and gradient descent algorithms.

This streamlined description consolidates the network's structure and functionality, emphasizing the flow from input through the series of layers to the final classification, and highlights the role of each layer in the process.

3.5 Transfer Learning Models

In the field of image recognition and classification research, transfer learning models play an essential role. They have not only advanced deep learning technology but also provided powerful tools for solving practical problems. Below are some widely recognized transfer learning models in academia and industry, along with their invention years: AlexNet (2012), VGGNet (2014), GoogLeNet (Inception-V1) (2014), ResNet (2015), Inception-V2/V3 (in 2015 and 2016, respectively), DenseNet (2016), the MobileNet series (MobileNet-V1 in 2017 and MobileNet-V2 in 2018), BERT (2018, mainly used for natural language processing but also applicable to image recognition tasks), and EfficientNet (2019). The successive introduction of these models represents significant milestones in the field of image recognition technology within deep learning, offering researchers and developers a diverse array of tools and technological options.

In this study, we selected MobileNet-V2, Inception-V3, and ResNet-18 as our transfer learning models for three main reasons: Firstly, MobileNet-V2 (Gulzar, 2023) focuses on optimizing computational efficiency while maintaining performance. This model significantly reduces the model size and computational requirements through the use of depthwise separable convolutions, maintaining high recognition accuracy, and making it particularly suitable for applications with limited computational resources. Secondly, Inception-V3 and ResNet-18 have been extensively validated in a variety of image classification tasks, demonstrating their powerful capability in feature extraction. Additionally, the selected models show good adaptability, being able to quickly adapt to different datasets and task requirements. This allows them to quickly achieve high performance on new image classification problems during the transfer learning process. Choosing these models helps us compare the transfer learning capabilities of different

architectures, providing a comprehensive perspective for assessing the effects of transfer learning.

Considering the limitations of hardware resources, the lightweight characteristics of MobileNet-V2 make it an ideal choice for deployment in resource-constrained environments, which is particularly important in practical applications. Lastly, the use of these models not only helps us explore new areas of transfer learning but also serves as a foundation for improving and innovating existing models, offering a certain degree of innovation. Taking into account the specific objectives of the research, available resources, expected application scenarios, and the specific needs of the research team, we believe that MobileNet-V2, Inception-V3, and ResNet-18 are appropriate choices for conducting transfer learning research.

Moving forward, we will present an overview of the three transfer learning models that we have constructed: MS-MobileNet-V2, MS-Inception-V3, and MS-ResNet-18.

3.5.1 MS-MobileNet-V2

As depicted in Figure 3.10, the MS-MobileNet-V2 architecture is a transfer learning model specifically designed for the task of microseismic event waveform recognition, based on the pre-trained MobileNet-V2 model (Avola et al., 2022). This architecture leverages transfer learning techniques to successfully transfer the general feature extraction capabilities of MobileNet-V2, honed on image recognition tasks, to the identification of microseismic waveform data. Here are the specific steps implemented in the MS-MobileNet-V2 transfer learning model:

1. **Data Preprocessing:** Initially, the raw microseismic time-series waveform data is converted into event waveform images (time-amplitude representation). This transformation aligns the data format with the model's input requirements. Subsequently, the waveform images are resized to 224×224 pixels to match the input layer dimensions of the MobileNet-V2 model.

2. **Transfer Learning Strategy:** During model initialization, the pre-trained parameters of MobileNet-V2 are employed. This strategy enables the model to capitalize on the knowledge gained from large-scale image datasets like ImageNet (Krizhevsky et al., 2017), providing a foundation for feature extraction from microseismic waveform data.

3. Feature Extraction: The inverted residual blocks and linear bottleneck structures of MobileNet-V2 are utilized to extract features from the preprocessed waveform images. The design of these structures helps maintain the effectiveness of feature extraction while reducing computational complexity.

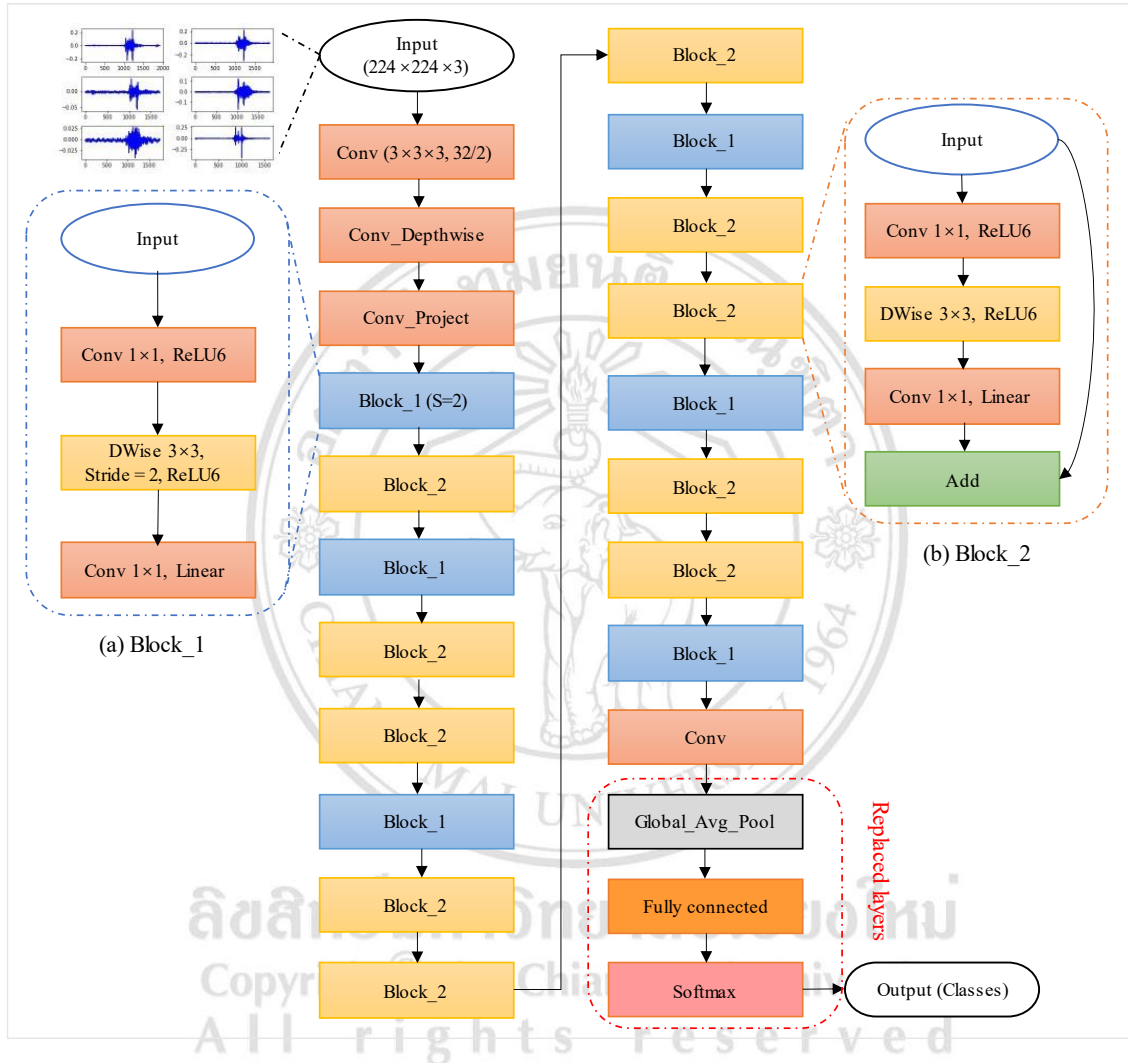


Figure 3.10 Transfer learning model for microseismic event waveform identification and classification based on MobileNet-V2 (MS-MobileNet-V2).

4. Classification Layer Adjustment: To cater to the specific classification task, the last three layers of the MobileNet-V2 model are replaced. This includes a fully connected layer, a softmax layer, and an output layer. The fully connected layer is parameterized to 4, corresponding to the four anticipated categories of event classification.

5. Model Training and Evaluation: Finally, the model is trained using microseismic data from three mines. During training, validation and test sets are used to assess the model's performance. Evaluation metrics such as accuracy, recall, and F1 score are employed to provide a comprehensive view of the model's performance.

Through this process, the MS-MobileNet-V2 model can efficiently recognize microseismic events, offering a novel technical approach for mine safety monitoring and disaster prediction. This model not only reduces reliance on a large amount of annotated data but also, due to its lightweight nature, is suitable for deployment in environments with limited computational resources (Bichri et al., 2023).

3.5.2 MS-ResNet-18

The MS-ResNet-18 model, a deep learning model for microseismic event waveform recognition and classification through transfer learning (Figure 3.11), is designed based on the residual network ResNet-18 developed by Microsoft Research (Zhao et al., 2022). It is optimized for the classification and identification tasks of microseismic signals. ResNet-18, a shallower network in the ResNet series, consists of 18 stacked residual blocks. These blocks effectively address the vanishing gradient problem during the training of deep networks by introducing skip connections, enabling the network to learn more complex functional mappings (Alinsaif et al., 2020).

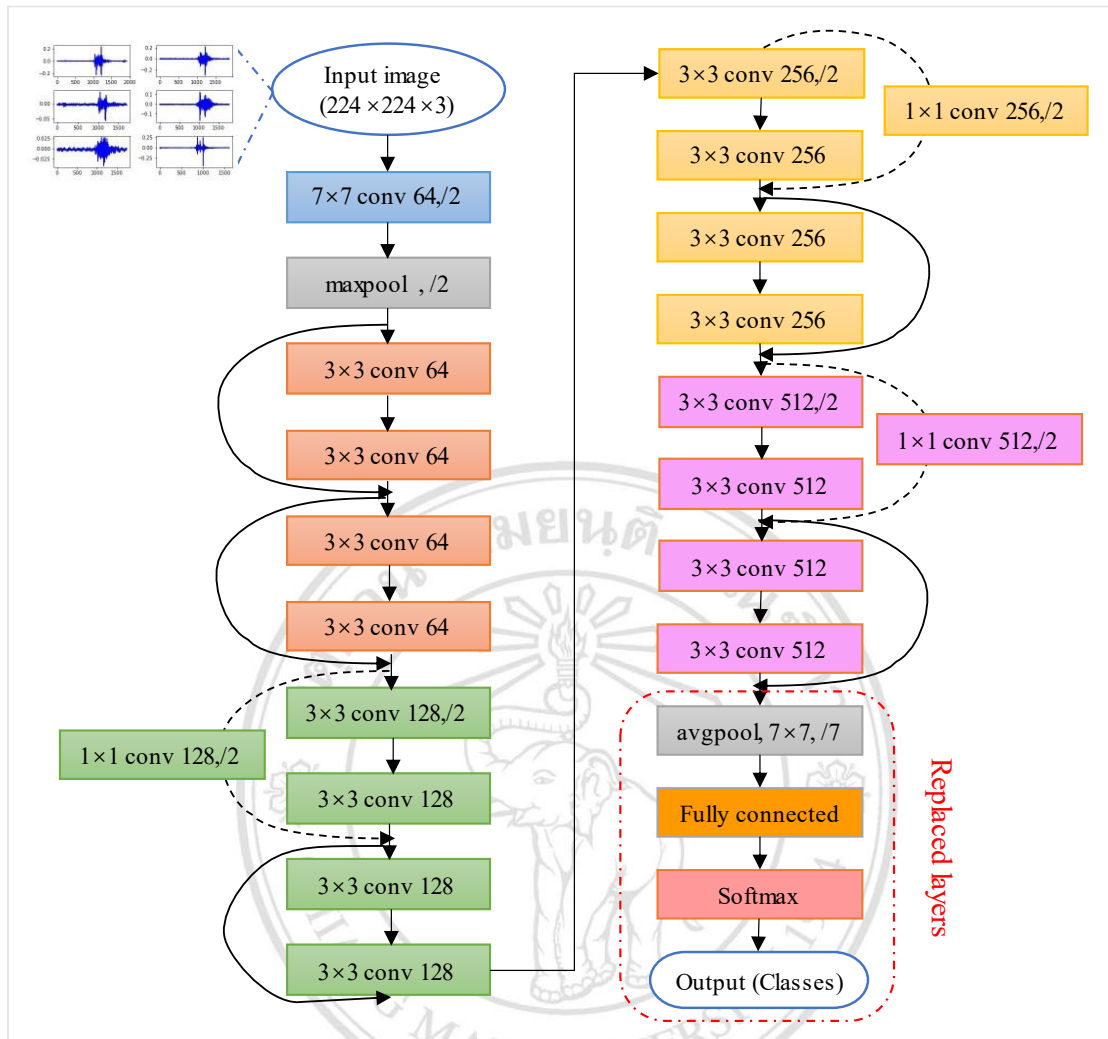


Figure 3.11 Transfer learning model for microseismic event waveform identification and classification based on ResNet-18 (MS-ResNet-18).

The MS-ResNet-18 model leverages the deep residual learning (He et al., 2015) framework of ResNet-18, capable of capturing deep features and patterns within microseismic waveform data. Utilizing transfer learning techniques, MS-ResNet-18 inherits the pre-trained weights of ResNet-18 obtained from large-scale image recognition datasets. These weights encapsulate rich knowledge of visual features, which, when transferred to the task of recognizing microseismic waveform data, can significantly enhance the model's learning efficiency and performance on the new task.

The implementation steps of MS-ResNet-18 also follow the standard transfer learning process. During the data preprocessing phase, the original microseismic waveform data is transformed into a format suitable for model input, including adjusting

data size and normalization. Subsequently, the pre-trained weights of ResNet-18 are loaded as the initial state of the network, and the network structure is appropriately fine-tuned according to the characteristics of the microseismic waveform data. Then, the model's output layer is customized according to specific classification tasks, and the network weights are further optimized through the training process. Finally, the model's performance is evaluated on separate validation and test sets, and the model is optimized based on the evaluation results.

Through transfer learning and fine-tuning, MS-ResNet-18 is expected to demonstrate good generalization and adaptability, capable of adjusting to different microseismic waveform datasets, providing an efficient and automated solution for microseismic monitoring in mines.

MobileNet-V2 and ResNet-18 all use 224×224 images because this size provides a good balance between computational efficiency and sufficient detail for accurate feature extraction. It allows the models to perform well across various visual recognition tasks while keeping the processing time and memory usage manageable. Additionally, this image size is a standard benchmark in the field, enabling consistent comparison of model performance.

3.5.3 MS-Inception-V3

The MS-Inception-V3 transfer learning model (Figure 3.12 and Figure 3.13) is based on the Inception-V3 network developed by Google and is constructed for the classification and identification tasks of microseismic signals. This architecture adopts the intricate design of the Inception-V3 network (Wang et al., 2019), particularly its unique Inception modules, which can process features of different scales in parallel, thereby effectively extracting key information from microseismic waveform data. Through transfer learning, MS-Inception-V3 inherits the knowledge that Inception-V3 has learned from large-scale image recognition datasets and applies it to the identification task of microseismic waveforms, significantly improving the model's training efficiency and performance for specific tasks. Additionally, MS-Inception-V3 can be fine-tuned to adapt to specific microseismic waveform datasets, demonstrating good generalization and adaptability (Lin et al., 2019).

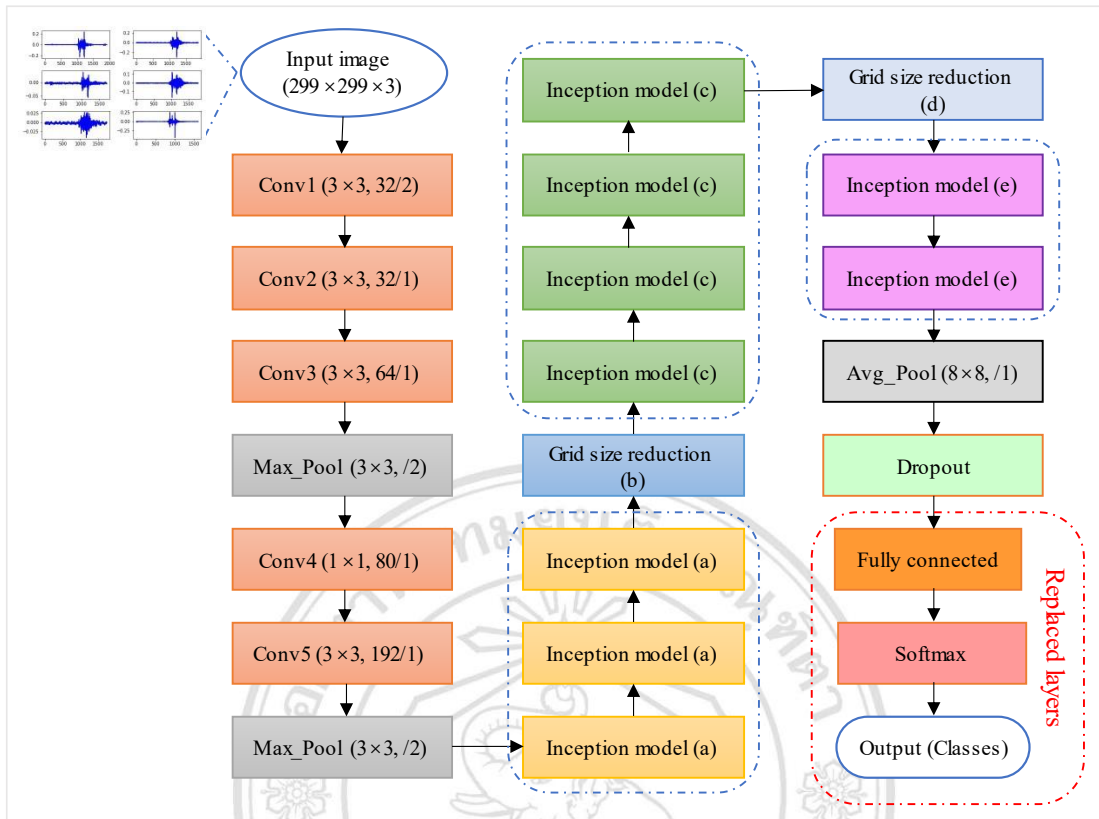


Figure 3.12 Transfer learning model for microseismic event waveform identification and classification based on Inception-V3 (MS-Inception-V3).

The implementation steps of MS- follow the standard transfer learning process. During the data preprocessing phase, the original microseismic waveform data is converted into an image format and size suitable for model input (299×299 pixels). The model was trained on the ImageNet dataset with this resolution, which ensures that the pre-trained weights are well-suited for images of this size. Subsequently, the pre-trained Inception-V3 model weights are loaded to initialize the network. The model's output layer is then customized to fit the specific classification task, and the network weights are further optimized through the training process. Finally, the model's performance is evaluated using separate validation and test sets, and the model is optimized based on the evaluation results. The MS-Inception-V3 architecture can be widely applied to automatic microseismic event classification, real-time mine monitoring and early warning, as well as geological structure analysis, providing an efficient and automated solution for the field of seismic monitoring.

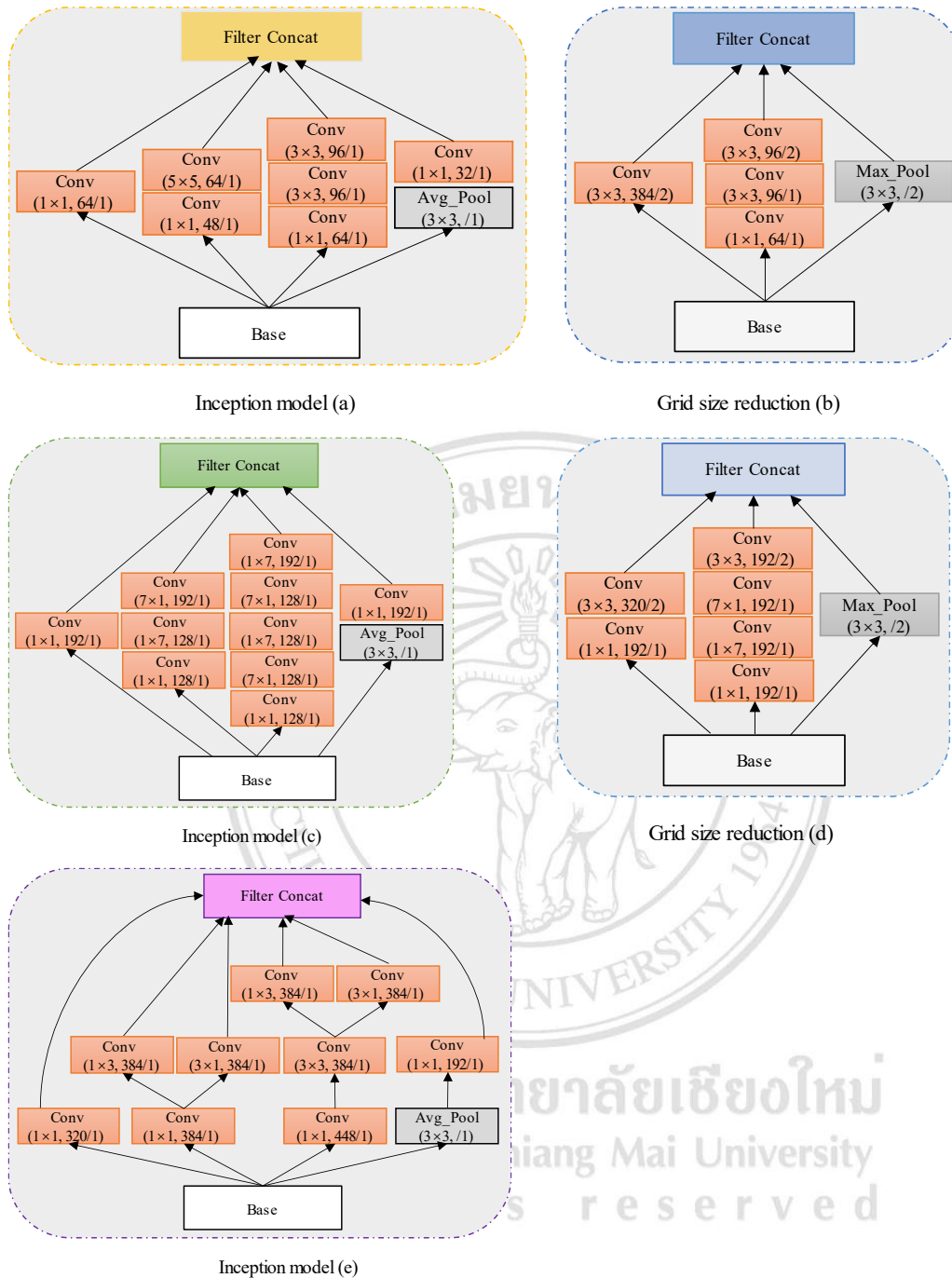


Figure 3.13 Detailed structure of five inception models (a~e) in MS-Inception-V3.

Based on existing research, Table 3.4 summarizes the key architectural parameters of the three transfer learning models, including the number of convolutional layers, the size and number of kernels, the stride, and the count of parameters. From the table, it can be seen that the MobileNet-V2 model has approximately 53 convolutional layers with a kernel size of 3×3 , varying numbers of kernels across different layers, and a stride of 1 for most layers, totaling about 3.47 million parameters. ResNet-18 consists of 18

convolutional layers, also with 3×3 kernel sizes, starting with 64 filters in the first layer, doubling in number with each residual block up to 512, with a parameter count of approximately 11.18 million. Inception-V3's convolutional layers involve multiple Inception modules of different scales, with varying numbers of kernels and strides within each module according to the design, primarily using 1×1 , 3×3 , and 5×5 kernels, and has a model parameter count of about 23.8 million.

Table 3.4 Key architectural parameters of transfer learning models

Model	Number of Convolutional Layers	Convolutional Kernel Size	Number of Convolutional Kernels	Stride	Number of Parameters
MobileNet-V2	About 53 layers	3×3	Varies by layer, adhering to a specific design philosophy	Primarily 1	About 3.47M
ResNet-18	18 layers	3×3	Begins with 64, doubling with each layer progression	2 for the first layer, 1 for subsequent layers	About 11.18M
Inception-V3	About 48 layers	1×1 , 3×3 , 5×5	Differs between modules, tailored according to the architectural design	Differs between modules	About 23.8M

Notes:

- The "Number of Convolutional Kernels" for MobileNet-V2 indicates variation across layers in accordance with its design principles.
- For ResNet-18, the number of convolutional kernels initiates at 64 in the first layer and exponentially increases with each successive layer.
- Inception-V3 features convolutional layers with varying kernel sizes (1×1 , 3×3 , and 5×5), and both the number of kernels and stride are tailored to the specific requirements of each module.

3.6 Evaluation Metrics

When evaluating the performance of machine learning models, it is crucial to use appropriate evaluation metrics. In order to comprehensively assess the performance and accuracy of our model, we have adopted a series of evaluation metrics including accuracy, precision, recall, F1 score, Kappa coefficient, and confusion matrix. These metrics quantify the accuracy, robustness, and generalization ability of the model, helping us objectively evaluate its performance in solving specific tasks. The following will provide a detailed description of each evaluation metric, including the rationale for its selection, calculation formula, and interpretation.

1. Accuracy

Accuracy is one of the most intuitive evaluation metrics, measuring the overall correctness of the classification model's predictions (Tharwat, 2020). It represents the proportion of correctly classified samples among the total number of samples. The calculation Equation (3.23) is as follows:

$$Accuracy = \frac{TP + TN}{TP + TN + FP + FN} \quad (3.23)$$

where TP represents true positives, the number of samples correctly predicted as positive; TN represents true negatives, the number of samples correctly predicted as negative; FP represents false positives, the number of samples incorrectly predicted as positive; FN represents false negatives, the number of samples incorrectly predicted as negative. A higher accuracy indicates a better overall predictive ability of the model.

2. Precision

Precision measures the proportion of true positive predictions out of all positive predictions made by the classifier (Vujovic, 2021). The calculation Equation (3.24) for precision is as follows:

$$Precision = \frac{TP}{TP + FP} \quad (3.24)$$

Precision helps us evaluate the rate of false alarms, i.e., the cases where negative samples are incorrectly predicted as positive. A higher precision implies fewer false positive predictions when classifying positive samples.

3. Recall

Recall measures the proportion of true positive predictions out of all actual positive samples (Powers, 2020). The calculation Equation (3.25) for the recall is as follows:

$$Recall = \frac{TP}{TP + FN} \quad (3.25)$$

Recall helps us evaluate the rate of missed detections, i.e., the cases where positive samples are incorrectly predicted as negative. A higher recall implies capturing a larger proportion of actual positive samples.

4. F1-Score

The F1-Score is the harmonic mean of precision and recall, providing a comprehensive measure of both precision and recall in classification models (Yacouby et al., 2020). The calculation Equation (3.26) for the F1-Score is as follows:

$$F1\ Score = \frac{2 \times (Precision \times Recall)}{Precision + Recall} \quad (3.26)$$

The F1-Score combines precision and recall, giving them equal weight. When both precision and recall are high, the F1-Score will also be high, indicating a balanced performance in predicting both positive and negative samples.

5. Kappa coefficient

The Kappa coefficient, also known as Cohen's Kappa, is used to measure the accuracy of classification models, particularly when evaluating the reliability and consistency of classification results (Cohen, 1960). It takes into account the effect of random agreement. The formula for calculating the Kappa coefficient is as follows (Equation (3.27)):

$$\left\{ \begin{array}{l} Kappa = \frac{P_o - P_e}{1 - P_e} \\ P_o = \frac{\sum_i n_{ii}}{N} \\ P_e = \sum_i \left(\frac{n_{i \cdot} \cdot n_{\cdot i}}{N^2} \right) \end{array} \right. \quad (3.27)$$

where P_o is the observed agreement (i.e., the proportion of actual classification that matches the true classification), and P_e is the expected agreement (i.e., the proportion of agreement expected by chance).

Construct a confusion matrix (Contingency Table) with actual categories and predicted categories as dimensions.

Calculate the observed agreement P_o , where n_{ii} is the element on the diagonal of the confusion matrix (representing the number of correctly classified samples). N is the total number of samples.

Calculate the expected agreement P_e , where n_i is the total number of samples in the i -th row. n_i is the total number of samples in the i -th column.

Substitute P_o and P_e into the Kappa coefficient formula to calculate *Kappa*.

6. Confusion matrix

The confusion matrix is an intuitive tabular representation that shows the relationship between the classifier's predicted results and the true class labels, providing a visual display of the classifier's classification performance (Valero-Carreras et al., 2023). Each cell in the confusion matrix represents the prediction results for a specific sample, including true positives, false positives, true negatives, and false negatives.

In multi-class classification problems, the confusion matrix can be used to visualize the classifier's classification results and calculate metrics such as accuracy, recall, and F1 score for each class. It provides detailed correspondence between the classifier's predicted results and the true class labels, helping evaluate the model's performance across different classes.

For a four-class classification problem, the structure of the confusion matrix becomes more complex as it needs to account for the classification results of four different categories. The confusion matrix will be a 4×4 matrix, summarizing the model's correct and incorrect predictions, broken down by each class. Each cell represents a combination of actual and predicted categories.

Assuming we have four categories: 1, 2, 3, and 4. The structure of the confusion matrix is as follows (Table 3.5):

Table 3.5 The basic structure of a four-class confusion matrix

Predicted Class \ Actual Class	Actual Class 1	Actual Class 2	Actual Class 3	Actual Class 4
Predicted Class 1	C11	C12	C13	C14
Predicted Class 2	C21	C22	C23	C24
Predicted Class 3	C31	C32	C33	C34
Predicted Class 4	C41	C42	C43	C44

- Rows represent the predicted categories.
- Columns represent the actual categories.
- Each cell C_{ij} represents the number of instances where the actual category is j and the predicted category is i .

➤ Explanation of the Confusion Matrix

- **Diagonal Elements (C_{ij}):**

- These elements represent the number of instances that were correctly classified.
- For example, C_{11} indicates the number of instances correctly predicted as class 1.

- **Off-Diagonal Elements (C_{ij} for $i \neq j$):**

- These elements represent the number of instances that were misclassified.
- For example, C_{12} indicates the number of instances that actually belong to class 2 but were predicted as class 1.

➤ Key Metrics Derived from the Confusion Matrix

Several important metrics can be derived from the confusion matrix to evaluate the model's performance:

- **Accuracy:**

- Accuracy is the ratio of the number of correctly classified instances to the total number of instances.

- $$Accuracy = \frac{\sum_{i=1}^4 C_{ii}}{\sum_{i=1}^4 \sum_{j=1}^4 C_{ij}}$$

- **Precision** (for each class):

- The precision of a class is the ratio of the number of instances correctly predicted as that class to the total number of instances predicted as that class.

- For class i : $Precision_i = \frac{C_{ii}}{\sum_{j=1}^4 C_{ij}}$ ($i = 1, 2, 3, 4$)

- **Recall** (for each class):
 - The recall of a class is the ratio of the number of instances correctly predicted as that class to the total number of instances that actually belong to that class.
 - For class i : $Recall_i = \frac{C_{ii}}{\sum_{j=1}^4 C_{ji}}$ ($i = 1, 2, 3, 4$)
- **F1-Score** (for each class):
 - The F1-Score is the harmonic mean of precision and recall.
 - For class i : $F1\ Score_i = \frac{2 \times Precision_i \times Recall_i}{Precision_i + Recall_i}$

To comprehensively evaluate the model's performance, perform similar calculations for each category.

In conclusion, each evaluation metric has its specific objectives and application scenarios. Choosing appropriate evaluation metrics and conducting comprehensive analysis and interpretation will contribute to a thorough assessment of the performance and effectiveness of machine learning models.

3.7 Summary

This chapter provides an overview of the data and methodology used to achieve fast and accurate identification and classification of four types of microseismic monitoring events (microseisms, blasts, rock drilling, and noise) in mining environments. Firstly, by transforming raw waveform data into waveform graphs and utilizing expert knowledge and manual identification, sample databases of 6-channel microseismic event waveform graphs are established for mines A, B, and C. Subsequently, the theoretical knowledge and algorithm principles of using HOG-SML, convolutional neural networks, and transfer learning based on deep learning are introduced to explore the most suitable machine learning algorithms for microseismic signal identification and classification.

To objectively evaluate the model's performance, extensive real data is used for training and testing, followed by a detailed explanation of the definition, selection rationale, and corresponding calculation formulas for each evaluation metric. By

comparing metrics such as accuracy, precision, recall, F1 score, and Kappa coefficient, the best-performing model is determined.

The ultimate goal is to provide intelligent technological support for microseismic monitoring and promote the intelligent transformation and safe development of mining operations.



ลิขสิทธิ์มหาวิทยาลัยเชียงใหม่
Copyright© by Chiang Mai University
All rights reserved

CHAPTER 4

RESULTS

4.1 Introduction

This chapter presents the process and outcomes of experiments conducted using three common machine-learning techniques. Firstly, we utilize the HOG feature extraction method in conjunction with shallow machine learning classifiers to achieve automatic recognition and classification of microseismic event waveforms. This approach addresses the challenge of manually designing feature extraction in traditional machine learning methods and leverages the advantages of shallow machine learning algorithms, which require fewer computational resources and offer faster processing speeds. Secondly, we refine existing convolutional neural network structures to construct a simple CNN model, training it from scratch to obtain a model that demonstrates strong performance in both efficiency and accuracy. Thirdly, we make comprehensive use of existing image classification models and employ transfer learning techniques to achieve high-accuracy models. Through experimentation with these three methods, we conduct a comprehensive comparative analysis of the results, aiming to identify the optimal models and approaches. This will aid readers and fellow researchers in making informed and appropriate decisions.

4.2 Experimental Environment

This section will introduce the experimental environment and infrastructure of this study from both hardware and software perspectives.

1. Hardware Infrastructure

This study utilized a computer equipped with a graphics processing unit (GPU, NVIDIA GeForce GTX 1050 Ti) as the experimental platform. The processor operated at a base clock frequency of 2.5GHz, featuring 8 processing cores from the

high-performance Intel 11th generation Core i7 series, thus providing substantial computational power for the experiments. The computer was equipped with 16GB of memory and had a storage configuration consisting of a 500GB solid-state drive (SSD) and a 2TB hard disk drive (HDD), offering ample space for data storage and processing.

2. Software System

On the software side, Python was utilized for acoustic data processing and waveform graph conversion. Furthermore, MATLAB R2021b was employed to implement HOG feature extraction and perform training and testing of the classification models. Additionally, we used MATLAB's Deep Learning Toolbox to implement convolutional neural network (CNN) models and transfer learning models. MATLAB, a widely-used high-performance numerical computing software, is renowned for its extensive mathematical function library and robust plotting capabilities, supporting diverse applications such as data analysis, algorithm development, signal processing, image processing, and machine learning. These hardware and software configurations provided a reliable foundation for microseismic event waveform recognition and classification.

4.3 Results of the HOG-SML Method

The combination of histogram of oriented gradients and shallow machine learning (HOG-SML) algorithms was utilized. Initially, the HOG algorithm was employed to extract feature vectors from microseismic event waveforms, serving as inputs for the shallow learning models. Subsequently, linear classifiers, decision tree classifiers, KNN classifiers, Fisher discriminant classifiers, and SVM classifiers were constructed.

4.3.1 K-fold Cross-Validation

During the model training process, we adopted the five-fold cross-validation method to evaluate the model's performance and enhance its generalization ability. The basic principle involves dividing the training data into five mutually exclusive subsets, with four for model training and one for model validation. Each subset had the opportunity to act as the validation set, resulting in five sets of performance evaluations. Ultimately, the average of these five results was considered as the evaluation of the model's performance, providing more stable and reliable performance metrics.

The reason for selecting $k = 5$ over 7 or 10 was to balance efficiency and reliability. While using a higher number of folds could offer more precise performance evaluations, it would also escalate computational costs and time consumption. Five-fold cross-validation is commonly regarded as a practical and effective choice of folds, maintaining relatively lower computational overhead while ensuring evaluation accuracy. Additionally, the balanced division of training and validation sets in five-fold cross-validation aids in better assessing the model's generalization capability and stability. Therefore, in this study, we opted for five-fold cross-validation as the method for evaluating model performance.

By employing five-fold cross-validation, the model underwent multiple rounds of training and validation on different training and validation sets. This helped in detecting potential overfitting, where good performance on one subset but poor performance on others may indicate overfitting issues. Multiple training and validation cycles on diverse data subsets contributed to a more comprehensive understanding of the model's adaptability to various data distributions. Consequently, this led to an enhancement in the model's generalization performance, making it more effective when dealing with new, unseen data. Through cross-validation, we were also able to optimize the model's hyperparameters. For instance, different hyperparameter combinations could be explored in each fold, and the model with the best performance on the validation set was chosen. This process assisted in identifying the optimal hyperparameter configuration, thereby improving the model's overall performance. Table 4.1 presents the performance results of five shallow machine learning models obtained through five-fold cross-validation on training datasets from Mines A, B, and C. This table provides a comprehensive evaluation of the generalization capabilities of each model across the different datasets.

Table 4.1 The results of five-fold cross-validation of shallow machine learning models on three datasets

Dataset	Model	Validation accuracy					
		fold_1	fold_2	fold_3	fold_4	fold_5	Average_val
A	SVM	95.62	95.43	96.79	96.11	95.52	95.89
	Linear Classifier	96.20	96.79	96.11	94.46	95.03	95.72
	Decision Tree	81.79	82.59	82.10	81.81	81.60	81.98
	KNN	88.90	89.20	89.69	89.59	91.72	89.82
	Fisher Discriminant	95.23	94.75	94.07	94.65	94.64	94.67
B	SVM	96.65	96.94	97.71	96.56	96.56	96.88
	Linear Classifier	95.60	97.23	96.85	96.46	97.04	96.64
	Decision Tree	91.30	90.26	91.02	92.35	91.59	91.30
	KNN	94.84	95.89	96.08	95.12	96.18	95.62
	Fisher Discriminant	97.42	96.94	96.94	97.42	95.89	96.92
C	SVM	96.89	96.25	96.14	96.55	96.85	96.54
	Linear Classifier	96.40	96.81	96.51	96.36	97.00	96.62
	Decision Tree	84.70	85.08	86.50	85.00	85.15	85.29
	KNN	93.03	92.24	91.94	92.24	93.21	92.53
	Fisher Discriminant	95.16	95.28	94.86	95.05	95.28	95.13

From Table 4.1, it is evident that there are differences in the accuracy rates of each model after undergoing five rounds of training and validation. The SVM and Linear models have demonstrated higher validation accuracy and stability across all datasets, especially with the SVM achieving an average validation accuracy of 96.88% on dataset B. The Decision Tree model has relatively poorer performance on all datasets, with the lowest average validation accuracy. The KNN model shows an improvement on dataset B, but still falls below the SVM and Linear models overall. The Discriminant analysis shows exceptional stability on dataset B, but exhibits greater fluctuations on other datasets. In summary, the SVM and Linear models perform the most impressively on these datasets, while the Decision Tree model requires further optimization to enhance its performance.

To evaluate the training efficiency of five shallow machine learning models across different datasets, we recorded the training time for each classification model, with the experimental results presented in Figure 4.1. The intuitive display of the bar chart reveals that the KNN classifier has the shortest training time, followed closely by the linear classifier. The decision tree and SVM have relatively longer training times, while the discriminant classifier has the longest training time among all models, particularly when

processing the large sample dataset C, where the time taken increases significantly. Across all datasets, the Linear model has demonstrated a faster training time, making it an ideal choice for scenarios requiring a quick response. The KNN model, due to the simplicity of its algorithm, also maintains a faster training speed across all datasets. These analytical results provide us with insights into the performance differences of different models on various datasets, helping us to select the appropriate model and optimize the training process to enhance the overall efficiency of machine learning projects.

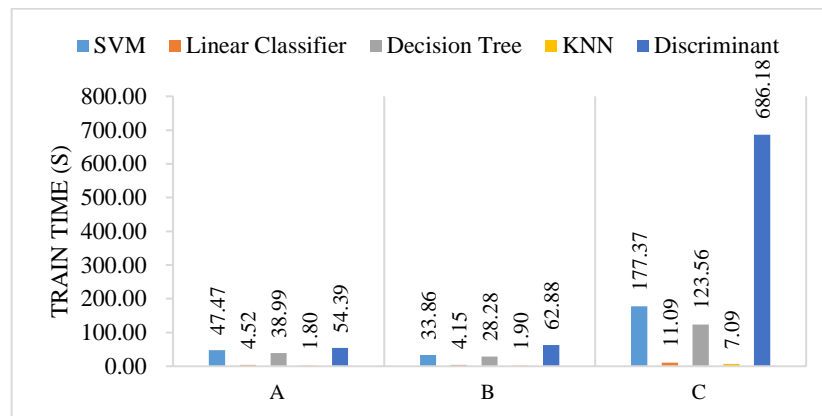


Figure 4.1 Training time of shallow learning models on three training sets.

4.3.2 Testing Results

Upon completing the training of classifiers, we conducted a final performance evaluation of the models using independent test sets. These test sets contained data that the model had not encountered previously, aiming to simulate new data scenarios that the model may face in real-world applications. This step is crucial for assessing the model's generalization capability. As mentioned earlier, we utilized metrics such as accuracy, precision, recall, F1 score, and Kappa coefficient to evaluate the model's performance on the test sets. Additionally, we employed confusion matrices to provide a more detailed classification presentation of the test results. The specific experimental results are as follows: Table 4.2 documents the accuracy and Kappa coefficients of these five classifiers on datasets A, B, and C. Figure 4.2 illustrates their testing durations on the three different test sets.

Table 4.2 Performance of shallow machine learning models on three mine test datasets

Dataset	Metrics	Shallow machine learning models				
		SVM	Linear	Tree	KNN	Discriminant
A	Accuracy (%)	97.12	96.65	82.94	91.2	94.55
	Kappa	0.961	0.954	0.767	0.880	0.925
B	Accuracy (%)	96.25	96.41	90.90	95.26	96.87
	Kappa	0.946	0.948	0.870	0.932	0.955
C	Accuracy (%)	96.79	97.21	86.68	92.17	95.68
	Kappa	0.956	0.961	0.816	0.891	0.940

The analysis from Table 4.2 indicates that on Dataset A, the SVM model achieves the highest accuracy at 97.12%, demonstrating its effectiveness in making correct predictions. Additionally, the SVM model has the highest Kappa statistic of 0.961, indicating strong agreement between predicted and actual classifications. On Dataset B, the Discriminant model shows the highest scores for both accuracy and Kappa, with 96.87% and 0.955 respectively, signifying its superior performance on this dataset. For Dataset C, the Linear model outperforms others, with an accuracy of 97.21% and a Kappa of 0.961.

In summary, the Linear and SVM models consistently exhibit high accuracy and Kappa values across all datasets, suggesting their robustness and reliability. The performance of the Tree model varies significantly, with lower accuracy and Kappa compared to other models. The KNN and Discriminant models show improved performance on Datasets B and C. These findings can inform model selection based on the specific characteristics of different datasets, positioning the Linear and SVM models as strong contenders due to their consistently high performance.

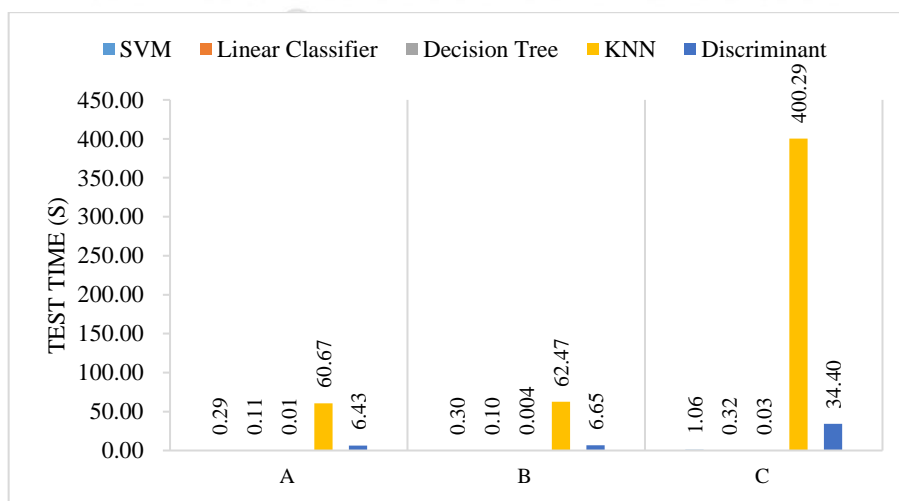


Figure 4.2 The testing time of shallow learning models on three testing sets.

The bar chart 4.2 illustrates the test times in seconds for five shallow machine learning models across three mining test datasets. The Tree model exhibits the shortest test times, being less than 1 millisecond for datasets A and B, and only 3 milliseconds for dataset C. In contrast, KNN has the longest test times, with an exceptionally high duration of 400 seconds on dataset C, significantly outpacing the other models. Both Linear and SVM models maintain low test times across all datasets, indicating high testing efficiency. The Discriminant model shows low test times for datasets A and B, but experiences an increase on dataset C. The data highlights the notable variance in testing efficiency among different models when applied to various datasets.

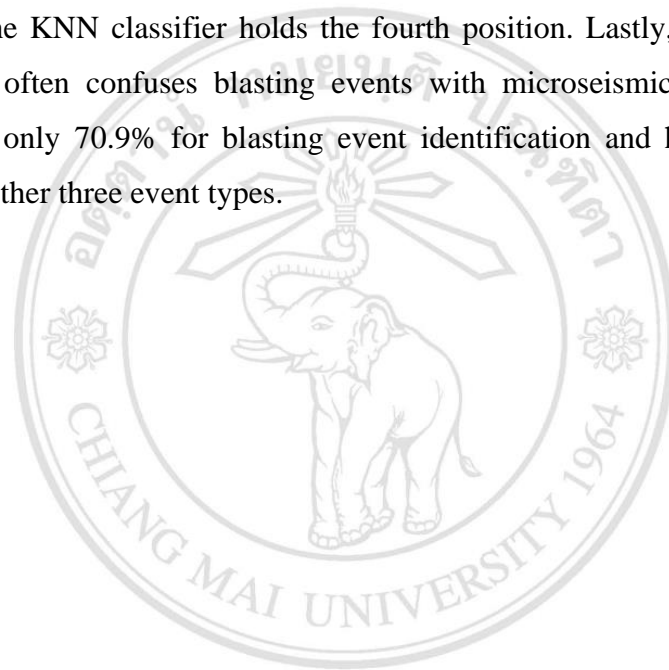
Furthermore, we used confusion matrices to meticulously demonstrate the classification performance of each model across different event categories, as depicted in Figure 4.3, Figure 4.4, and Figure 4.5.

For a clear analysis and comparison, the F1-Scores are calculated and displayed at the bottom of the confusion matrix. As shown in Figure 4.3, on the test dataset from Mine A, the SVM classifier demonstrates the best overall performance with the highest precision, recall, and F1-Scores for each class. Notably, it achieves the best classification for noise events (F1-Score of 98.6%), followed closely by microseismic events (F1-Score of 97.1%), with drilling and blasting events showing similar performance. The Linear classifier performs second best, with high precision across all four events. The discriminant classifier ranks third, particularly effective in noise event identification. The KNN classifier shows average results. Lastly, the decision tree classifier performs the weakest, with recall and precision rates around 80% for each event class, indicating the need for further improvement.

On the test dataset from Mine B, the sample size for blast events is the smallest (70), approximately one-sixth of the quantity of other event categories. As shown in Figure 4.4, the discriminant classifier performs the best overall, particularly in identifying microseismic events, with an F1 score of 98.3%. In terms of identifying blast events, the discriminant classifier also excels, with a recall rate and F1 score of 87.1% and 90.4%, respectively. The linear classifier has the highest precision for blast event identification (96.5%), but its recall rate is only 78.6%. For drilling events, both the discriminant and linear classifiers demonstrate high identification accuracy. The SVM model's

performance in microseismic event identification is second only to the discriminant classifier. The KNN classifier has the highest precision for microseismic event identification, at 97.8%, but its recall rate is lower than that of the discriminant classifier and SVM. Although the decision tree classifier performs better on test set B than on test set A, with an accuracy rate of 90.9%, it is still the weakest among the five models.

On the test dataset from Mine C, the linear classifier demonstrates the best overall performance, achieving the highest F1-scores for noise, drilling, microseismic, and blasting events. The SVM classifier ranks second, followed by the discriminant classifier in third place. The KNN classifier holds the fourth position. Lastly, the decision tree classifier, which often confuses blasting events with microseismic events, shows a precision rate of only 70.9% for blasting event identification and has relatively low accuracy for the other three event types.



ลิขสิทธิ์มหาวิทยาลัยเชียงใหม่
Copyright© by Chiang Mai University
All rights reserved

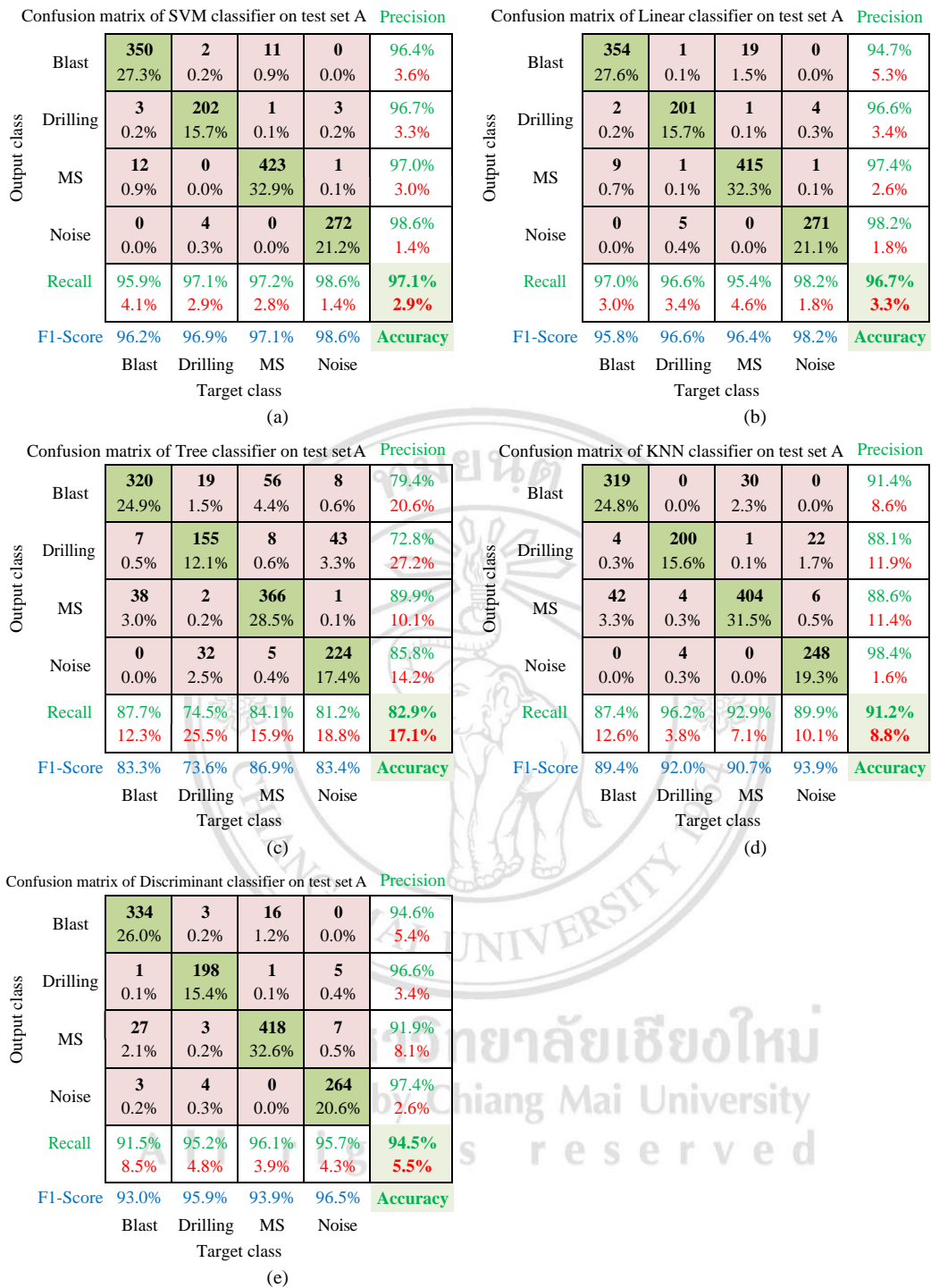


Figure 4.3 The confusion matrices of shallow machine learning models on test set A.

Confusion matrix of SVM classifier on test set B Precision

Output class	Blast	59 4.5%	0 0.0%	5 0.4%	0 0.0%	92.2% 7.8%
	Drilling	0 0.0%	398 30.4%	0 0.0%	19 1.5%	95.4% 4.6%
	MS	11 0.8%	0 0.0%	395 30.2%	0 0.0%	97.3% 2.7%
	Noise	0 0.0%	14 1.1%	0 0.0%	407 31.1%	96.7% 3.3%
	Recall	84.3% 15.7%	96.6% 3.4%	98.8% 1.3%	95.5% 4.5%	96.3% 3.7%
F1-Score	88.1%	96.0%	98.0%	96.1%	Accuracy	
	Blast	Drilling	MS	Noise	Target class	

(a)

Confusion matrix of Linear classifier on test set B Precision

Output class	Blast	55 4.2%	0 0.0%	2 0.2%	0 0.0%	96.5% 3.5%
	Drilling	0 0.0%	400 30.6%	0 0.0%	18 1.4%	95.7% 4.3%
	MS	15 1.1%	0 0.0%	398 30.4%	0 0.0%	96.4% 3.6%
	Noise	0 0.0%	12 0.9%	0 0.0%	408 31.2%	97.1% 2.9%
	Recall	78.6% 21.4%	97.1% 2.9%	99.5% 0.5%	95.8% 4.2%	96.4% 3.6%
F1-Score	86.6%	96.4%	97.9%	96.5%	Accuracy	
	Blast	Drilling	MS	Noise	Target class	

(b)

Confusion matrix of Tree classifier on test set B Precision

Output class	Blast	48 3.7%	3 0.2%	25 1.9%	0 0.0%	63.2% 36.8%
	Drilling	0 0.0%	382 29.2%	4 0.3%	32 2.4%	91.4% 8.6%
	MS	22 1.7%	0 0.0%	368 28.1%	3 0.2%	93.6% 6.4%
	Noise	0 0.0%	27 2.1%	3 0.2%	391 29.9%	92.9% 7.1%
	Recall	68.6% 31.4%	92.7% 7.3%	92.0% 8.0%	91.8% 8.2%	90.9% 9.1%
F1-Score	65.8%	92.0%	92.8%	92.3%	Accuracy	
	Blast	Drilling	MS	Noise	Target class	

(c)

Confusion matrix of KNN classifier on test set B Precision

Output class	Blast	61 4.7%	0 0.0%	7 0.5%	0 0.0%	89.7% 10.3%
	Drilling	0 0.0%	395 30.2%	1 0.1%	28 2.1%	93.2% 6.8%
	MS	9 0.7%	0 0.0%	392 30.0%	0 0.0%	97.8% 2.2%
	Noise	0 0.0%	17 1.3%	0 0.0%	398 30.4%	95.9% 4.1%
	Recall	87.1% 12.9%	95.9% 4.1%	98.0% 2.0%	93.4% 6.6%	95.3% 4.7%
F1-Score	88.4%	94.5%	97.9%	94.6%	Accuracy	
	Blast	Drilling	MS	Noise	Target class	

(d)

Confusion matrix of Discriminant classifier on test set B Precision

Output class	Blast	61 4.7%	0 0.0%	4 0.3%	0 0.0%	93.8% 6.2%
	Drilling	0 0.0%	406 31.0%	0 0.0%	21 1.6%	95.1% 4.9%
	MS	9 0.7%	0 0.0%	396 30.3%	1 0.1%	97.5% 2.5%
	Noise	0 0.0%	6 0.5%	0 0.0%	404 30.9%	98.5% 1.5%
	Recall	87.1% 12.9%	98.5% 1.5%	99.0% 1.0%	94.8% 5.2%	96.9% 3.1%
F1-Score	90.4%	96.8%	98.3%	96.7%	Accuracy	
	Blast	Drilling	MS	Noise	Target class	

(e)

Figure 4.4 The confusion matrices of shallow machine learning models on test set B.

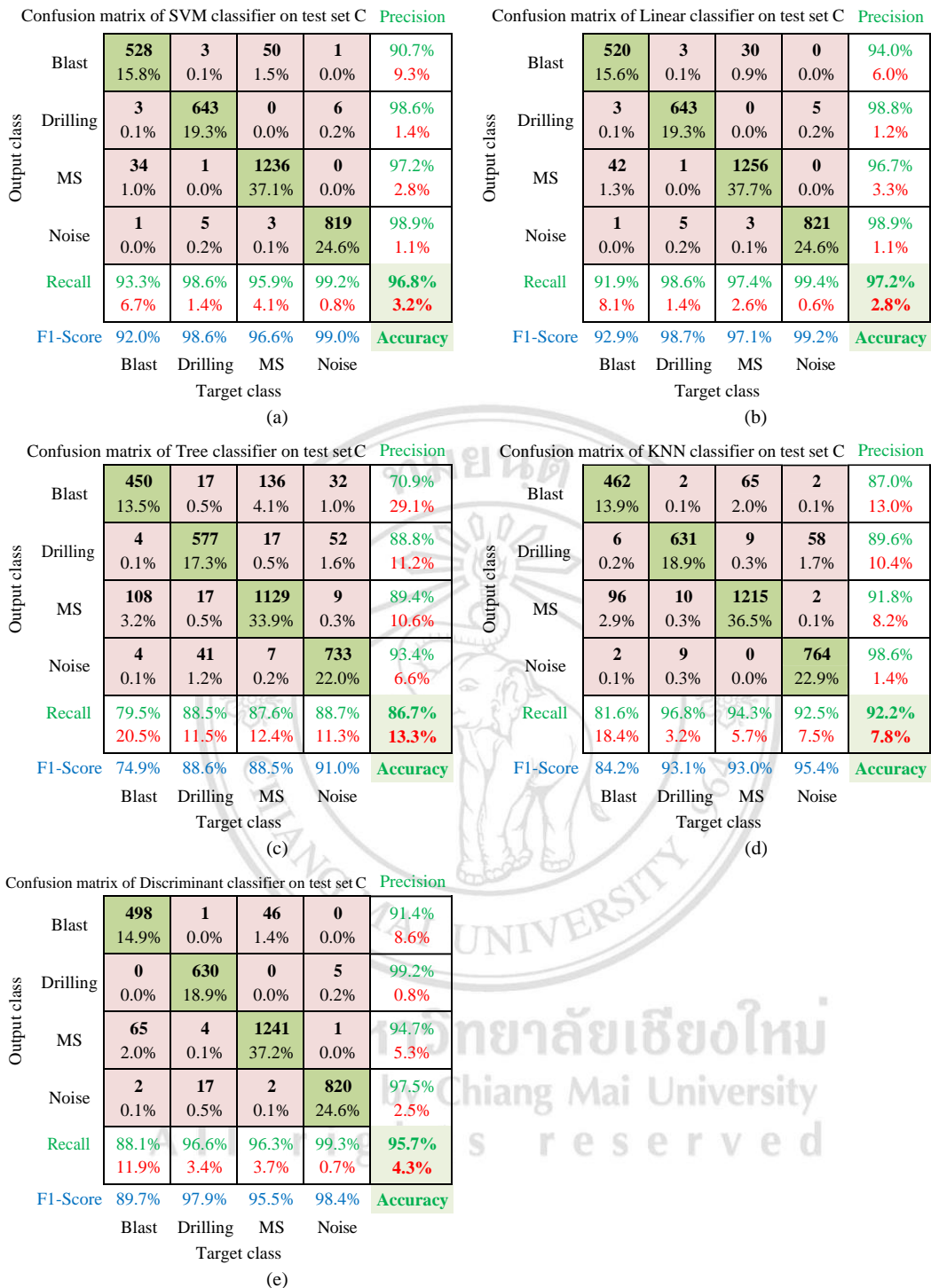


Figure 4.5 The confusion matrices of shallow machine learning models on test set C.

After a comprehensive analysis of the test datasets from Mines A, B, and C, we conclude that different datasets, due to their varying feature complexities and distributions of event counts, have a significant impact on the performance of classification models. Overall, the Linear and SVM classifiers perform well in most cases

due to their stability and high accuracy, especially suitable for datasets with uniform feature distribution and high-dimensional data. The Discriminant classifier demonstrates advantages when dealing with datasets with imbalanced samples. The KNN classifier, though easy to implement, may be affected by noisy data when the feature dimension is high. The Decision Tree, while highly interpretable, is prone to overfitting with complex datasets. Therefore, choosing the most appropriate model requires a comprehensive consideration of data characteristics, task requirements, and the specific strengths of the models, along with performance evaluation through methods such as cross-validation to ensure that the selected model can achieve optimal classification performance in specific application scenarios.

4.4 Results of MS-CNN Model

4.4.1 The Impact of Hyperparameters on Model Performance

During the training process of CNNs, the setting of hyperparameters typically involves selecting appropriate initialization methods to promote a reasonable distribution of network weights, determining the learning rate and its decay strategy to balance training speed and prevent oscillation, setting batch size to balance computational efficiency and memory usage, configuring optimizers to suit specific problems and data characteristics, and adjusting network architecture-related parameters (such as convolutional kernel size, number of layers, and connection methods) through experiments to improve the model's generalization ability and performance. In addition, hyperparameter settings must consider avoiding overfitting, ensuring the model's performance on unseen data, and using cross-validation and independent test sets to verify the effectiveness of hyperparameter choices.

The selection of hyperparameters has a significant impact on the results of machine learning models. The optimizer plays a crucial role in the training process, adjusting the model's parameters to minimize the loss function. The choice of optimizer determines the direction and step size of parameter updates. Commonly used optimizers include Gradient Descent, SGDM (Stochastic Gradient Descent with Momentum), Adam (Kingma et al., 2014), RMSprop (Root Mean Square Propagation), etc. The initial learning rate is the step size of the optimization algorithm at the start, determining the degree of parameter updates based on the gradient of the loss function. The learning rate typically starts with

a value that promotes the reduction of training loss and is then adjusted according to the observed training performance. An excessively high learning rate may lead to an overshoot, while an overly low learning rate can result in a slow training process.

The maximum number of training epochs refers to the number of times the model completely uses the training dataset for training. An epoch means that the model has viewed all training samples once. Generally, more epochs can improve model performance but also increase the risk of overfitting. The appropriate number of iterations depends on the complexity of the model and the size of the dataset. Batch size refers to the number of samples in the model's training set used for backpropagation in a single weight update. A smaller mini-batch size can provide better generalization, while a larger batch size can speed up training but may lead to instability during the training process. The optimal batch size is usually determined based on the model's structure and the performance of the hardware used. In this experiment, recognition accuracy was chosen as the main metric for evaluating the performance of the image recognition model. The higher the recognition accuracy on the test set, the better the model's performance is.

To visually demonstrate the impact of different hyperparameter settings on the performance of the MS-CNN model, this study used dataset A as a benchmark and systematically compared the combined effects of different optimizers (SGDM and Adam), learning rates (0.1, 0.001, 0.0001), batch sizes (8, 16, 32), and the number of iterations (8, 10, 20). The results of these experiments are detailed in Table 4.3, highlighting the influence of hyperparameter tuning on model performance.

Based on the data analysis from Table 4.3, several key observations can be made:

1. Choice of Optimizer: The Adam optimizer generally demonstrates higher accuracy compared to SGDM, likely due to the superiority of the Adam algorithm in automatically adjusting the learning rate.

2. Sensitivity to Learning Rate: The learning rate significantly impacts model performance. For instance, a decrease in the learning rate from 0.001 to 0.0001 (row NO.1 vs. NO.9) results in a drop in accuracy, indicating that a smaller learning rate is not always better. At the same time, a higher learning rate (such as 0.1, rows NO.24 & 25) leads to a significant performance decline, showing that an excessively large learning rate can impair the model's convergence and accuracy.

Table 4.3 Performance comparison of the MS-CNN model on dataset A under different hyperparameter settings

NO.	Optimizer	Learning rate	Epochs	Batch size	Accuracy (%)
1	sgdm	0.001	8	32	96.73
2	sgdm	0.001	8	16	97.20
3	sgdm	0.001	8	8	96.88
4	sgdm	0.001	10	8	96.34
5	sgdm	0.001	10	16	96.73
6	sgdm	0.001	10	32	96.34
7	sgdm	0.001	20	32	96.88
8	sgdm	0.0001	20	32	96.03
9	sgdm	0.0001	8	32	94.78
10	sgdm	0.0001	10	32	95.33
11	sgdm	0.01	8	32	95.25
12	sgdm	0.01	10	32	96.65
13	sgdm	0.01	20	32	96.26
14	adam	0.001	8	32	97.43
15	adam	0.001	8	16	97.20
16	adam	0.001	10	32	97.20
17	adam	0.001	8	8	96.81
18	adam	0.001	10	8	97.43
19	adam	0.001	10	16	97.98
20	adam	0.0001	8	32	96.81
21	adam	0.0001	10	32	96.50
22	adam	0.01	8	32	96.18
23	adam	0.01	10	32	96.26
24	adam	0.1	8	32	86.37
25	adam	0.1	10	32	89.95

3. Balance Between Iterations and Batch Size: The number of iterations and batch size need to be coordinated to achieve optimal performance. For example, with 10 iterations, a smaller batch size (such as 16, row NO.15) usually yields higher accuracy compared to a larger batch size (such as 32, row NO.16). Moreover, an excessive number of iterations (such as 20, row NO.13) does not bring additional performance improvements and may lead to overfitting.

4. Consideration of Hardware Resources: Hardware resource limitations must be taken into account when selecting hyperparameters. A larger batch size, while

accelerating training speed, may exceed the processing capacity of the hardware, resulting in reduced training efficiency.

In summary, the rational selection of hyperparameters is crucial for model performance. In practical applications, it is necessary to fine-tune and optimize based on specific tasks and hardware conditions to find the optimal combination of hyperparameters that maximizes model performance.

4.4.2 Hyperparameter Optimization

In the field of deep learning, the tuning of hyperparameters has a decisive impact on the model's generalization ability and training efficiency. This study aims to explore the optimal combination of hyperparameters through a systematic approach to ensure model performance while minimizing the time required for training. In this study, we used the control variable method to optimize hyperparameters, with the aim of achieving the best model performance. Specific hyperparameter settings can be found in Table 4.4.

Table 4.4 Hyperparameter settings of the MS-CNN model during training

Hyperparameter	Value	Description
Optimizer	Adam	Use the Adam optimizer for gradient descent optimization.
Initial Learning Rate	0.001	The learning rate at the start of training.
Max Epochs	8	The maximum number of epochs for training the model.
Mini-Batch Size	32	The number of samples used in each gradient descent update.
Data Shuffle	Every-epoch	Randomly shuffle the data once at the beginning of each training epoch.
Validation Frequency	10	Perform a performance evaluation on the validation set after every specified number of mini-batches.

Firstly, we fixed the learning rate, number of iterations, and batch size, and conducted an exhaustive comparison of different optimization algorithms. Through in-depth analysis of the model's loss and accuracy on the training and validation sets, we found that the Adam optimizer demonstrated superior performance across multiple evaluation metrics. Therefore, we selected Adam as the optimization algorithm for this study. Subsequently, keeping the batch size and number of iterations constant, we finely adjusted the learning rate and found that when the learning rate was set to 0.001, the model's accuracy on the test set significantly increased while maintaining a low training

loss. To prevent model overfitting, we further optimized the number of iterations and found that when set to 8, the model achieved a lower and stable training loss while maintaining a high validation accuracy. Finally, we optimized the batch size and found that with other hyperparameters held constant, when the batch size was set to 32, the model's accuracy on the validation set exceeded 96%, and the training loss was also kept at a low level. Through this series of hyperparameter adjustments, we successfully enhanced the model's performance, laying a solid foundation for subsequent research.

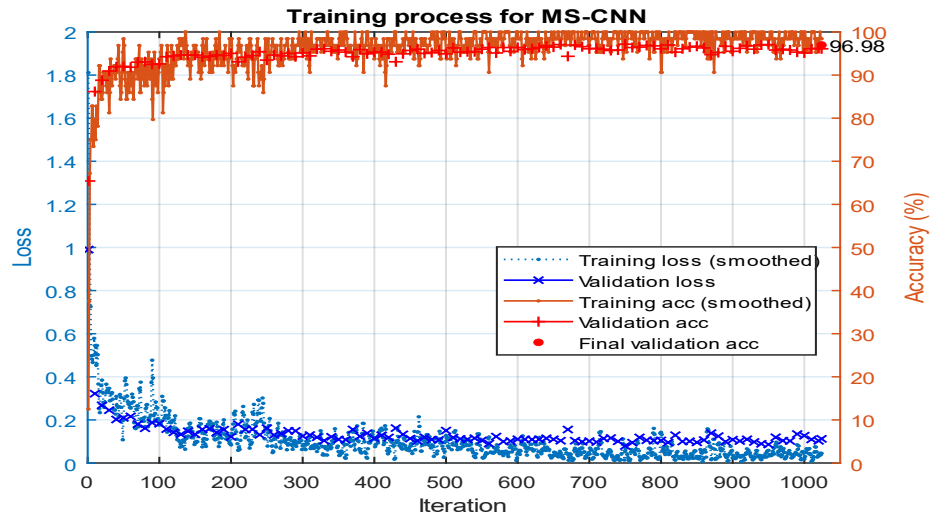
4.4.3 Training Process

1. Changes in Loss and Accuracy During the Training Process

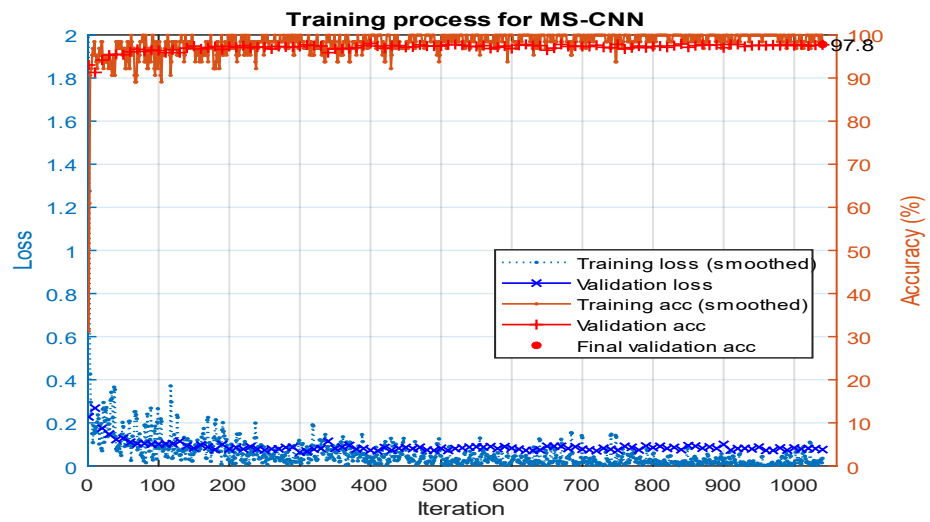
In this study, we conducted exhaustive training experiments on datasets from three different mines (named A, B, and C) using a five-fold cross-validation method. Through visualization, we presented the changes in loss and accuracy on the training and validation sets as the training cycles and iteration numbers increased, as shown in Figure 4.6. In the figure, the left y-axis represents loss, and the right y-axis represents accuracy. To maintain a reasonable length and avoid repetition, we only displayed the training process diagram of the model that performed optimally on the validation set.

Evaluate model training effectiveness by visualizing changes in loss and accuracy, providing an intuitive understanding of the model's learning curve and training process effectiveness. Detecting overfitting involves noticing a continuous decrease in loss and increase in accuracy on the training set, while the validation set shows increasing loss and decreasing accuracy. Underfitting is identified when both training and validation sets exhibit high loss and low accuracy, indicating a need for increased model complexity or extended training epochs.

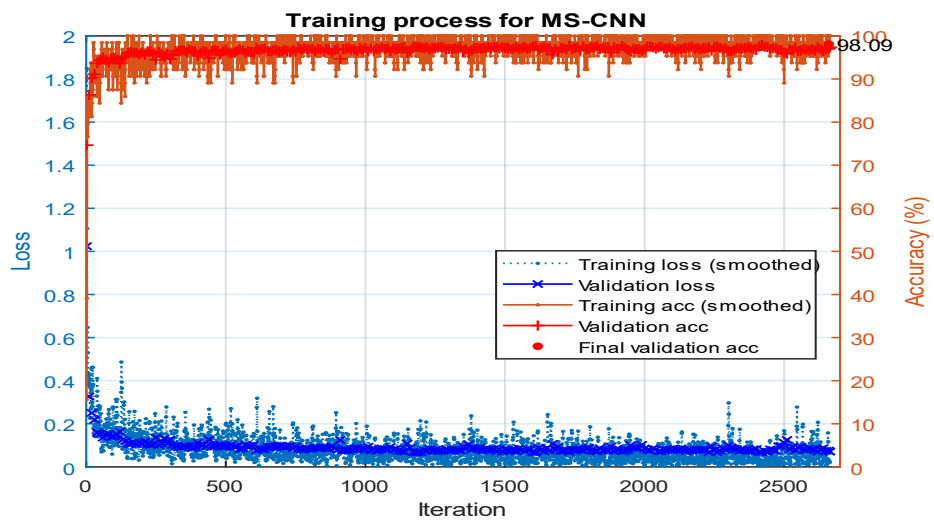
To optimize the model, observe the training curves and adjust parameters like learning rate and batch size as needed. This proactive approach helps refine the training process and enhances overall model performance.



(a) Training process of MS-CNN on dataset A



(b) Training process of MS-CNN on dataset B



(c) Training process of MS-CNN on dataset C

Figure 4.6 Training process of the MS-CNN model on different mine datasets.

➤ Loss Change Plot:

- **Meaning:** The loss function measures the difference between the model's predictions and the true labels. Common loss functions include cross-entropy loss and mean squared error.
- **Purpose:** Monitoring the loss function's changes helps us understand the model's learning progress. At the beginning of training, the loss value is usually high, and it should gradually decrease as the number of iterations increases.
- **Significance:** By observing the loss change plot, we can determine if the model is learning effectively. If the loss value does not decrease significantly or fluctuates greatly, it may be necessary to adjust the learning rate, optimizer, or model architecture.

➤ Accuracy Change Plot:

- **Meaning:** Accuracy measures the proportion of correctly predicted samples to the total number of samples. For classification tasks, accuracy is a direct performance metric.
- **Purpose:** Tracking the changes in accuracy can evaluate the model's performance improvement on the training and validation sets. Typically, accuracy is low at the start of training and should gradually increase with more iterations.
- **Significance:** By analyzing the accuracy change plot, we can assess the model's training effectiveness. If accuracy significantly improves on the training set but performs poorly on the validation set, it may indicate overfitting, necessitating the use of regularization, data augmentation, or adjusting the model's complexity.

These diagrams are important tools for understanding the dynamics of model learning and assessing its generalization ability. They not only record the adjustment and optimization trajectory of the model at various iterative stages but also lay a solid foundation for subsequent model optimization work and in-depth data analysis.

Taking Figure 4.6(a) as an example, we analyzed the training process of the MS-CNN model. The figure detailed the smoothed accuracy and loss curves during the training process, as well as the accuracy and loss values obtained on the validation set. Overall, it demonstrated the training progress of the MS-CNN model on dataset A,

capturing the dynamic changes and results of accuracy and loss on both the training and validation sets. The training process was efficiently completed in 7 minutes, comprising 8 epochs, with each epoch containing 128 iterations, totaling 1,024 iterations. Validation was performed every 10 iterations. The training was conducted on a single GPU, with the learning rate maintained at a constant level of 0.001. From the numerical values in the figure, after 40 iterations, the model's accuracy basically stabilized at and above 90%, and the loss was maintained at and below 0.23. As the number of iterations increased, the model's accuracy and loss gradually stabilized and ultimately remained at their optimal values. The final validation accuracy of the model was 96.98%.

2. Five-Fold Cross-Validation Experimental Results

Additionally, we have thoroughly documented and analyzed the training efficiency and validation accuracy of the MS-CNN model on different datasets. The experimental results can be found in Table 4.5.

Table 4.5 MS-CNN model training results with five-fold cross-validation

Results	Validation accuracy (%)			Training time (s)		
	Fold_No.	A	B	C	A	B
1	96.98	96.94	97.86	429.32	441.16	2012.36
2	96.89	97.23	98.09	496.89	481.22	2068.55
3	96.21	97.33	97.34	467.07	443.66	2056.21
4	96.89	97.80	97.30	416.71	406.00	2026.12
5	96.49	97.71	96.51	497.48	444.76	2138.19
Average	96.69	97.40	97.42	461.49	443.36	2060.29

Through meticulous data analysis, we observed that the MS-CNN model demonstrated the highest validation accuracy on dataset C, reaching a peak of 98%. Considering the variance in sample sizes across datasets A, B, and C, which are 5138, 5232, and 13334 samples respectively, dataset C contains approximately 2.6 times the number of samples compared to dataset A, while dataset B has 94 more samples than A, accounting for about 39% of the sample size of dataset C. This gradient difference in sample sizes directly influenced the training duration: datasets A and B had similar training times, both under 8 minutes, whereas dataset C required a longer duration, approximately 35 minutes.

Based on the correlation analysis between sample size and training duration, it is reasonable to infer that although dataset C has 2.5 times the samples of A, its training time is nearly 4.3 times that of A. Despite dataset B having only 1.8% more samples than A, its training time is comparable to A, and in some cases, even shorter. It should be emphasized that the proportional relationship between training time and sample size we propose is an approximate inference based on the current data and not a strict mathematical ratio. In practical applications, training duration is influenced by a multitude of factors, including but not limited to the complexity of the samples, the complexity of the model architecture, and hardware performance. This comprehensive consideration is crucial for understanding the efficiency and accuracy during the model training process and provides valuable insights for future model optimization and algorithmic improvements.

4.4.4 Testing Results

Table 4.6 presents the performance of the MS-CNN model on three different test sets (A, B, C). Across all test sets, the model's test accuracy exceeded 97%, with an average accuracy of 97.58%, indicating the MS-CNN model's excellent performance on all datasets. The Kappa statistic, a key measure of classification consistency, has a mean value of 0.968, nearly approaching perfect consistency, further confirming the model's high reliability in classification tasks. In terms of test time, we observed that test set B had the shortest test time of 3.28 seconds, while test set C had the longest test time of 9.07 seconds, indicating a significant correlation between test time and the scale and complexity of the datasets. Despite variations in test times across different datasets, overall, the MS-CNN model not only shows excellent performance in classification accuracy but also achieves a high level of consistency.

Table 4.6 Performance of the MS-CNN model on different test sets

Dataset	Test-accuracy (%)	Kappa	Test-time (s)
A	97.43	0.966	3.78
B	97.71	0.970	3.28
C	97.60	0.968	9.07

Figure 4.7 provides a detailed illustration of the MS-CNN model's performance on specific classification tasks across different test sets through confusion matrices.

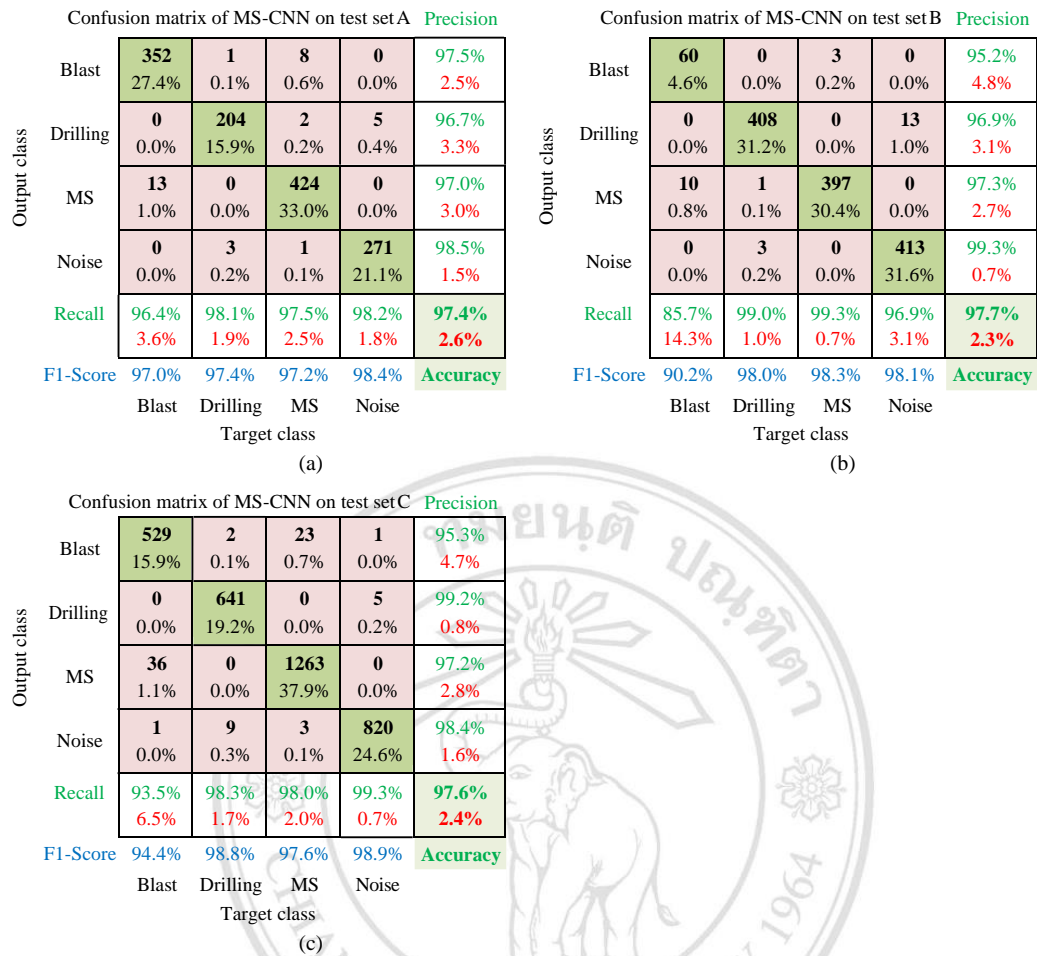


Figure 4.7 Confusion matrices of the MS-CNN model on three test datasets.

In the confusion matrix for test set A, the MS-CNN model demonstrated good classification accuracy. Specifically, the Blast category achieved a correct identification rate of 97.5%, the highest among the three datasets, although approximately 2.4% of samples were incorrectly classified as microseismic events (MS). The identification precision for the Drilling category was 96.7%, with 3.3% of samples misclassified as noise or drilling events. The identification precision for microseismic events was 97%, with 3% of samples misclassified as blasting events. The Noise category had the highest correct identification rate at 98.5%, indicating the model's high accuracy in noise recognition, although a small number of samples may have been misclassified as drilling or microseismic events.

In the confusion matrix for test set B, the MS-CNN model also showed high classification performance. The precision for the Blast category reached 95.2%, with 4.6%

of samples incorrectly classified as microseismic events. The Drilling category had a correct identification rate of 96.9%, with 3.1% of samples incorrectly categorized as noise events. The precision for microseismic events was 97.3%, despite a certain proportion of samples being prone to misclassification as blasting events. The Noise category performed the best with a 99.3% precision, further proving the model's effectiveness in differentiating noise from other categories such as microseismic events.

The confusion matrix for test set C shows that the model's overall performance on this dataset is equally remarkable. Specifically, the correct identification rate for the Blast category was 95.3%, slightly higher than test set B, although most misclassified samples were primarily misclassified as microseismic events. The Drilling category had a very high correct identification rate of 99.2%, with only 0.8% of samples misclassified as noise events. The precision for microseismic events was 97.2%, and the precision for the Noise category was 98.4%. These results indicate that the MS-CNN model also demonstrated strong capabilities in distinguishing between drilling, noise, and other categories when processing test set C. Overall, the results of these confusion matrices not only validate the MS-CNN model's classification capabilities across all test sets but also highlight its generalization performance in different environments.

4.5 Results of the Transfer Learning method

4.5.1 Hyperparameter Settings

Based on our experience with hyperparameter settings in the MS-CNN model, we compared the training effects of using the SGDM and Adam optimizers. After careful consideration, we selected SGDM for its momentum component, which helps the model converge more quickly and stabilizes the training process by reducing oscillations. Setting the initial learning rate to 0.001 provided a good balance for the model to start learning without making large jumps in the weight space, which can be crucial in fine-tuning a model that has already been pre-trained.

Max epochs to 8 was a strategic choice to ensure that the model does not overfit the training data. This number of epochs allows the model sufficient time to adjust to the specifics of the new task without excessive training that could lead to poor generalization. Choosing a mini-batch size of 32 was a compromise between computational efficiency and the model's ability to generalize from the training data. This size is large enough to

provide a good estimate of the gradient for the optimization while keeping the noise level that comes with smaller batch sizes, which can be beneficial for training stability.

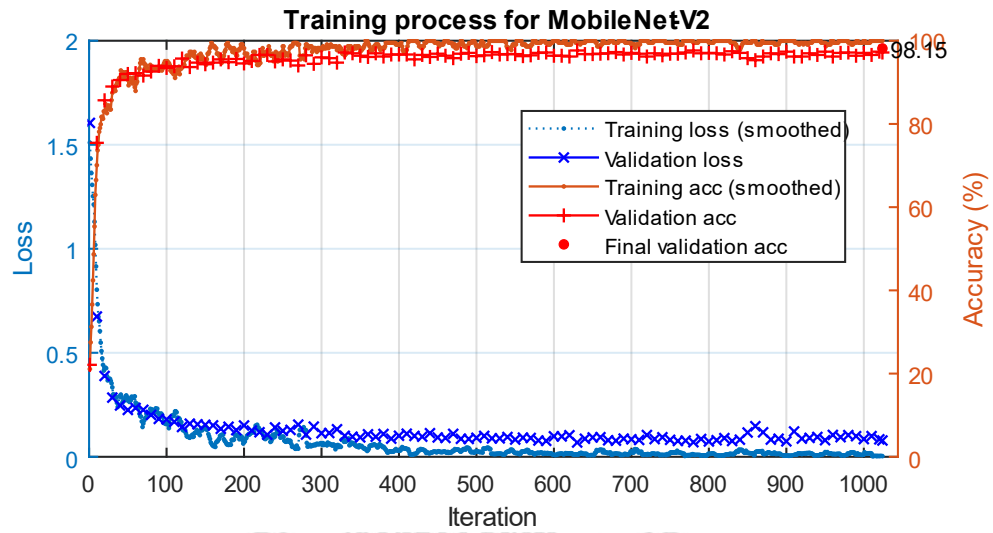
Shuffling the data every epoch ensures that the model does not develop any bias towards the order of training samples, promoting a more robust learning process. Lastly, setting a validation frequency of every 10 iterations allows for a regular assessment of the model's performance on unseen data, which is crucial for making informed decisions about when to stop training to avoid overfitting.

These hyperparameter settings collectively form a training strategy that is not only efficient and stable but also highly adaptable to the nuances of the task at hand. By carefully tuning these hyperparameters, we aimed to enhance the model's ability to generalize well to new data while maintaining high accuracy and reducing reliance on extensive manual tuning.

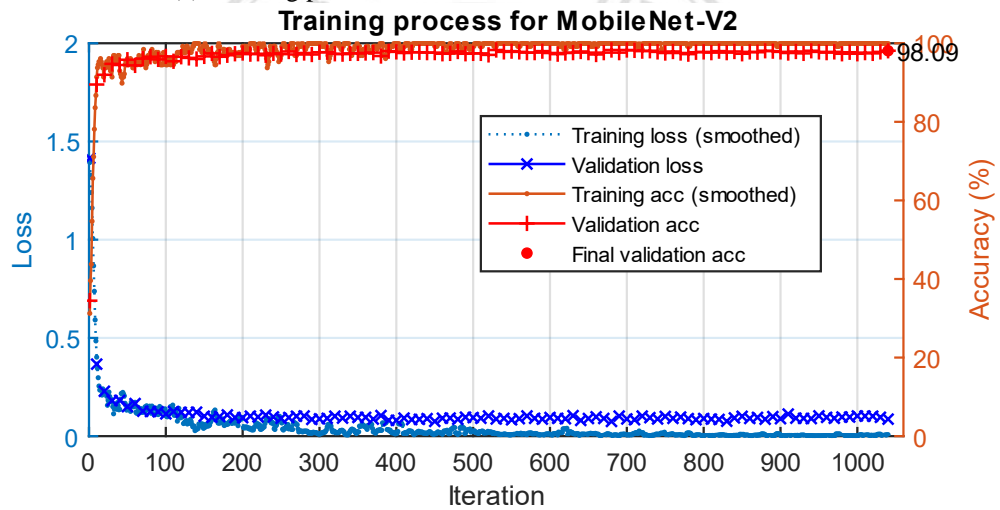
4.5.2 Training Process

In this study, we selected datasets from three different mines (labeled A, B, and C) for model training and conducted an in-depth analysis of the performance changes during the training process. Using dual-axis charts, we clearly demonstrated the evolution of loss and accuracy on the training and validation sets for the three transfer learning models: MS-MobileNet-V2, MS-ResNet-18, and MS-Inception-V3, as the training cycles and iteration numbers increased. Figures 4.8, 4.9, and 4.10 correspond to the performance changes of the aforementioned models, respectively. These charts reveal the optimization trajectory of the models during the iterative process, laying the foundation for subsequent model improvements and in-depth data analysis.

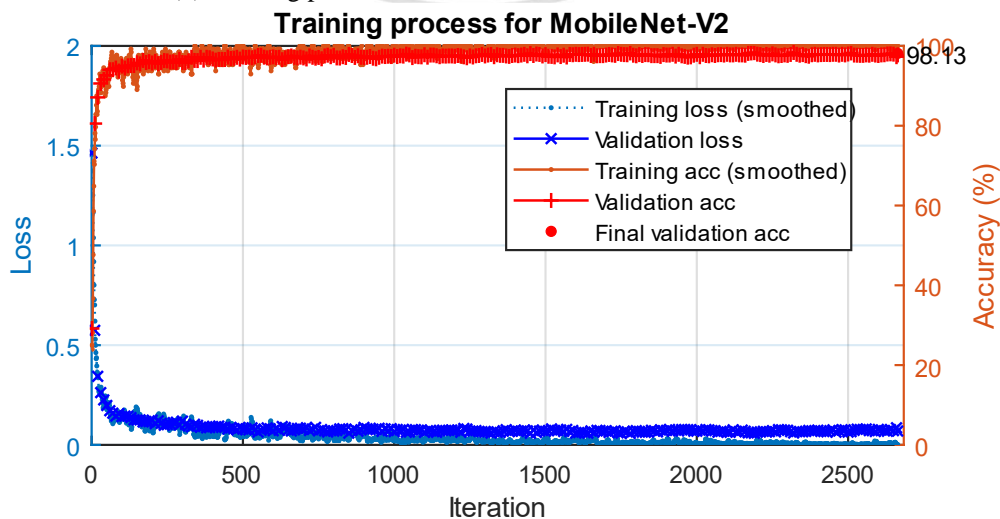
Taking the results in Figure 4.8 as an example for analysis, the MS-MobileNet-V2 model showed consistency in the training process across the three different datasets, including the dynamic changes and results of accuracy and loss on the training and validation sets. It can be seen from the figure that after completing a training cycle on dataset A, the model's validation accuracy stabilized above 90%. On datasets B and C, the model's convergence speed was faster. As the number of iterations increased, the model's accuracy and loss gradually stabilized and ultimately remained at optimal values. The final validation accuracy of the model reached above 98%.



(a) Training process of the MS-MobileNet-V2 model on dataset A

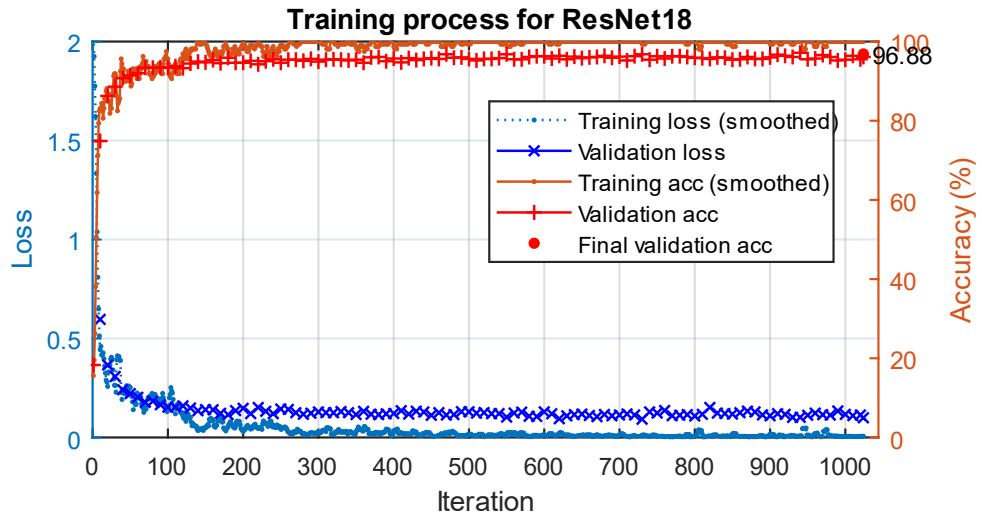


(b) Training process of the MS-MobileNet-V2 model on dataset B

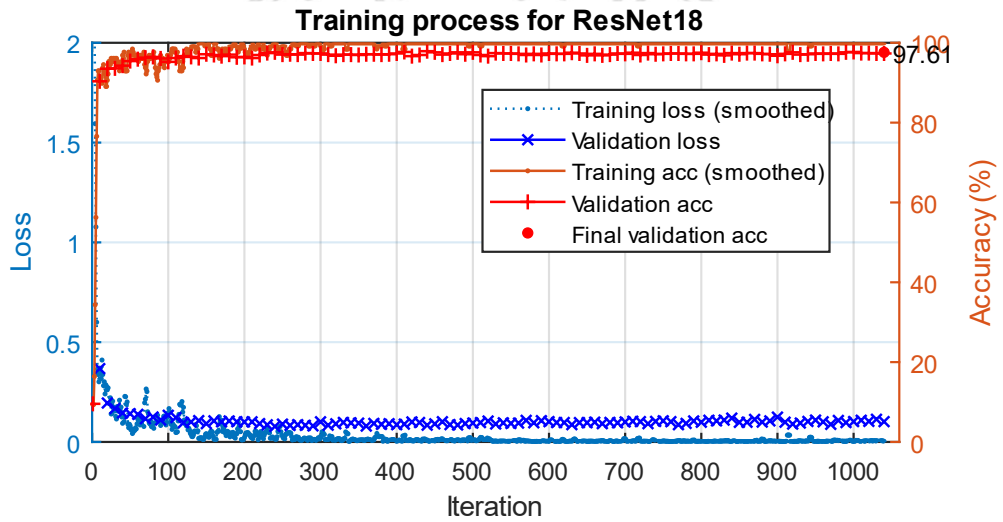


(c) Training process of the MS-MobileNet-V2 model on dataset C

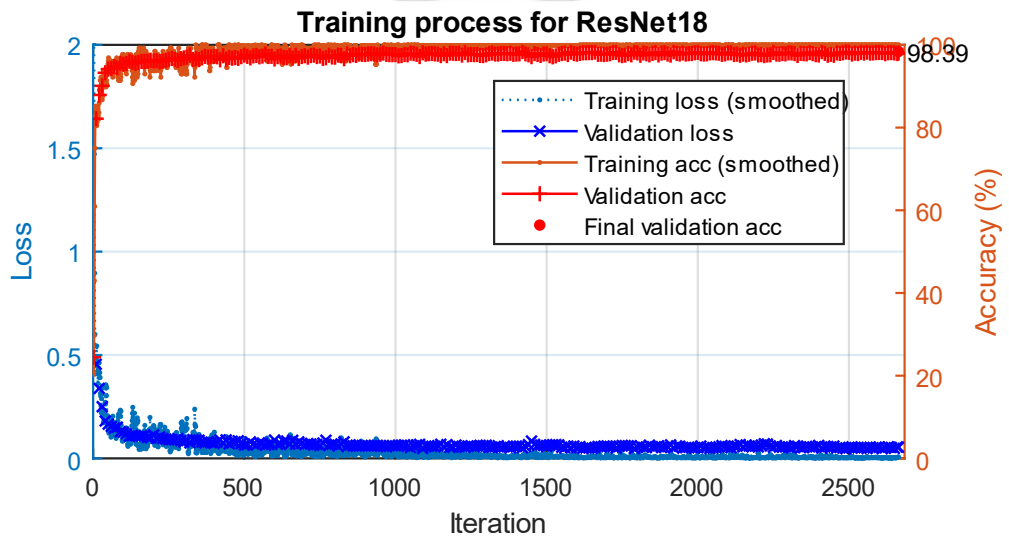
Figure 4.8 Training process of the MS-MobileNet-V2 model on three datasets.



(a) Training process of the MS-ResNet-18 model on dataset A

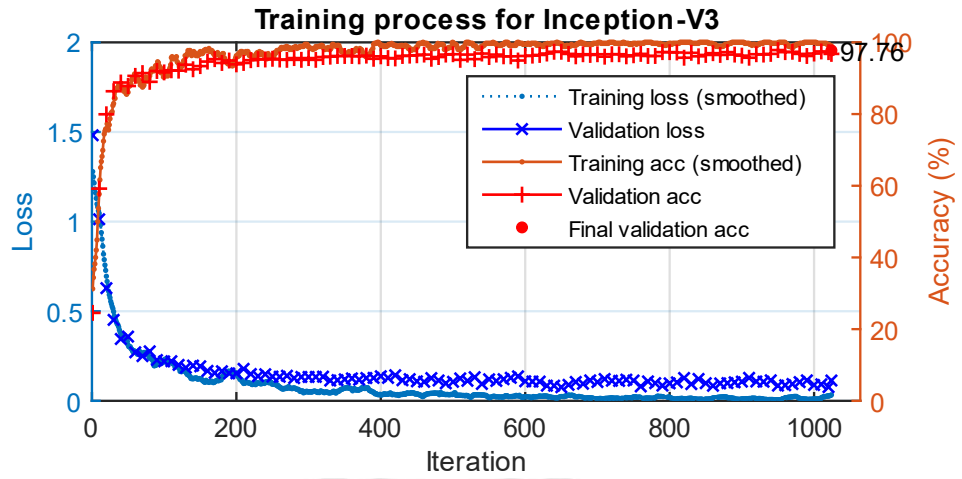


(b) Training process of the MS-ResNet-18 model on dataset B

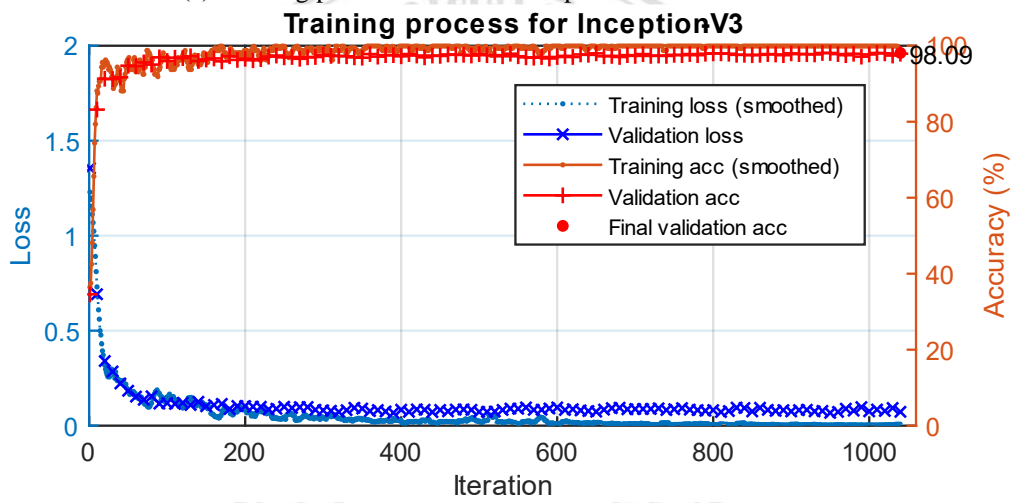


(c) Training process of the MS-ResNet-18 model on dataset C

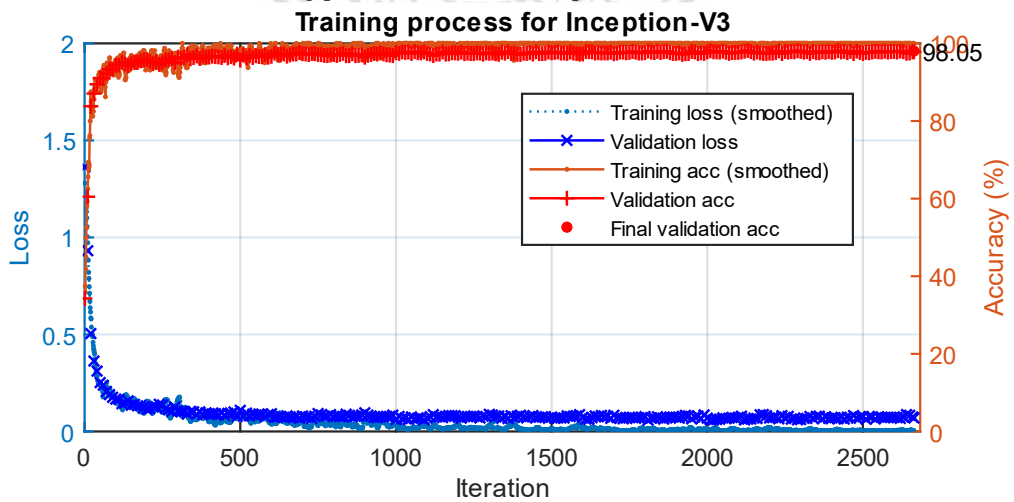
Figure 4.9 Training process of the MS-ResNet-18 model on three datasets.



(a) Training process of the MS-Inception-V3 model on dataset A



(b) Training process of the MS-Inception-V3 model on dataset B



(c) Training process of the MS-Inception-V3 model on dataset C

Figure 4.10 Training process of the MS-Inception-V3 model on three datasets.

Through these charts, we not only recorded the gradual improvement of model performance but also provided a key perspective for assessing the model's generalization ability. The consistency of the model's performance across different datasets further confirms its generalization capability. Looking at the changes in the loss function: in the initial stage of training, the loss is high because the transfer learning model needs to adapt to the recognition and classification tasks of microseismic event waveform diagrams. In the middle stage, as training progresses, the loss gradually decreases, indicating that the model is learning and recognizing the features of microseismic event waveform diagrams. In the later stage, the loss function tends to stabilize, indicating that the model has adapted well to the target task.

Looking at the improvement in accuracy: in the early training period, the accuracy is relatively low because the model has not yet adapted to the new task. As training progresses, the accuracy significantly improves, indicating that the model's performance is continuously improving. In the later stages of training, the accuracy reaches a higher level and tends to stabilize. Through detailed performance analysis, we can gain a deeper understanding of the model's learning dynamics, ensuring its effectiveness and robustness in practical applications.

4.5.3 Testing Results

Table 4.7 provides a detailed account of how three models—MS-MobileNet-V2, MS-ResNet18, and MS-Inception-V3—fare in terms of accuracy, training time, test time, and Kappa statistics on datasets A, B, and C.

Table 4.7 Performance of transfer learning models on different datasets

Model	Dataset	Train time(s)	Test time(s)	Accuracy (%)	Kappa
MS-MobileNet-V2	A	1630.74	10.28	98.21	0.976
	B	1703.02	10.13	98.01	0.974
	C	7311.72	24.05	98.26	0.977
MS-ResNet18	A	909.93	5.78	98.13	0.975
	B	927.71	5.91	97.55	0.968
	C	4329.12	11.99	98.11	0.975
MS-Inception-V3	A	8702.44	17.39	98.71	0.983
	B	8788.83	41.58	97.55	0.968
	C	37211.09	98.94	98.17	0.976

The MS-MobileNet-V2 model shows a high level of accuracy, consistently scoring above 98% across all datasets. It has a slight decrease in accuracy from dataset A to B, followed by a marginal increase in dataset C. The Kappa statistic for this model is also very high, indicating excellent agreement between predicted and actual labels, with minimal prediction errors.

In contrast, the MS-ResNet18 model demonstrates a slightly lower but still impressive accuracy, with the shortest training times among the three models. This suggests that MS-ResNet18 is not only accurate but also efficient in terms of computational resources required for training, making it a strong candidate for real-world applications where time and computational power are critical.

MS-Inception-V3, while achieving the highest accuracy on dataset A, shows a significant increase in training time on dataset C, which is considerably longer than the other two models. Despite this, it maintains a high accuracy and Kappa statistic, indicating robust performance. However, the longer training time may be a consideration when choosing this model for tasks where training speed is a concern.

In summary, all three models exhibit strong performance with high accuracy and Kappa values. MS-MobileNet-V2 stands out for its consistency and high Kappa statistic, MS-ResNet18 for its training efficiency, and MS-Inception-V3 for its top accuracy on dataset A, albeit with a longer training time on dataset C. These models offer valuable insights and a solid foundation for further exploration and application in the realm of transfer learning for image classification.

- Results of confusion matrices

We utilized confusion matrices to elaborate on the relationships between the real labels and model-predicted labels for transfer learning models across different categories. Figure 4.10 presents the confusion matrix for MS-MobileNet-V2 on three distinct test sets (A, B, C), while Figures 4.11 and 4.12 correspond to the confusion matrices for MS-ResNet-18 and MS-Inception-V3 models, respectively. In these matrices, rows represent model-predicted class labels, and columns represent actual class labels. The values on the diagonal reflect the correct prediction count for each class, directly influencing the model's classification performance.

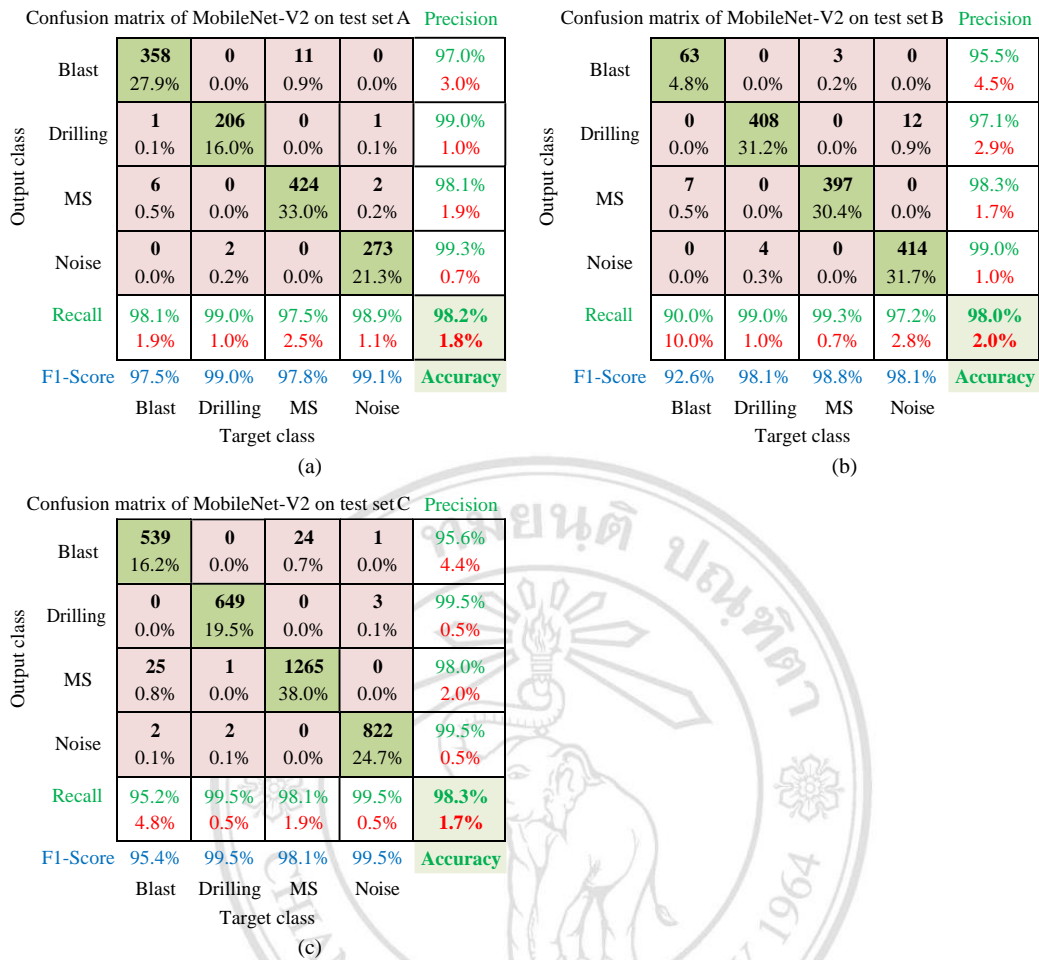


Figure 4.11 Confusion matrix of the MS-MobileNet-V2 model on various test datasets.

Taking the confusion matrix of MS-MobileNet-V2 on test set A (Figure 4.11(a)) as an example for analysis, we observed the highest precision for the Noise event (99.3%), showcasing the model's excellent performance in noise event recognition, with 273 samples correctly classified and only 3 samples misclassified. The precision for Drilling events was 99%, while for MS events, it was 98.1%. In contrast, the precision for Blast events was relatively lower at 97%, primarily due to the similarity between microseismic and blasting events, leading to potential confusion in the model's differentiation.

By comparing and analyzing the confusion matrices across the three test sets, we can explore the model's performance across different datasets. Overall, the MS-MobileNet-V2 model demonstrates excellent classification performance across all three datasets, particularly excelling in noise event recognition with a 99% precision rate across all datasets, indicating a high level of recognition capability for this category. For the core

category of microseismic events, the model achieves a precision rate of 98% across all datasets, further validating its robustness in key categories.

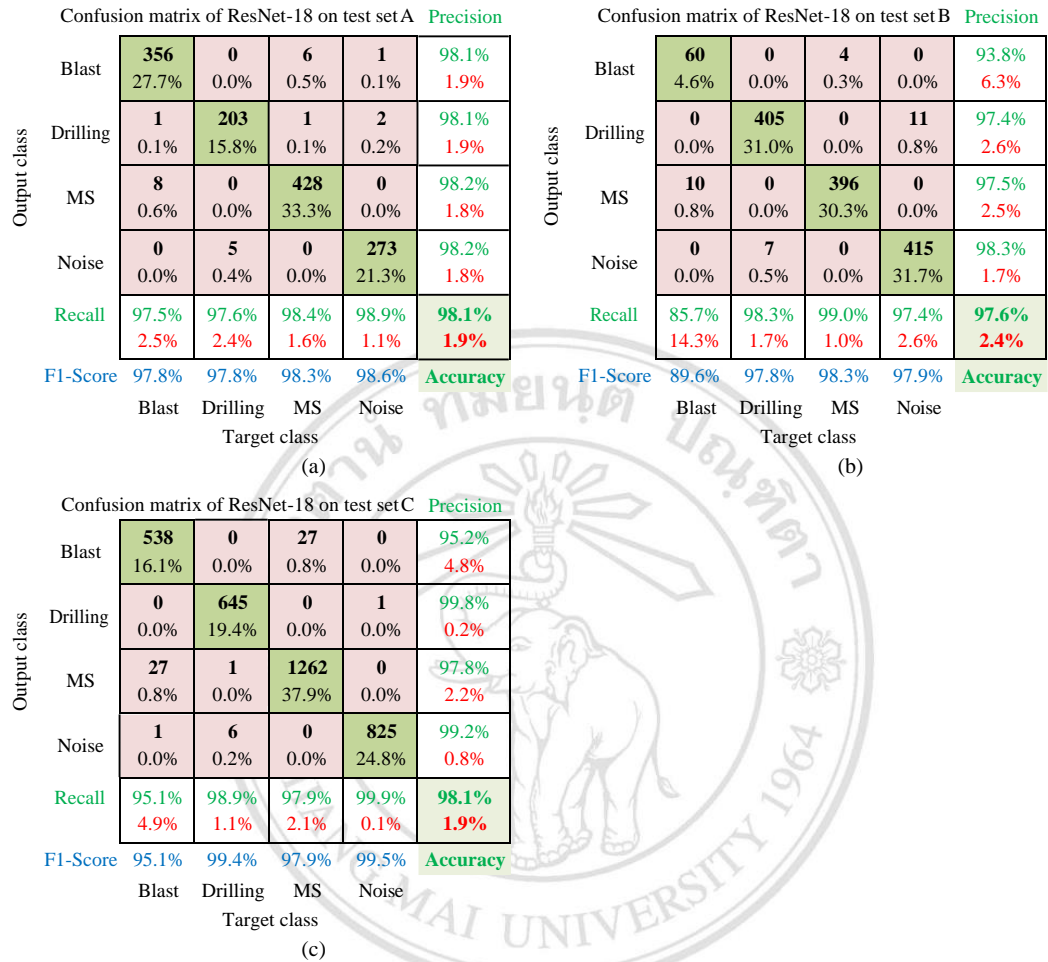


Figure 4.12 Confusion matrix of the MS-ResNet-18 model on various test datasets.

Upon a comprehensive analysis of the performance of the MS-ResNet-18 model across different test sets (Figure 4.12), we observed consistently good performance in classifying various categories, despite minor category confusion. For instance, in test set A, the precision rates for Blast and Drilling events were both 98.1%, while for MS and Noise events, they were 98.2%. In test set B, the precision rate for Blast events was slightly lower at 93.8%, with Drilling and MS events at 97.4% and 97.5%, respectively, and Noise events reaching 98.3%. In test set C, Blast events had a precision rate of 95.2%, while Drilling, MS, and Noise events exhibited higher precision rates of 99.8%, 97.8%, and 99.2%, respectively. These results indicate that, despite minor confusion in certain categories, the ResNet-18 model maintains a high overall classification accuracy, particularly excelling in recognizing Noise and Drilling events.

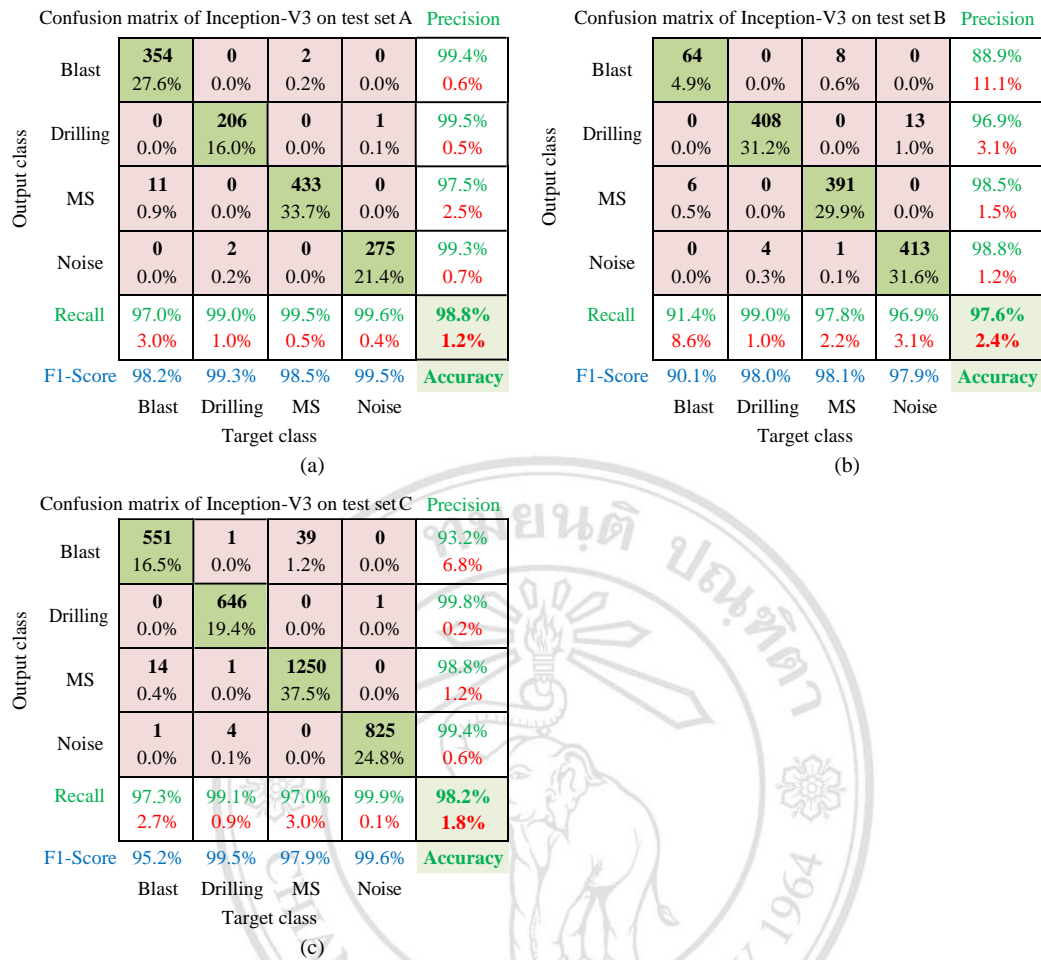


Figure 4.13 Confusion matrix of the MS-Inception-V3 model on various test datasets.

The confusion matrix results for the MS-Inception-V3 model across different test sets (Figure 4.13) also demonstrate high classification accuracy, especially in distinguishing between Drilling and Noise events. For Blast events, the model achieved precision rates of 99.4% and 93.2% in test sets A and C, respectively, but dropped to 88.9% in test set B. The precision rates for MS events were 97.5%, 98.5%, and 98.8% in test sets A, B, and C, respectively. Despite minor category misclassifications, overall, the Inception-V3 model maintains high classification performance across different test sets, displaying good generalization capabilities and robustness.

In conclusion, the overall performance of the transfer learning models across the three test sets is satisfactory. Despite some category confusion, the models demonstrate high precision in identifying key event categories. Future research efforts could focus on reducing confusion between categories to enhance the models' classification accuracy and reliability.

4.6 Summary

Considering the feature complexity and event distribution of the three datasets, along with the overall performance of the five shallow machine learning classification models, we can conclude that no single model is universally applicable; each has its own strengths and limitations. Selecting the appropriate model involves considering the characteristics of the dataset, the requirements of the classification task, and the performance of the model. In practical applications, it may be necessary to use methods such as cross-validation to assess the performance of different models, thereby making the most suitable choice. Additionally, model tuning and feature engineering are crucial for enhancing classification performance.

Compared to HOG combined with shallow machine learning models, CNNs offer the advantage of automatically learning complex feature representations from data. With their multi-layer architecture, CNNs can capture a hierarchy of features—from simple to complex—which makes them highly effective for processing high-dimensional data such as images. Moreover, CNNs facilitate end-to-end learning, directly mapping input data to classification outcomes, thereby simplifying the model-building process.

In the task of identifying and classifying microseismic events, transfer learning models have demonstrated significant performance. Specifically, the Inception-V3 model exhibited the highest recognition accuracy (98.71%), closely followed by the MobileNet-V2 model (98.26%). Notably, the ResNet-18 model maintained high recognition accuracy (98.13%) while also possessing significant recognition efficiency advantages, making it particularly useful in applications requiring rapid response.

Considering all metrics, the advantages of Inception-V3 and MobileNet-V2 in recognition accuracy, along with the balance achieved by ResNet-18 between efficiency and accuracy, provide robust technical support for the automatic detection and classification of microseismic events. The performance of these models not only validates the potential of transfer learning in practical applications but also offers valuable insights for future research and applications.

Proper selection of hyperparameters is crucial for the performance of deep learning models. In practice, it is necessary to meticulously tune and optimize hyperparameters

based on specific tasks and hardware conditions to achieve the best combination and maximize model performance.



ลิขสิทธิ์มหาวิทยาลัยเชียงใหม่
Copyright© by Chiang Mai University
All rights reserved

CHAPTER 5

DISCUSSIONS

5.1 Introduction

In this chapter, we have conducted an in-depth analysis of the key findings from the research on intelligent identification and classification of microseismic events, and discussed the significance of these results at both the theoretical and practical levels. The chapter begins with an overview of the main outcomes of microseismic event identification, reiterates the performance metrics of the classification models, and provides an in-depth explanation of the factors contributing to the model performance.

Furthermore, this chapter engages in a comprehensive discussion of the machine learning techniques employed, including their strengths and limitations, as well as the specific impact of data preprocessing, feature selection, and model selection on the results. In terms of methodology, the chapter evaluates the effectiveness and reliability of the research methods and discusses the rationality of the experimental design and data analysis approaches. At the same time, we honestly analyze the main limitations and challenges encountered during the research process and discuss the potential impact of these limitations on the research findings and conclusions.

Finally, based on these limitations, we propose directions for future research aimed at further improving model performance and expanding its application scope, thereby laying the foundation for the future development of intelligent identification and classification technology for microseismic events.

5.2 Analysis of Results

Based on the experimental results in Chapter 4, our research yielded the following key findings: (1) The pattern recognition approach using HOG features extracted from waveform images, combined with shallow machine learning methods, demonstrated

promising results. Specifically, we utilized five common classifiers (SVM, Linear, Decision Tree, KNN, and Fisher Discriminant). Notably, the SVM classifier outperformed others using dataset A, achieving an accuracy of 97.12% and a Kappa statistic of 0.961. (2) We also implemented a convolutional neural network model, which surpassed the HOG-SVM method in both accuracy and robustness. Our MS-CNN model excelled with an accuracy of 97.43% and a Kappa statistic of 0.966 on dataset A. (3) Lastly, employing transfer learning techniques, we built target models (MS-MobileNet-V2, MS-ResNet-18, and MS-Inception-V3) for microseismic event recognition and classification tasks based on pre-trained deep learning models, resulting in further enhancements. Among them, the MS-Inception-V3 model achieved the highest accuracy of 98.71% on dataset A.

5.2.1 Analysis of Training Time Differences

The training time of different models is influenced by factors such as model complexity and optimization algorithms. Among the five shallow machine learning models compared, the discriminative models and SVM models have longer training times. This is primarily because they require numerous iterations and optimization steps to determine the optimal decision boundary or hyperplane. The decision tree model has the next longest training time, likely due to its need for feature selection, tree construction, and handling a large amount of data partitioning and node optimization tasks. In contrast, the linear model benefits from its straightforward classification mechanism, resulting in a lighter computational load and shorter training time. The KNN model has the shortest training time because it only involves storing training samples and classifying based on distance, lacking complex training steps.

Compared to shallow machine learning models, deep learning models based on convolutional neural networks require a large number of iterations and optimizations to find the best parameters, and their training time is closely related to the chosen hyperparameters, including the optimizer, learning rate, training epochs, and batch size. With specific hyperparameter configurations, the average training time of the MS-CNN model we built is about 10 times that of the SVM model.

For transfer learning models, due to their complex network structures and the large number of parameters involved, their training time is longer than the MS-CNN model.

Although transfer learning uses pre-trained models to reduce the training burden, it still requires data preprocessing, network parameter fine-tuning, and hyperparameter adjustment for specific tasks, all of which require additional time. Moreover, deep learning models typically rely on powerful computational resources, and if resources are limited, they will also increase training time. Therefore, when using DNN for transfer learning, it is necessary to consider the complexity of the model, available computational resources, and training strategies to improve training efficiency.

The above analysis helps us understand the trade-offs in the training efficiency of different models and provides guidance for choosing the appropriate model.

5.2.2 Analysis of Testing Time Differences

Testing time is primarily influenced by the computational complexity required for model predictions and the number of samples. Among the five shallow machine learning models compared, the KNN model has the longest testing time because it needs to calculate the distance between each test sample and all training samples, and then identify the nearest neighbors. This computationally intensive process results in longer testing times with large training datasets. In contrast, the decision tree model performs the best in terms of testing time as it relies on pre-established decision boundaries for predictions, involving minimal computation. The SVM and linear models also demonstrate short testing times, approaching real-time computational capabilities. The Fisher discriminant model has relatively longer testing times due to more complex linear operations involved compared to the SVM and linear models.

For transfer learning models based on deep neural networks, testing time is closely related to the complexity of the network structure and the number of parameters. ResNet-18 shows performance close to or even superior to the discriminant model in testing due to its streamlined network structure and a smaller number of parameters. This indicates that network efficiency and optimization play a key role in fast inference.

MobileNet-V2, though optimized for mobile and edge computing environments, may have its unique lightweight design, such as depthwise separable convolutions, resulting in testing times approximately twice that of ResNet-18. This difference emphasizes the impact of architectural choices on testing efficiency.

Inception-V3 has a more complex network structure and more parameters, making its testing time relatively longer. However, compared to the KNN model, Inception-V3's testing time is still within an acceptable range. This suggests that despite model complexity, proper optimization and computational resource management can still achieve reasonable testing speeds.

The MS-CNN model we built is superior in testing efficiency compared to the three aforementioned transfer learning models, likely due to its balanced network design and effective use of computational resources. However, compared to models with lower computational demands such as decision trees, SVM, and linear models, there is still room for improvement in the testing efficiency of CNN models. This suggests that although CNN models have advantages in feature learning capabilities, further model simplification and acceleration strategies may be needed in resource-constrained environments.

In summary, the differences in testing times of machine learning models can be attributed to the complexity of the network structure, the number of parameters, and the demand for computational resources. Understanding these factors is crucial for selecting models suitable for specific application scenarios and guides us on how to improve testing efficiency through model optimization and hardware acceleration.

5.2.3 Analysis of Model Performance Differences

1. Analysis of Model Performance Variations on the Same Dataset

In dataset A, microseismic events are the most prevalent, accounting for 34% of the total, followed by blasting events at 28%, noise events at 22%, and drilling events the least with only 16%. Although there is an imbalance in the quantity of events, this distribution is representative of the actual data collection in most mines. Therefore, we selected dataset A to analyze the performance differences among various models.

Among the five shallow learning models, the SVM model performed the best, with an identification accuracy of 97.12% and a Kappa coefficient of 0.961. The SVM model stood out due to its ability to find the optimal hyperplane for decision boundaries, effectively handling high-dimensional space issues; the use of kernel tricks to deal with nonlinear problems without explicit mapping; robustness to outliers and noise, focusing only on support vectors that affect the decision boundary; and enhancing generalization

ability by maximizing the margin. Moreover, as a mature algorithm, SVM has a broad research base and community support, allowing it to perform well in multi-class classification problems.

Our MS-CNN model further improved upon the SVM, increasing the accuracy by 0.31 percentage points and the Kappa coefficient by 0.005. The CNN model is superior to SVM because its deep architecture can automatically learn hierarchical features directly from raw data, thereby enhancing representational and classification accuracy.

The three transfer learning models all demonstrated excellent performance, with identification accuracies all above 98% and Kappa coefficients above 0.975. Their high performance is mainly due to the use of pre-trained weights on large-scale datasets (such as ImageNet), which have learned rich feature representations and have been further adapted to the microseismic event identification and classification tasks through fine-tuning. As a result, they can leverage rich feature representations and make highly accurate predictions. In particular, the Inception-V3 model performed the best among all models, with an identification accuracy of 98.71% and a Kappa coefficient of 0.983. This achievement is attributed to Inception-V3's efficient architectural design, including parallel convolutional branches and spatial aggregation, which balance the integration of features at different scales, as well as the possible application of optimized hyperparameters and advanced regularization techniques, all of which contribute to improving the model's performance and generalization ability.

In summary, the model performance analysis on dataset A shows that while shallow learning models like SVM show robustness, deep learning methods, especially CNN and transfer learning models, offer significant improvements in accuracy and reliability, highlighting their great potential for advanced event identification and classification in mining applications.

2. Analysis of Model Performance Variations on Different Datasets

To evaluate the generalizability and stability of the models, in addition to the dataset from Mine A, we have also included datasets from Mines B and C. Dataset B has a similar total number of samples to A (B has 118 more samples than A), with noise events accounting for the largest proportion, followed by drilling and microseismic events, and the fewest blasting events. The proportion of these four types of events from largest to

smallest is approximately: 32%, 32%, 31%, and 5%. Dataset C has the largest total number of samples (greater than the sum of datasets A and B), with microseismic events being the most frequent (about 39%), noise events second (about 24%), blasting events third (about 20%), and the fewest drilling events (about 17%).

Dataset A serves as the core of our experiment, providing a representative sample set and establishing a benchmark for model training and validation. Dataset B is designed to assess the stability of the models when faced with class distribution imbalances, which is crucial for common challenges in practical applications. Dataset C is used to explore the potential impact of data volume on model performance and its generalization ability, which is particularly critical for large-scale datasets. Through these monitoring datasets from three mines, we can comprehensively evaluate the performance of the models under different conditions, ensuring their effectiveness and reliability in diverse application scenarios.

When analyzing the performance of shallow learning models on datasets A, B, and C, we found that the SVM and Linear models demonstrated similar and outstanding overall performance. This may be attributed to their effectiveness in finding optimal decision boundaries in high-dimensional feature spaces and their good adaptation to the characteristics of the datasets. In contrast, the Discriminant model also performed well but was slightly inferior to the SVM and Linear models, possibly due to differences in model complexity or generalization ability. The performance of KNN and Decision Tree models fluctuated significantly, with lower accuracy and consistency, possibly due to their higher sensitivity to dataset size, class imbalance, noise sensitivity, or parameter settings. These factors indicate that while the SVM and Linear models perform robustly on these datasets, other models may require further adjustment and optimization to improve their performance and generalization ability on specific datasets.

The MS-CNN model outperformed the best shallow learning model, SVM, on all three datasets, possibly because it leveraged the deep architecture of convolutional neural networks to automatically extract complex features from the data, especially when dealing with data that has spatial correlations or high-dimensional structures. Additionally, the MS-CNN model may have better adapted to the diversity and complexity of the datasets through its strong generalization ability and effective

regularization techniques, thus maintaining a very high level of identification accuracy and Kappa coefficients.

The three transfer learning models performed well on all datasets, but MobileNet-V2, due to its lightweight architecture, showed particularly stable 98% accuracy on all three datasets, while ResNet-18 and Inception-V3 experienced a slight decrease in accuracy on dataset B. This may be due to the uneven class distribution in dataset B, which negatively affects models sensitive to class imbalance, while MobileNet-V2 may be more robust to such imbalances.

Analysis of the classification models for four types of events based on precision, recall, and F1 score indicates that noise events and drilling events, with their distinct waveform characteristics and high recognizability, tend to be better identified across various classification models. Next in line are microseismic events, while blasting events, which share many similar features with microseismic events, are more prone to misclassification, leading to lower precision, recall, and F1 scores.

In dataset A, despite the proportion of samples for noise events and drilling events being less than that for blasting and microseismic events, the identification effect for both is still very good. Due to the larger number of microseismic event samples, its identification effect is better than that of blasting events. Particularly in dataset B, the identification effect for microseismic events is the best, but because there are too few samples for blasting events, the insufficient sample size leads to inadequate training of the model on this category, resulting in a lower identification accuracy for blasting events and a slight decrease in overall model performance.

In dataset C, although the sample size for noise events and drilling events is not as large as for microseismic events, their identification effects are better than that of microseismic events. This may be related to the test sample size reaching more than 500, while the sample size for blasting events is less than 500. The increased likelihood of misclassifying blasting events as microseismic events thus reduces the precision, recall, and F1 scores for microseismic events.

Overall, on the A, B, and C mining datasets, the SVM model in shallow learning, the MS-CNN model, and the transfer learning models have all demonstrated good performance across multiple evaluation metrics. Different models exhibit some variation

in the identification effect for different types of events, allowing us to choose the appropriate model for classification based on specific task requirements.

5.3 Comparison with Existing Work

To demonstrate the strengths of our research methodology, this study conducted a thorough comparison of the results with existing research in the field. Based on dataset A, we trained and tested the following models: the CNN model proposed in reference [55], the transfer learning model AlexNet from reference [108], and the transfer learning-based DNN models, including GoogLeNet and ResNet-50, as presented in reference [53]. These comparisons not only validate the effectiveness of our approach but also highlight its relative standing in the current research landscape.

Table 5.1 presents a performance comparison between shallow learning models, CNN models, and transfer learning-based DNN models with existing research methods on dataset A. Among the shallow machine learning methods, we selected the best-performing model, HOG-SVM, as a representative. Since training and testing times, accuracy, and Kappa coefficients can comprehensively reflect the efficiency and accuracy of the models, this section focuses on comparing these four key evaluation metrics.

To emphasize the main indicators and simplify the analysis, this section does not delve into a detailed comparison of single-class evaluation metrics such as precision, recall, and F1-score, allowing readers to more directly grasp the performance differences between models.

Table 5.1 Comparative experimental results of existing research methods and the method of this study

Model	Accuracy (%)	Kappa	Training time (s)	Testing time (s)
CNN [55]	94.5	0.926	139	3.33
AlexNet [108]	95.33	0.938	714.25	4.08
GoogLeNet [53]	97.43	0.966	1020.99	6.64
ResNet-50 [53]	97.74	0.970	2612.67	11.65
HOG-SVM	97.12	0.961	47.47	0.29
MS-CNN	97.43	0.966	461.49	3.78
ResNet-18	98.13	0.975	909.93	5.78
MobileNet-V2	98.21	0.976	1630.74	10.28
Inception-V3	98.71	0.983	8702.44	17.39

The experimental results indicate that the Inception-V3 model achieves the highest accuracy (98.71%) and Kappa coefficient (0.983), demonstrating its superior performance in classification tasks with high consistency and accuracy. The MobileNet-V2 and ResNet-18 follow closely with accuracies of 98.21% and 98.13%, respectively, and also exhibit high Kappa coefficients, indicating good generalization capabilities.

The HOG-SVM model shows a significant efficiency advantage, with the shortest training and testing times, making it highly suitable for applications requiring rapid response. In contrast, the Inception-V3 model has the longest training and testing times, which may affect its application in real-time systems.

The MS-CNN model matches GoogLeNet in terms of accuracy and Kappa coefficient but has shorter training and testing times, showing a better performance balance. Although MobileNet-V2 has slightly lower accuracy and Kappa coefficient compared to Inception-V3, its significantly reduced training and testing times suggest a clear advantage in speed and efficiency.

The models proposed in this study, including HOG-SVM, MS-CNN, MS-ResNet-18, MS-MobileNet-V2, and MS-Inception-V3, are competitive with the models in existing research in terms of accuracy and Kappa coefficient, and have improved training and testing times.

Overall, the analysis of Table 5.1 emphasizes the trade-offs to consider when selecting a model. If the application scenario demands high prediction speed, HOG-SVM may be the most appropriate choice. For applications that pursue the highest accuracy and can tolerate longer training times, the Inception-V3 and MobileNet-V2 models may be more favored. The models proposed in this study, especially MS-CNN, ResNet-18, and MobileNet-V2, show competitiveness in accuracy, Kappa coefficient, training, and testing times, offering a variety of choices for specific needs.

5.4 Analysis of the Advantages of This Study

5.4.1 Advantages of HOG-Shallow Machine Learning Method

To overcome the limitations of traditional manual identification of microseismic events, we have integrated existing research to propose an image recognition and classification model based on computer vision. To address the issue of relying on manual

experience for feature extraction, we employed the HOG method to automatically extract features from microseismic waveform images, which were then input into commonly used classifiers. To select the appropriate classifier, we constructed and compared five models.

The experimental results demonstrate that the Shallow Machine Learning (SML) approach combined with HOG is feasible. These five models (HOG-SVM, HOG-Linear, HOG-Tree, HOG-KNN, HOG-Discriminant) have achieved satisfactory performance across different mining datasets. In terms of overall evaluation metrics—accuracy and Kappa coefficient—the SVM classifier performed the best, exhibiting strong stability. Regarding single-class evaluation metrics—precision, recall, and F1 score—the SVM model outperformed others across all four event categories.

Taking dataset A as an example, the SVM model showed high accuracy in identifying noise and microseismic events, with F1 scores of 0.986 and 0.971, respectively. However, in terms of training and testing time, the Linear classifier had the highest computational efficiency, at 4.52 seconds and 0.11 seconds, respectively.

On dataset C, the Linear classifier displayed the highest accuracy and consistency. The SVM classifier also performed well in most cases, especially on dataset B, where its performance in microseismic event identification was second only to the Discriminant classifier, highlighting its robust capability in handling high-dimensional data. The Discriminant classifier showed the best performance when dealing with dataset B, which had an imbalanced sample size. Although the KNN classifier is simple and intuitive, its performance on certain datasets was not outstanding, particularly susceptible to noise influence when the feature dimension is high. The Decision Tree classifier performed well on simple datasets but was prone to overfitting on complex datasets, leading to a decrease in performance (Curram et al., 1994).

Overall, combining HOG with shallow machine learning methods for microseismic event recognition and classification offers multiple advantages. Firstly, the HOG technique effectively extracts crucial features such as edges and textures from waveform images, aiding in capturing key information about microseismic events and enhancing classification accuracy. Secondly, the low dimensionality of features extracted by HOG reduces the complexity of the feature space, leading to faster model training and improved

prediction efficiency. Additionally, HOG features exhibit a certain level of robustness to variations in lighting, rotation, and scaling, ensuring stable performance in microseismic event recognition and classification tasks across different environments.

By combining with shallow machine learning methods like SVM and linear classifiers, rapid classifier construction is achievable, particularly excelling on small-scale datasets. Moreover, this approach is characterized by strong interpretability, assisting researchers in understanding the decision-making processes of the model and providing valuable insights for further optimization and enhancement.

In summary, leveraging HOG in conjunction with shallow machine learning methods provides an effective, efficient, and interpretable approach for microseismic event recognition and classification, offering convenience and practicality in microseismic research.

5.4.2 Advantages of CNN Method

The convolutional neural network model has multiple advantages in the recognition and classification of microseismic events (Liu et al., 2021). Firstly, CNN possesses strong feature learning capabilities, utilizing layered convolution and pooling operations to automatically learn high-level features from data without the need for manual feature design, effectively capturing complex patterns and key features within microseismic event data. Secondly, the CNN structure can effectively preserve spatial information, particularly suitable for processing data with spatial structures like images and waveform data, aiding in accurately distinguishing different categories of microseismic events. Additionally, CNN exhibits a certain degree of invariance and generalization to handle data variations such as translation, scaling, and rotation, enhancing the model's adaptability.

Through multi-layer network structures, CNN can learn abstract feature representations from data, thereby improving classification accuracy (Liu et al., 2021). Most importantly, CNN excels when working with large-scale datasets, demonstrating high recognition accuracy and stability, making it suitable for complex microseismic event identification tasks, providing a robust and efficient tool for microseismic research.

In comparison to the HOG-SML method, CNN offers advantages such as strong feature learning capabilities, preservation of spatial information, adaptability to data

variations, and deep feature learning. However, CNN may require more computational resources, lack interpretability, have risks of overfitting, and necessitate a substantial amount of labeled data for training. Despite CNN's outstanding performance in complex pattern recognition and feature extraction, it faces challenges like high computational costs, poor model interpretability, and risks of overfitting. When selecting the appropriate method, a comprehensive consideration of specific application requirements and available resources is essential.

5.4.3 Advantages of Transfer Learning Method

Transfer learning models offer multiple advantages in the recognition and classification of microseismic events (Jin et al., 2024). Firstly, by leveraging pre-trained model parameters on large-scale datasets, transfer learning accelerates the learning process on microseismic event datasets, enhancing model performance and generalization capability. Secondly, in scenarios with limited data, transfer learning demonstrates higher sample efficiency, effectively utilizing the knowledge from pre-trained models to improve the accuracy of microseismic event classification. Rapid convergence is also a benefit of transfer learning, as models have learned universal features, resulting in quicker training processes on microseismic event data, thereby saving time and resources.

Moreover, transfer learning models exhibit strong adaptability, flexibly adjusting to the characteristics of different microseismic event datasets, enhancing generalization to new data and increasing model adaptability and stability (Xie et al., 2024). Importantly, transfer learning helps address the issue of data sparsity in microseismic event datasets by transferring learned features to compensate for missing data, effectively enhancing classification performance. These advantages make transfer learning models a powerful tool for handling microseismic event recognition and classification tasks, providing crucial support for research and practical applications.

In the task of microseismic event recognition and classification, the HOG-SML method stands out for its high computational efficiency and strong interpretability. Through simple feature extraction and fast computation, HOG can quickly extract features on small-scale datasets (Han et al., 2020). Additionally, shallow machine learning methods like SVM possess strong interpretability, aiding in understanding the model's workings. However, the feature representation capability of HOG may be limited,

potentially failing to capture complex data patterns, and restricting its application in challenging tasks.

On the other hand, the CNN method demonstrates robust feature learning capabilities and adaptability, automatically learning high-level features and handling data with spatial structures, thereby enhancing classification accuracy. However, CNN models require substantial computational resources and data support, with training processes being time-consuming, and their complex structures lacking interpretability, making their decision-making processes challenging to understand (Papadimitroulas et al., 2021).

Furthermore, transfer learning methods leverage pre-trained model parameters to accelerate the training process, enhancing model performance and generalization, particularly showing higher sample efficiency with limited data. However, transfer learning models may need adaptation to specific microseismic event datasets, facing challenges in domain adaptation, and may perform poorly in cases of data mismatch or overfitting, requiring careful handling. In conclusion, for microseismic event recognition and classification tasks, selecting the appropriate method requires a comprehensive consideration of their strengths and limitations, aligning with specific task requirements and available resources to achieve optimal recognition and classification outcomes.

5.5 Summary

In summary, the HOG-shallow machine learning method excels in computational efficiency and interpretability, but is limited in feature representation capability; the CNN method shines in feature learning and adaptability, yet demands significant computational resources; while the transfer learning method offers advantages in parameter transfer and sample efficiency, caution is needed regarding domain adaptability and risks of overfitting. When selecting the appropriate method, it is essential to consider specific task requirements, data characteristics, and available resources.

CHAPTER 6

CONCLUSIONS AND FUTURE RESEARCH

6.1 Summary of the Study

This study aims to enhance the sample quality, recognition efficiency, and accuracy of microseismic event data through machine learning methods. Meticulously selected microseismic monitoring data collected on-site from three mines in China underwent thorough preprocessing to eliminate irrelevant and anomalous data. By transforming the raw waveform data into six-channel event waveform images and meticulously annotating them under the strict guidance of domain experts, we obtained an image dataset covering four event categories: microseismic events, blasts, rock drilling, and noise, ensuring the reliability of training data and evaluation samples.

To address the key research objectives and questions, we proposed the following solutions:

1. To automate the process of identifying microseismic signals, alleviate the burden of manual analysis, and enhance recognition efficiency, we adopted a strategy that combines HOG features with shallow machine learning.

2. To further improve the efficiency and accuracy of identification and classification, we introduced convolutional neural networks and developed the optimized model, MS-CNN.

3. To enhance the model's generalization and robustness in recognizing microseismic event waveform images, we employed a transfer learning approach based on DNN, encompassing advanced models such as ResNet-18, MobileNet-V2, and Inception-V3.

Through a comprehensive evaluation using overall performance metrics (such as training and testing time, accuracy, Kappa coefficient) and single classification metrics (precision, recall, and F1 score), we conducted a thorough assessment of model

performance and compared it with other methods in the current research field. The evaluation results indicate that the microseismic event recognition and classification models proposed in this study exhibit outstanding performance in terms of recognition accuracy, classification efficiency, and generalization capabilities.

- Summary of main research findings:

1. In this study, the HOG algorithm was employed to automatically extract local gradient orientation histograms of images as features, and five classifiers were constructed: SVM, Linear, Decision Tree, KNN, and Fisher Discriminant. These models were trained and tested using microseismic monitoring datasets from three mines. Experimental results showed that the HOG-SVM model performed the best, achieving a classification accuracy of over 97% on dataset A with a testing time of only 0.29 seconds. This confirms that combining HOG with shallow machine learning methods can ensure high accuracy and recognition efficiency without increasing model complexity or processing time, enabling the automation of microseismic signal identification.

2. By introducing CNN and applying optimization techniques such as regularization and dropout, the MS-CNN model developed in our study demonstrated outstanding performance. On dataset A, the testing time of the MS-CNN model was approximately 3.78 seconds, with a recognition accuracy of 97.43%, representing an improvement of about 3 percentage points compared to existing CNN models in research.

3. Utilizing transfer learning techniques, the three deep neural network models (ResNet-18, MobileNet-V2, and Inception-V3) constructed in our study exhibited excellent performance. On dataset A, all these models achieved recognition accuracies exceeding 98%, with the MS-Inception-V3 model notably reaching an accuracy of 98.71% and a high Kappa coefficient of 0.983. Compared to existing transfer learning models in research, the models proposed in our study achieved an increase of approximately 1 percentage point in accuracy.

- Major research contributions:

This study has made significant contributions in the field of intelligent recognition of microseismic events:

1. Innovative Dataset Creation: Created high-quality microseismic event waveform databases from three mines, encompassing key events such as microseismic events, blasts, rock drilling, and noise. These databases not only provide solid data support for automated identification research of microseismic events but also ensure the repeatability and comparability of research results, laying a foundation for academic development and practical applications in this field.

2. Automated Microseismic Signal Identification: By combining HOG feature extraction with shallow machine learning techniques, we achieved efficient automated identification of microseismic signals, reducing the labor intensity of manual analysis while maintaining the simplicity and efficiency of the model.

3. Optimization of Model Architecture: Designed the MS-CNN model, a convolutional neural network optimized specifically for microseismic event recognition tasks. Through fine parameter tuning and regularization strategies, we further improved the model's recognition accuracy.

4. Application and Extension of Transfer Learning Models: Innovatively applied transfer learning models based on deep neural networks, including ResNet-18, MobileNet-V2, and Inception-V3. These models not only demonstrated outstanding performance in the recognition and classification of microseismic events but also showcased robust generalization capabilities to new data, providing more accurate and robust intelligent recognition tools for seismic monitoring.

In summary, this study has achieved significant results in enhancing the identification efficiency of microseismic signals and optimizing the accuracy of models, while also providing valuable data support for the monitoring of mining disasters. These outcomes not only accelerate the advancement of mine safety monitoring technology but also offer new perspectives and tools for research in this field.

6.2 Implications

In the following discussion, we will explore the significance of our research findings from two perspectives: their contribution to theoretical development and their practical application:

1. Theoretical Significance

Our research contributes to the existing body of knowledge by offering novel insights into the identification and classification of microseismic events. The theoretical frameworks that underpin machine learning models, such as SVM and CNN, have been enriched by our empirical findings, which validate and expand upon current theories.

The results have influenced our understanding of how complex patterns within microseismic data can be effectively recognized and differentiated by sophisticated algorithms, deepening the theoretical discourse on the capabilities and limitations of both shallow and deep learning methods in analyzing microseismic data.

2. Practical Significance

The practical implications of our research are substantial, particularly in the fields of mine safety and seismic disaster monitoring. The models and methods developed in this study can be directly applied to enhance real-time microseismic event detection systems, thereby improving risk assessment and mitigation strategies.

By translating these research outcomes into practical tools, mining companies can benefit from more accurate and efficient microseismic monitoring, informing decision-making processes and potentially preventing catastrophic events. Our findings also have practical applications in other industries where seismic activity is critical, contributing to safety management.

In summary, the theoretical contributions of this research advance our scientific comprehension of microseismic phenomena and the application of machine learning technologies, while its practical applications provide tangible benefits for improving safety protocols and decision-making in seismically active environments.

6.3 Limitations

In this study, there are several limitations to consider:

1. Quality, Quantity, and Representativeness of the Dataset

The quality, quantity, and representativeness of the dataset have significant impacts on the model's training and generalization abilities. Poor quality or limited quantity of

data may restrict the model's performance and applicability, while the representativeness of the dataset can affect the model's performance in real-world scenarios.

2. Choice of Classification Models and Optimization Algorithms

The subjective nature and limitations in selecting classification models and optimization algorithms may lead to different performance outcomes. The performance of other models and algorithms may not have been fully explored.

3. Parameter Settings

Parameter settings play a crucial role in the performance and generalization ability of the model. Limitations in parameter selection and adjustment in this study may have influenced the final performance and stability of the model.

4. Limitations of Hardware Resources

Constraints in hardware resources can impact the efficiency and scale of model training and testing. Limited hardware resources may restrict the model's size and complexity, affecting its performance.

5. Comparative Analysis

Limitations in the comparative analysis may stem from the inability to cover all possible comparative models or algorithms comprehensively, leading to constraints in evaluating and generalizing the research findings. Biases or incompleteness in the comparative analysis could also affect the accuracy of the research conclusions.

Clearly identifying and discussing these limitations contributes to a more comprehensive understanding of the scope and applicability of the research findings, providing guidance and recommendations for future research.

6.4 Future Research

Based on the current study, several suggestions for future research are proposed:

1. Enhanced Dataset Collection: Future research could focus on expanding and improving the dataset used for microseismic event recognition. This may involve collecting data from a wider range of sources or incorporating more diverse and representative samples to enhance the model's performance and generalization ability.

2. **Advanced Model Development:** Further research could explore the development of more advanced and sophisticated models for microseismic event recognition. This may include incorporating ensemble learning techniques (S. Jiang et al., 2018), attention mechanisms, or exploring the potential of deep reinforcement learning in improving the accuracy and efficiency of the recognition process.

3. **Optimization and Parameter Tuning:** Future studies could delve deeper into the optimization of classification models and fine-tuning of parameters to enhance the performance and robustness of the models. Exploring novel optimization algorithms or conducting sensitivity analysis on key parameters could further improve the model's effectiveness.

4. **Real-world Application and Validation:** It is essential to conduct real-world application and validation of the developed models in practical scenarios related to engineering safety, geological exploration, or seismic monitoring. Assessing the models' performance in diverse and complex environments will provide valuable insights into their applicability and effectiveness.

5. **Integration of Multi-modal Data:** Future research could explore the integration of multi-modal data sources, such as incorporating seismic waveforms with other geophysical data or sensor information. This integration could provide a more comprehensive understanding of seismic events and improve the accuracy of event recognition systems.

By addressing these future research suggestions, advancements can be made in the field of microseismic event recognition, leading to more robust and efficient models for various applications in engineering, geology, and seismic monitoring.

6.5 Summary

This research has made significant contributions to the field of microseismic event recognition through the application of machine learning techniques. By meticulously selecting data from three mining sites in China and developing advanced classification models, this study has demonstrated the potential for enhancing the sample quality, recognition efficiency, and accuracy of microseismic event data.

The key findings of this research highlight the effectiveness of combining HOG features with shallow machine learning methods, introducing CNNs, and utilizing transfer learning models for improved generalization and robustness. The evaluation results have shown exceptional performance in terms of accuracy, classification efficiency, and generalization capabilities.

Overall, this research underscores the importance of automated microseismic signal identification and the development of optimized classification models for various applications in engineering safety, geological exploration, and seismic monitoring. The findings emphasize the significance of advancing intelligent recognition techniques for microseismic events, contributing to the advancement of research in seismic monitoring practices.

In conclusion, the contributions of this study not only validate the superiority of the proposed models but also showcase their potential applications in real-world scenarios. The research's significance lies in its ability to enhance automated recognition processes, improve monitoring systems, and provide valuable insights for further advancements in the field of microseismic event recognition.

REFERENCES

- Abdalzaher, M. S., Soliman, M. S., El-Hady, S. M., Benslimane, A., & Elwekeil, M. (2022). A Deep Learning Model for Earthquake Parameters Observation in IoT System-Based Earthquake Early Warning. *IEEE Internet of Things Journal*, 9(11), 8412–8424. <https://doi.org/10.1109/JIOT.2021.3114420>
- Alarfaj, F. K., Malik, I., Khan, H. U., Almusallam, N., Ramzan, M., & Ahmed, M. (2022). Credit Card Fraud Detection Using State-of-the-Art Machine Learning and Deep Learning Algorithms. *IEEE Access*, 10, 39700–39715. <https://doi.org/10.1109/ACCESS.2022.3166891>
- Alinsaif, S., & Lang, J. (2020). Histological Image Classification using Deep Features and Transfer Learning. In *2020 17th Conference on Computer and Robot Vision (CRV)* (pp. 101–108). <https://doi.org/10.1109/CRV50864.2020.00022>
- Alzubaidi, L., Zhang, J., Humaidi, A. J., Al-Dujaili, A., Duan, Y., Al-Shamma, O., Santamaría, J., Fadhel, M. A., Al-Amidie, M., & Farhan, L. (2021). Review of deep learning: concepts, CNN architectures, challenges, applications, future directions. *Journal of Big Data*, 8(1), 1–74. <https://doi.org/10.1186/s40537-021-00444-8>
- Anikiev, D., Birnie, C., Waheed, U. B., Alkhalifah, T., Gu, C., Verschuur, D. J., & Eisner, L. (2023). Machine learning in microseismic monitoring. *Earth-Science Reviews*, 239, 104371. <https://doi.org/10.1016/j.earscirev.2023.104371>
- Apicella, A., Donnarumma, F., Isgrò, F., & Prevete, R. (2021). A survey on modern trainable activation functions. *Neural Networks*, 138, 14–32. <https://doi.org/10.1016/j.neunet.2021.01.026>
- Arrowsmith, S. J., Trugman, D. T., MacCarthy, J., Bergen, K. J., Lumley, D., & Magnani, M. B. (2022). Big Data Seismology. *Reviews of Geophysics*, 60(2), e2021RG000769. <https://doi.org/10.1029/2021RG000769>

- Avola, D., Bacciu, A., Cinque, L., Fagioli, A., Marini, M. R., & Taiello, R. (2022). Study on transfer learning capabilities for pneumonia classification in chest-x-rays images. *Computer Methods and Programs in Biomedicine*, 221, 106833. <https://doi.org/10.1016/j.cmpb.2022.106833>
- Azevedo, B. F., Rocha, A. M. A. C., & Pereira, A. I. (2024). Hybrid approaches to optimization and machine learning methods: a systematic literature review. *Machine Learning*, 113(7), 4055–4097. <https://doi.org/10.1007/s10994-023-06467-x>
- Bahri, A., Ghofrani Majelan, S., Mohammadi, S., Noori, M., & Mohammadi, K. (2020). Remote Sensing Image Classification via Improved Cross-Entropy Loss and Transfer Learning Strategy Based on Deep Convolutional Neural Networks. *IEEE Geoscience and Remote Sensing Letters*, 17(6), 1087–1091. <https://doi.org/10.1109/LGRS.2019.2937872>
- Barnewold, L., & Lottermoser, B. G. (2020). Identification of digital technologies and digitalisation trends in the mining industry. *International Journal of Mining Science and Technology*, 30(6), 747–757. <https://doi.org/10.1016/j.ijmst.2020.07.003>
- Basnet, P. M. S., Jin, A., & Mahtab, S. (2024). Developing an explainable rockburst risk prediction method using monitored microseismicity based on interpretable machine learning approach. *Acta Geophysica*, 72(4), 2597–2618. <https://doi.org/10.1007/s11600-024-01338-y>
- Bergen, K. J., Johnson, P. A., De Hoop, M. V., & Beroza, G. C. (2019). Machine learning for data-driven discovery in solid Earth geoscience. *Science*, 363(6433), eaau0323. <https://doi.org/10.1126/science.aau0323>
- Bi, L., Xie, W., & Zhao, J. (2019). Automatic recognition and classification of multi-channel microseismic waveform based on DCNN and SVM. *COMPUTERS & GEOSCIENCES*, 123, 111–120. <https://doi.org/10.1016/j.cageo.2018.10.008>

- Bi, X., Zhang, C., He, Y., Zhao, X., Sun, Y., & Ma, Y. (2021). Explainable time–frequency convolutional neural network for microseismic waveform classification. *Information Sciences*, 546, 883–896.
<https://doi.org/10.1016/j.ins.2020.08.109>
- Bichri, H., Chergui, A., & Hain, M. (2023). Image Classification with Transfer Learning Using a Custom Dataset: Comparative Study. *Procedia Computer Science*, 220, 48–54. <https://doi.org/10.1016/j.procs.2023.03.009>
- Binder, G., & Chakraborty, D. (2019). Detecting microseismic events in downhole distributed acoustic sensing data using convolutional neural networks. *SEG Technical Program Expanded Abstracts 2019*, 4864–4868.
<https://doi.org/10.1190/segam2019-3214863.1>
- Brownlee, J. (2016). *Machine Learning Mastery With Python: Understand Your Data, Create Accurate Models, and Work Projects End-to-End*. Machine Learning Mastery.
- Caffagni, E., Eaton, D. W., Jones, J. P., & van der Baan, M. (2016). Detection and analysis of microseismic events using a Matched Filtering Algorithm (MFA). *Geophysical Journal International*, 206(1), 644–658.
<https://doi.org/10.1093/gji/ggw168>
- Campbell, C., & Ying, Y. (2022). *Learning with Support Vector Machines*. Springer Nature.
- Cano, E. V., Akram, J., & Peter, D. B. (2021). Automatic seismic phase picking based on unsupervised machine-learning classification and content information analysis. *Geophysics*, 86(4), V299–V315. <https://doi.org/10.1190/geo2020-0308.1>
- Cao, A., Dou, L., Yan, R., Jiang, H., Lu, C., Du, T., & Lu, Z. (2009). Classification of microseismic events in high stress zone. *Mining Science and Technology (China)*, 19(6), 718–723. [https://doi.org/10.1016/S1674-5264\(09\)60131-9](https://doi.org/10.1016/S1674-5264(09)60131-9)
- Cao, A. Y., Liu, Y. Q., Yang, X., Li, S., & Liu, Y. P. (2022). FDNet: Knowledge and Data Fusion-Driven Deep Neural Network for Coal Burst Prediction. *Sensors*, 22(8). <https://doi.org/10.3390/s22083088>

- Cervantes, J., Garcia-Lamont, F., Rodríguez-Mazahua, L., & Lopez, A. (2020). A comprehensive survey on support vector machine classification: Applications, challenges and trends. *Neurocomputing*, 408, 189–215.
<https://doi.org/10.1016/j.neucom.2019.10.118>
- Chakraborty, M., Das, M., & Aruchamy, S. (2022). Micro-Seismic Event Detection using statistical feature extraction and machine learning techniques. In 2022 IEEE 7th International conference for Convergence in Technology (I2CT) (pp. 1–5).
<https://doi.org/10.1109/I2CT54291.2022.9824819>
- Chandra, M. A., & Bedi, S. S. (2021). Survey on SVM and their application in imageclassification. *International Journal of Information Technology*, 13(5), 1–11. <https://doi.org/10.1007/s41870-017-0080-1>
- Chapelle, O., Haffner, P., & Vapnik, V. N. (1999). Support vector machines for histogram-based image classification. *IEEE Transactions on Neural Networks*, 10(5), 1055–1064. <https://doi.org/10.1109/72.788646>
- Chen, H., Xue, S., & Zheng, X. (2022). Coal mine microseismic identification and first-arrival picking based on Conv-LSTM-Unet. *Acta Geophysica*, 71(1), 161–173.
<https://doi.org/10.1007/s11600-022-00898-1>
- Chen, J., Lian, Y., & Li, Y. (2020). Real-time grain impurity sensing for rice combine harvesters using image processing and decision-tree algorithm. *Computers and Electronics in Agriculture*, 175, 105591.
<https://doi.org/10.1016/j.compag.2020.105591>
- Chen, Y. (2018). Fast waveform detection for microseismic imaging using unsupervised machine learning. *Geophysical Journal International*, 215(2), 1185–1199.
<https://doi.org/10.1093/gji/ggy348>
- Chen, Y. (2020). Automatic microseismic event picking via unsupervised machine learning. *Geophysical Journal International*, 222(3), 1750–1764.
<https://doi.org/10.1093/gji/ggaa186>

- Chen, Y. K., Zhang, G. Y., Bai, M., Zu, S. H., Guan, Z., & Zhang, M. (2019). Automatic Waveform Classification and Arrival Picking Based on Convolutional Neural Network. *Earth and Space Science*, 6(7), 1244–1261.
<https://doi.org/10.1029/2018ea000466>
- Chen, Y., Saad, O. M., Savvaidis, A., Chen, Y., & Fomel, S. (2022). 3D Microseismic Monitoring Using Machine Learning. *Journal of Geophysical Research: Solid Earth*, 127(3), e2021JB023842. <https://doi.org/10.1029/2021JB023842>
- Cheng, G., Chen, J., Wei, Y., Chen, S., & Pan, Z. (2023). A Coal Gangue Identification Method Based on HOG Combined with LBP Features and Improved Support Vector Machine. *Symmetry*, 15(1), 202. <https://doi.org/10.3390/sym15010202>
- Choi, W. C., Kim, C., Cheon, D., & Pyun, S. (2019). Automatic Classification of Microseismic Signals Related to Mining Activities by Supervised Learning. In 81st EAGE Conference and Exhibition 2019 (pp. 1–5). London, UK,: European Association of Geoscientists & Engineers. <https://doi.org/10.3997/2214-4609.201900757>
- Choi, W., Pyun, S., & Cheon, D. (2024). Automatic microseismic signal classification for mining safety monitoring using the WaveNet classifier. *Geophysical Prospecting*, 72(2), 315–332. <https://doi.org/10.1111/1365-2478.13398>
- Chugh, R. S., Bhatia, V., Khanna, K., & Bhatia, V. (2020). A Comparative Analysis of Classifiers for Image Classification. In 2020 10th International Conference on Cloud Computing, Data Science & Engineering (Confluence) (pp. 248–253). <https://doi.org/10.1109/Confluence47617.2020.9058042>
- Cohen, J. (1960). A Coefficient of Agreement for Nominal Scales. *Educational and Psychological Measurement*, 20(1), 37–46.
<https://doi.org/10.1177/001316446002000104>
- Cortes, C., & Vapnik, V. (1995). Support-vector networks. *Machine Learning*, 20(3), 273–297. <https://doi.org/10.1007/BF00994018>

- Cui, F., Sun, J., Lai, X., Jia, C., & Zhang, S. (2023). Study on the Energy Release Law of Overburden Rock Breaking and Anti-Rockburst Technology in the Knife Handle Working Face of a Gently Inclined Coal Seam. *Applied Sciences*, 13(21), 11809. <https://doi.org/10.3390/app132111809>
- Curram, S. P., & Mingers, J. (1994). Neural Networks, Decision Tree Induction and Discriminant Analysis: an Empirical Comparison. *Journal of the Operational Research Society*, 45(4), 440–450. <https://doi.org/10.1057/jors.1994.62>
- Dalal, N., & Triggs, B. (2005). Histograms of Oriented Gradients for Human Detection. In 2005 IEEE Computer Society Conference on Computer Vision and Pattern Recognition (CVPR'05) (Vol. 1, pp. 886–893). San Diego, CA, USA: IEEE. <https://doi.org/10.1109/CVPR.2005.177>
- Deepak, S., & Ameer, P. M. (2019). Brain tumor classification using deep CNN features via transfer learning. *Computers in Biology and Medicine*, 111, 103345. <https://doi.org/10.1016/j.combiomed.2019.103345>
- Di, Y., Wang, E., Li, Z., Liu, X., Huang, T., & Yao, J. (2023). Comprehensive early warning method of microseismic, acoustic emission, and electromagnetic radiation signals of rock burst based on deep learning. *International Journal of Rock Mechanics and Mining Sciences*, 170, 105519. <https://doi.org/10.1016/j.ijrmms.2023.105519>
- Ding, L., Cao, L., Zhang, G., & Pan, Y. (2022). Improved mine microseismic event recognition method combining neural network and transfer learning. In 2022 9th International Conference on Behavioural and Social Computing (BESC) (pp. 1–7). <https://doi.org/10.1109/BESC57393.2022.9995230>
- Ding, L., Chen, Z., Pan, Y., & Song, B. (2022). Mine Microseismic Time Series Data Integrated Classification Based on Improved Wavelet Decomposition and ELM. *Cognitive Computation*, 14(4), 1526–1546. <https://doi.org/10.1007/s12559-022-09997-z>
- Ding, S., Zhao, X., Zhang, J., Zhang, X., & Xue, Y. (2019). A review on multi-class TWSVM. *Artificial Intelligence Review*, 52(2), 775–801. <https://doi.org/10.1007/s10462-017-9586-y>

- Dong, L., Sun, D., Li, X., Ma, J., Chen, G., & Zhang, C. (2016). A statistical method to identify blasts and microseismic events and its engineering application, 35, 1423–1433. <https://doi.org/10.13722/j.cnki.jrme.2015.1007>
- Dong, L.-J., Wesseloo, J., Potvin, Y., & Li, X.-B. (2016). Discriminant models of blasts and seismic events in mine seismology. *International Journal of Rock Mechanics and Mining Sciences*, 86, 282–291. <https://doi.org/10.1016/j.ijrmms.2016.04.021>
- Dong, Longjun, Hu, Q., Tong, X., & Liu, Y. (2020). Velocity-Free MS/AE Source Location Method for Three-Dimensional Hole-Containing Structures. *Engineering*, 6(7), 827–834. <https://doi.org/10.1016/j.eng.2019.12.016>
- Dong, Longjun, & Li, X. (2023). *Velocity-Free Localization Methodology for Acoustic and Microseismic Sources*. Singapore: Springer Nature Singapore. <https://doi.org/10.1007/978-981-19-8610-9>
- Dong, Longjun, Li, X., Tang, L., & Gong, F. (2011). Mathematical functions and parameters for microseismic source location without pre-measuring speed. *Yanshilixue Yu Gongcheng Xuebao/Chinese Journal of Rock Mechanics and Engineering*, 30, 2057–2067.
- Dong, Longjun, Shu, H., Tang, Z., & Yan, X. (2023). Microseismic event waveform classification using CNN-based transfer learning models. *International Journal of Mining Science and Technology*, 33(10), 1203–1216. <https://doi.org/10.1016/j.ijmst.2023.09.003>
- Dong, Longjun, Sun, D., Shu, W., Li, X., & Zhang, L. (2019). Statistical Precursor of Induced Seismicity Using Temporal and Spatial Characteristics of Seismic Sequence in Mines, 218, 409–420. https://doi.org/10.1007/978-3-030-12111-2_38
- Dong, Long-jun, Tang, Z., Li, X., Chen, Y., & Xue, J. (2020). Discrimination of mining microseismic events and blasts using convolutional neural networks and original waveform. *Journal of Central South University*, 27(10), 3078–3089. <https://doi.org/10.1007/s11771-020-4530-8>

- Dong, Longjun, Tao, Q., Hu, Q., Deng, S., Chen, Y., Luo, Q., & Zhang, X. (2022). Acoustic emission source location method and experimental verification for structures containing unknown empty areas. *International Journal of Mining Science and Technology*, 32(3), 487–497.
<https://doi.org/10.1016/j.ijmst.2022.01.002>
- Dong, Longjun, Wesseloo, J., Potvin, Y., & Li, X. (2016). Discrimination of Mine Seismic Events and Blasts Using the Fisher Classifier, Naive Bayesian Classifier and Logistic Regression. *Rock Mechanics and Rock Engineering*, 49(1), 183–211.
<https://doi.org/10.1007/s00603-015-0733-y>
- Du, J., Chen, J., Pu, Y., Jiang, D., Chen, L., & Zhang, Y. (2021). Risk assessment of dynamic disasters in deep coal mines based on multi-source, multi-parameter indexes, and engineering application. *Process Safety and Environmental Protection*, 155, 575–586. <https://doi.org/10.1016/j.psep.2021.09.034>
- Duan, Y., Shen, Y., Canbulat, I., Luo, X., & Si, G. (2021). Classification of clustered microseismic events in a coal mine using machine learning. *Journal of Rock Mechanics and Geotechnical Engineering*, 13(6), 1256–1273.
<https://doi.org/10.1016/j.jrmge.2021.09.002>
- Fagan, D., Van Wijk, K., & Rutledge, J. (2013). Clustering revisited: A spectral analysis of microseismic events. *GEOPHYSICS*, 78(2), KS41–KS49.
<https://doi.org/10.1190/geo2012-0323.1>
- Fan, X., Cheng, J., Wang, Y., Li, S., Yan, B., & Zhang, Q. (2022). Automatic Events Recognition in Low SNR Microseismic Signals of Coal Mine Based on Wavelet Scattering Transform and SVM. *Energies*, 15(7), 2326.
<https://doi.org/10.3390/en15072326>
- Feng, G.-L., Feng, X.-T., Chen, B., Xiao, Y.-X., & Yu, Y. (2015). A Microseismic Method for Dynamic Warning of Rockburst Development Processes in Tunnels. *Rock Mechanics and Rock Engineering*, 48(5), 2061–2076.
<https://doi.org/10.1007/s00603-014-0689-3>

- Feng, Q., Han, L., Pan, B., & Zhao, B. (2022). Microseismic Source Location Using Deep Reinforcement Learning. *IEEE Transactions on Geoscience and Remote Sensing*, 60, 1–9. <https://doi.org/10.1109/TGRS.2022.3182991>
- Feng, Q., Han, L., Zhao, B., & Li, Q. (2023). Microseismic Events Recognition via Joint Deep Clustering With Residual Shrinkage Dense Network. *IEEE Transactions on Geoscience and Remote Sensing*, 61, 1–11. <https://doi.org/10.1109/TGRS.2023.3314149>
- Feng, X.-T., Liu, J., Chen, B., Xiao, Y., Feng, G., & Zhang, F. (2017). Monitoring, Warning, and Control of Rockburst in Deep Metal Mines. *Engineering*, 3(4), 538–545. <https://doi.org/10.1016/j.eng.2017.04.013>
- Foody, G. M., & Mathur, A. (2004). A relative evaluation of multiclass image classification by support vector machines. *IEEE Transactions on Geoscience and Remote Sensing*, 42(6), 1335–1343. <https://doi.org/10.1109/TGRS.2004.827257>
- Fu, S., Wang, X., Tang, J., Lan, S., & Tian, Y. (2024). Generalized robust loss functions for machine learning. *Neural Networks*, 171, 200–214. <https://doi.org/10.1016/j.neunet.2023.12.013>
- Fu, Y., & Aldrich, C. (2020). Deep Learning in Mining and Mineral Processing Operations: A Review. *IFAC-PapersOnLine*, 53(2), 11920–11925. <https://doi.org/10.1016/j.ifacol.2020.12.712>
- Ge, M. C. (2005). Efficient mine microseismic monitoring. *International Journal of Coal Geology*, 64(1–2), 44–56. <https://doi.org/10.1016/j.coal.2005.03.004>
- Gulzar, Y. (2023). Fruit Image Classification Model Based on MobileNetV2 with Deep Transfer Learning Technique. *Sustainability*, 15(3), 1906. <https://doi.org/10.3390/su15031906>
- Guo, C., Zhu, T., Gao, Y., Wu, S., & Sun, J. (2021). AEnet: Automatic Picking of P-Wave First Arrivals Using Deep Learning. *IEEE Transactions on Geoscience and Remote Sensing*, 59(6), 5293–5303. <https://doi.org/10.1109/TGRS.2020.3010541>

- Han, B., Wang, Y., Yang, Z., & Gao, X. (2020). Small-Scale Pedestrian Detection Based on Deep Neural Network. *IEEE Transactions on Intelligent Transportation Systems*, 21(7), 3046–3055. <https://doi.org/10.1109/TITS.2019.2923752>
- He, Jian, Li, H., Tuo, X., Wen, X., Rong, W., & He, X. (2022). Strong Noise-Tolerance Deep Learning Network for Automatic Microseismic Events Classification. *IEEE Transactions on Geoscience and Remote Sensing*, 60, 1–9. <https://doi.org/10.1109/TGRS.2022.3194351>
- He, Jiang, Dou, L., Gong, S., Li, J., & Ma, Z. (2017). Rock burst assessment and prediction by dynamic and static stress analysis based on micro-seismic monitoring. *International Journal of Rock Mechanics and Mining Sciences*, 93, 46–53. <https://doi.org/10.1016/j.ijrmms.2017.01.005>
- He, K., Zhang, X., Ren, S., & Sun, J. (2015). Deep Residual Learning for Image Recognition, 770–778.
- He, M., & Wang, Q. (2023). Rock dynamics in deep mining. *International Journal of Mining Science and Technology*, 33(9), 1065–1082. <https://doi.org/10.1016/j.ijmst.2023.07.006>
- Holtzman, B. K., Paté, A., Paisley, J., Waldhauser, F., & Repetto, D. (2018). Machine learning reveals cyclic changes in seismic source spectra in Geysers geothermal field. *Science Advances*, 4(5), eaao2929. <https://doi.org/10.1126/sciadv.aao2929>
- Huang, L., Li, J., Hao, H., & Li, X. (2018). Micro-seismic event detection and location in underground mines by using Convolutional Neural Networks (CNN) and deep learning. *Tunnelling and Underground Space Technology*, 81, 265–276. <https://doi.org/10.1016/j.tust.2018.07.006>
- Huang, M. Q., Ninić, J., & Zhang, Q. B. (2021). BIM, machine learning and computer vision techniques in underground construction: Current status and future perspectives. *Tunnelling and Underground Space Technology*, 108, 103677. <https://doi.org/10.1016/j.tust.2020.103677>

- Huang, W. L. (2019). Seismic signal recognition by unsupervised machine learning. *Geophysical Journal International*, 219(2), 1163–1180.
<https://doi.org/10.1093/gji/ggz366>
- Huang, W.-L., Gao, F., Liao, J.-P., & Chuai, X.-Y. (2021). A deep learning network for estimation of seismic local slopes. *Petroleum Science*, 18(1), 92–105.
<https://doi.org/10.1007/s12182-020-00530-1>
- Iannucci, R., Lenti, L., & Martino, S. (2020). Seismic monitoring system for landslide hazard assessment and risk management at the drainage plant of the Peschiera Springs (Central Italy). *Engineering Geology*, 277, 105787.
<https://doi.org/10.1016/j.enggeo.2020.105787>
- Ji, B., Xie, F., Wang, X., He, S., & Song, D. (2020). Investigate Contribution of Multi-Microseismic Data to Rockburst Risk Prediction Using Support Vector Machine With Genetic Algorithm. *IEEE Access*, 8, 58817–58828.
<https://doi.org/10.1109/ACCESS.2020.2982366>
- Jia, L., Chen, H., & Xing, K. (2022). Rapid classification of local seismic events using machine learning. *Journal of Seismology*, 26(5), 897–912.
<https://doi.org/10.1007/s10950-022-10109-5>
- Jiang, J., Stankovic, V., Stankovic, L., Parastatidis, E., & Pytharouli, S. (2023). Microseismic Event Classification With Time-, Frequency-, and Wavelet-Domain Convolutional Neural Networks. *IEEE Transactions on Geoscience and Remote Sensing*, 61, 1–14. <https://doi.org/10.1109/TGRS.2023.3262412>
- Jiang, R., Dai, F., Liu, Y., & Li, A. (2021). A novel method for automatic identification of rock fracture signals in microseismic monitoring. *Measurement*, 175, 109129.
<https://doi.org/10.1016/j.measurement.2021.109129>
- Jiang, R., Dai, F., Liu, Y., & Wei, M. (2020). An automatic classification method for microseismic events and blasts during rock excavation of underground caverns. *Tunnelling and Underground Space Technology*, 101, 103425.
<https://doi.org/10.1016/j.tust.2020.103425>

- Jiang, S., Lian, M. J., Lu, C. W., Gu, Q. H., Ruan, S. L., & Xie, X. C. (2018). Ensemble Prediction Algorithm of Anomaly Monitoring Based on Big Data Analysis Platform of Open-Pit Mine Slope. Complexity. <https://doi.org/10.1155/2018/1048756>
- JIANG Wenwu, YANG Zuolin, XIE Jianmin, & LI Jiafu. (2015). Application of FFT spectrum analysis to identify microseismic signals. *Science & Technology Review*, 33(2), 86–90. <https://doi.org/10.3981/j.issn.1000-7857.2015.02.013>
- Jin, S., Zhang, S., Gao, Y., Yu, B., & Zhen, S. (2024). Microseismic Event Recognition and Transfer Learning Based on Convolutional Neural Network and Attention Mechanisms. *Applied Geophysics*. <https://doi.org/10.1007/s11770-024-1058-y>
- Johnson, C. W., Ben-Zion, Y., Meng, H. R., & Vernon, F. (2020). Identifying Different Classes of Seismic Noise Signals Using Unsupervised Learning. *Geophysical Research Letters*, 47(15). <https://doi.org/10.1029/2020gl088353>
- Kan, J., Dou, L., Li, J., Song, S., Zhou, K., Cao, J., & Bai, J. (2022). Discrimination of Microseismic Events in Coal Mine Using Multifractal Method and Moment Tensor Inversion. *Fractal and Fractional*, 6(7), 361. <https://doi.org/10.3390/fractalfract6070361>
- Kang, H., Jiang, P., Feng, Y., Gao, F., Zhang, Z., & Liu, X. (2023). Application of Large-Scale Hydraulic Fracturing for Reducing Mining-Induced Stress and Microseismic Events: A Comprehensive Case Study. *Rock Mechanics and Rock Engineering*, 56(2), 1399–1413. <https://doi.org/10.1007/s00603-022-03061-w>
- Kang, Y., Wang, Y., Cheng, G., Song, Y., Yu, J., & Zhang, N. (2020). Classification of Microseismic Events and Blasts Using Deep Belief Network. In *2020 Chinese Control And Decision Conference (CCDC)* (pp. 5556–5561). IEEE. <https://doi.org/10.1109/CCDC49329.2020.9164062>
- Khayer, K., Hosseini Fard, E., Roshandel Kahoo, A., Soleimani Monfared, M., & Ahmadyfard, A. (2023). Integration of feature extraction, attribute combination and image segmentation for object delineation on seismic images. *Acta Geophysica*, 71(1), 275–292. <https://doi.org/10.1007/s11600-022-00921-5>

- Kingma, D., & Ba, J. (2014). Adam: A Method for Stochastic Optimization. *Computer Science*.
- Krawczyk, B., Woźniak, M., & Herrera, F. (2015). On the usefulness of one-class classifier ensembles for decomposition of multi-class problems. *Pattern Recognition*, 48(12), 3969–3982. <https://doi.org/10.1016/j.patcog.2015.06.001>
- Krizhevsky, A., Sutskever, I., & Hinton, G. E. (2017). ImageNet Classification with Deep Convolutional Neural Networks. *Communications of the Acm*, 60(6), 84–90. <https://doi.org/10.1145/3065386>
- Ku, B., Min, J., Ahn, J.-K., Lee, J., & Ko, H. (2021). Earthquake Event Classification Using Multitasking Deep Learning. *IEEE Geoscience and Remote Sensing Letters*, 18(7), 1149–1153. <https://doi.org/10.1109/LGRS.2020.2996640>
- LeCun, Y., Bengio, Y., & Hinton, G. (2015). Deep learning. *Nature*, 521(7553), 436–444. <https://doi.org/10.1038/nature14539>
- LeCun, Y., Boser, B., Denker, J. S., Henderson, D., Howard, R. E., Hubbard, W., & Jackel, L. D. (1989). Backpropagation Applied to Handwritten Zip Code Recognition. *Neural Computation*, 1(4), 541–551. <https://doi.org/10.1162/neco.1989.1.4.541>
- LeCun, Yann, Bottou, L., Bengio, Y., & Haffner, P. (1998). Gradient-based learning applied to document recognition. *Proceedings of the IEEE*, 86(11), 2278–2324. <https://doi.org/10.1109/5.726791>
- Li, Baolin, Wang, E., Li, Z., Niu, Y., Li, N., & Li, X. (2021). Discrimination of different blasting and mine microseismic waveforms using FFT, SPWVD and multifractal method. *Environmental Earth Sciences*, 80(1), 36. <https://doi.org/10.1007/s12665-020-09330-7>
- Li, Biao, Xu, N., Xiao, P., Xia, Y., Zhou, X., Gu, G., & Yang, X. (2023). Microseismic monitoring and forecasting of dynamic disasters in underground hydropower projects in southwest China: A review. *Journal of Rock Mechanics and Geotechnical Engineering*, 15(8), 2158–2177. <https://doi.org/10.1016/j.jrmge.2022.10.017>

- Li, C., Liu, J., Wang, C., Li, J., & Zhang, H. (2012). Spectrum characteristics analysis of microseismic signals transmitting between coal bedding. *Safety Science*, 50(4), 761–767. <https://doi.org/10.1016/j.ssci.2011.08.038>
- Li, F., Zhou, H., Wang, Z., & Wu, X. (2021). ADDCNN: An Attention-Based Deep Dilated Convolutional Neural Network for Seismic Facies Analysis With Interpretable Spatial–Spectral Maps. *IEEE Transactions on Geoscience and Remote Sensing*, 59(2), 1733–1744. <https://doi.org/10.1109/TGRS.2020.2999365>
- Li, Jiaming, Li, K., & Tang, S. (2023). Automatic arrival-time picking of P- and S-waves of microseismic events based on object detection and CNN. *Soil Dynamics and Earthquake Engineering*, 164, 107560. <https://doi.org/10.1016/j.soildyn.2022.107560>
- Li, Jiaming, Tang, S., Li, K., Zhang, S., Tang, L., Cao, L., & Ji, F. (2022). Automatic recognition and classification of microseismic waveforms based on computer vision. *Tunnelling and Underground Space Technology*, 121, 104327. <https://doi.org/10.1016/j.tust.2021.104327>
- Li, Jia-ming, Tang, S., Weng, F., Li, K., Yao, H., & He, Q. (2023). Waveform recognition and process interpretation of microseismic monitoring based on an improved LeNet5 convolutional neural network. *Journal of Central South University*, 30(3), 904–918.
- Li, Jiangfeng, Stankovic, L., Pytharouli, S., & Stankovic, V. (2021). Automated Platform for Microseismic Signal Analysis: Denoising, Detection, and Classification in Slope Stability Studies. *IEEE Transactions on Geoscience and Remote Sensing*, 59(9), 7996–8006. <https://doi.org/10.1109/TGRS.2020.3032664>
- Li, S., Ni, Y., Wang, Y., Shi, J., Zhang, S., Ge, Q., Zhang, G., Guang, D., Wu, X., Tang, C., & Yu, B. (2022). Highly sensitive fiber optic microseismic monitoring system for tunnel rockburst. *Measurement*, 189, 110449. <https://doi.org/10.1016/j.measurement.2021.110449>

- Li, X., Li, Z., Wang, E., Liang, Y., Li, B., Chen, P., & Liu, Y. (2018). PATTERN RECOGNITION OF MINE MICROSEISMIC AND BLASTING EVENTS BASED ON WAVE FRACTAL FEATURES. *Fractals*, 26(03), 1850029. <https://doi.org/10.1142/S0218348X18500299>
- Li, Z., Liu, F., Yang, W., Peng, S., & Zhou, J. (2022). A Survey of Convolutional Neural Networks: Analysis, Applications, and Prospects. *IEEE Transactions on Neural Networks and Learning Systems*, 33(12), 6999–7019. <https://doi.org/10.1109/TNNLS.2021.3084827>
- Li-li, L., & Chang-peng, J. (2009). Real-time Detection for Anomaly Data in Microseismic Monitoring System (pp. 307–310). Presented at the Computational Intelligence and Natural Computing, International Conference on, IEEE Computer Society. <https://doi.org/10.1109/CINC.2009.44>
- Lin, B. I., Wei, X. I. E., Junjie, Z. H. A. O., & Hui, Z. H. A. O. (2018). Automatic classification of multi-channel microseismic waveform based on DCNN-SPP. *Journal of Applied Geophysics*, 159, 446–452. <https://doi.org/10.1016/j.jappgeo.2018.09.022>
- Lin, C., Li, L., Luo, W., Wang, K. C. P., & Guo, J. (2019). Transfer Learning Based Traffic Sign Recognition Using Inception-v3 Model. *Periodica Polytechnica Transportation Engineering*, 47(3), 242–250. <https://doi.org/10.3311/PPtr.11480>
- Liu, L., Song, W. Q., Zeng, C., & Yang, X. H. (2021). Microseismic event detection and classification based on convolutional neural network. *Journal of Applied Geophysics*, 192. <https://doi.org/10.1016/j.jappgeo.2021.104380>
- Liu, R. (2021). Research on Feature Fusion Method of Mine Microseismic Signal Based on Unsupervised Learning. *Shock and Vibration*, 2021, 1–12. <https://doi.org/10.1155/2021/9544997>
- Liu, Y., Pu, H., & Sun, D.-W. (2021). Efficient extraction of deep image features using convolutional neural network (CNN) for applications in detecting and analysing complex food matrices. *Trends in Food Science & Technology*, 113, 193–204. <https://doi.org/10.1016/j.tifs.2021.04.042>

- Ma, C., Li, T., & Zhang, H. (2020). Microseismic and precursor analysis of high-stress hazards in tunnels: A case comparison of rockburst and fall of ground. *Engineering Geology*, 265, 105435.
<https://doi.org/10.1016/j.enggeo.2019.105435>
- Ma, C., Ran, X., Xu, W., Yan, W., Li, T., Dai, K., Wan, J., Lin, Y., & Tong, K. (2023). Fine Classification Method for Massive Microseismic Signals Based on Short-Time Fourier Transform and Deep Learning. *Remote Sensing*, 15(2), 502.
<https://doi.org/10.3390/rs15020502>
- Ma, C., Zhang, H., Lu, X., Ji, X., Li, T., Fang, Y., Yan, W., & Ran, X. (2023). A novel microseismic classification model based on bimodal neurons in an artificial neural network. *Tunnelling and Underground Space Technology*, 131, 104791.
<https://doi.org/10.1016/j.tust.2022.104791>
- Ma, Z., & Mei, G. (2021). Deep learning for geological hazards analysis: Data, models, applications, and opportunities. *Earth-Science Reviews*, 223, 103858.
<https://doi.org/10.1016/j.earscirev.2021.103858>
- Möller, D. P. F. (2023). Machine Learning and Deep Learning. In D. P. F. Möller (Ed.), *Guide to Cybersecurity in Digital Transformation: Trends, Methods, Technologies, Applications and Best Practices* (pp. 347–384). Cham: Springer Nature Switzerland. https://doi.org/10.1007/978-3-031-26845-8_8
- Mousavi, S. M., & Beroza, G. C. (2022). Deep-learning seismology. *Science*, 377(6607), eabm4470. <https://doi.org/10.1126/science.abm4470>
- Mousavi, S. M., & Beroza, G. C. (2023). Machine Learning in Earthquake Seismology. *Annual Review of Earth and Planetary Sciences*, 51(1), 105–129.
<https://doi.org/10.1146/annurev-earth-071822-100323>
- Mousavi, S. M., Horton, S. P., Langston, C. A., & Samei, B. (2016). Seismic features and automatic discrimination of deep and shallow induced-microearthquakes using neural network and logistic regression. *Geophysical Journal International*, 207(1), 29–46. <https://doi.org/10.1093/gji/ggw258>

- Mousavi, S. M., Zhu, W., Ellsworth, W., & Beroza, G. (2019). Unsupervised Clustering of Seismic Signals Using Deep Convolutional Autoencoders. *IEEE Geoscience and Remote Sensing Letters*, 16(11), 1693–1697.
<https://doi.org/10.1109/LGRS.2019.2909218>
- Orlic, N., & Loncaric, S. (2010). Earthquake—explosion discrimination using genetic algorithm-based boosting approach. *Computers & Geosciences*, 36(2), 179–185.
<https://doi.org/10.1016/j.cageo.2009.05.006>
- Othman, A., Iqbal, N., Hanafy, S. M., & Waheed, U. B. (2022). Automated Event Detection and Denoising Method for Passive Seismic Data Using Residual Deep Convolutional Neural Networks. *IEEE Transactions on Geoscience and Remote Sensing*, 60, 1–11. <https://doi.org/10.1109/TGRS.2021.3054071>
- Pan, S. J., & Yang, Q. (2010). A Survey on Transfer Learning. *IEEE Transactions on Knowledge and Data Engineering*, 22(10), 1345–1359.
<https://doi.org/10.1109/TKDE.2009.191>
- Papadimitroulas, P., Brocki, L., Christopher Chung, N., Marchadour, W., Vermet, F., Gaubert, L., Eleftheriadis, V., Plachouris, D., Visvikis, D., Kagadis, G. C., & Hatt, M. (2021). Artificial intelligence: Deep learning in oncological radiomics and challenges of interpretability and data harmonization. *Physica Medica*, 83, 108–121. <https://doi.org/10.1016/j.ejmp.2021.03.009>
- Peng, G., Tuo, X., Shen, T., & Lu, J. (2021). Recognition of Rock Micro-Fracture Signal Based on Deep Convolution Neural Network Inception Algorithm. *IEEE Access*, 9, 89390–89399. <https://doi.org/10.1109/ACCESS.2021.3086630>
- Peng, K., Tang, Z., Dong, L., & Sun, D. (2021). Machine Learning Based Identification of Microseismic Signals Using Characteristic Parameters. *Sensors*, 21(21), 6967. <https://doi.org/10.3390/s21216967>
- Peng, P. A., He, Z. X., Wang, L. G., & Jiang, Y. J. (2020). Automatic Classification of Microseismic Records in Underground Mining: A Deep Learning Approach. *IEEE Access*, 8, 17863–17876. <https://doi.org/10.1109/access.2020.2967121>

- Peng, P., He, Z., & Wang, L. (2019). Automatic Classification of Microseismic Signals Based on MFCC and GMM-HMM in Underground Mines. *Shock and Vibration*, 2019(1), 5803184. <https://doi.org/10.1155/2019/5803184>
- Peng, P., He, Z., Wang, L., & Jiang, Y. (2020). Microseismic records classification using capsule network with limited training samples in underground mining. *Scientific Reports*, 10(1), 13925. <https://doi.org/10.1038/s41598-020-70916-z>
- Pham, K., Kim, D., Park, S., & Choi, H. (2021). Ensemble learning-based classification models for slope stability analysis. *CATENA*, 196, 104886. <https://doi.org/10.1016/j.catena.2020.104886>
- Poernomo, A., & Kang, D.-K. (2018). Biased Dropout and Crossmap Dropout: Learning towards effective Dropout regularization in convolutional neural network. *Neural Networks*, 104, 60–67. <https://doi.org/10.1016/j.neunet.2018.03.016>
- Powers, D. M. W. (2020, October 10). Evaluation: from precision, recall and F-measure to ROC, informedness, markedness and correlation. *arXiv*. <https://doi.org/10.48550/arXiv.2010.16061>
- Qu, S., Guan, Z., Verschuur, E., & Chen, Y. (2020). Automatic high-resolution microseismic event detection via supervised machine learning. *GEOPHYSICAL JOURNAL INTERNATIONAL*, 222(3), 1881–1895. <https://doi.org/10.1093/gji/ggaa193>
- Rainio, O., Teuho, J., & Klén, R. (2024). Evaluation metrics and statistical tests for machine learning. *Scientific Reports*, 14(1), 6086. <https://doi.org/10.1038/s41598-024-56706-x>
- Rao, D., Shi, X., Zhou, J., Yu, Z., Gou, Y., Dong, Z., & Zhang, J. (2021). An Expert Artificial Intelligence Model for Discriminating Microseismic Events and Mine Blasts. *Applied Sciences*, 11(14), 6474. <https://doi.org/10.3390/app11146474>
- Rozza, A., Lombardi, G., Casiraghi, E., & Campadelli, P. (2012). Novel Fisher discriminant classifiers. *Pattern Recognition*, 45(10), 3725–3737. <https://doi.org/10.1016/j.patcog.2012.03.021>

- Schmidhuber, J. (2015). Deep learning in neural networks: An overview. *Neural Networks*, 61, 85–117. <https://doi.org/10.1016/j.neunet.2014.09.003>
- Schumacher, M., Holländer, N., & Sauerbrei, W. (1997). Resampling and cross-validation techniques: a tool to reduce bias caused by model building? *Statistics in Medicine*, 16(24), 2813–2827. [https://doi.org/10.1002/\(SICI\)1097-0258\(19971230\)16:24<2813::AID-SIM701>3.0.CO;2-Z](https://doi.org/10.1002/(SICI)1097-0258(19971230)16:24<2813::AID-SIM701>3.0.CO;2-Z)
- Setiawan, W., Utoyo, M. I., & Rulaningtyas, R. (2020). Transfer learning with multiple pre-trained network for fundus classification. *TELKOMNIKA (Telecommunication Computing Electronics and Control)*, 18(3), 1382–1388. <https://doi.org/10.12928/telkomnika.v18i3.14868>
- Shang, X., Li, X., Morales-Esteban, A., & Chen, G. (2017). Improving microseismic event and quarry blast classification using Artificial Neural Networks based on Principal Component Analysis. *Soil Dynamics and Earthquake Engineering*, 99, 142–149. <https://doi.org/10.1016/j.soildyn.2017.05.008>
- Shu, H., & Dawod, A. Y. (2023). Microseismic Monitoring Signal Waveform Recognition and Classification: Review of Contemporary Techniques. *Applied Sciences*, 13(23), 12739. <https://doi.org/10.3390/app132312739>
- Shu, H., Dawod, A. Y., Mu, L., & Tepsan, W. (2023). A Survey of Machine Learning Applications in Microseismic Signal Recognition and Classification. In *2023 15th International Conference on Software, Knowledge, Information Management and Applications (SKIMA)* (pp. 18–23). <https://doi.org/10.1109/SKIMA59232.2023.10387351>
- Shu, L., Liu, Z., Wang, K., Zhu, N., & Yang, J. (2022). Characteristics and Classification of Microseismic Signals in Heading Face of Coal Mine: Implication for Coal and Gas Outburst Warning. *Rock Mechanics and Rock Engineering*, 55(11), 6905–6919. <https://doi.org/10.1007/s00603-022-03028-x>
- Song, G., Cheng, J., & Grattan, K. T. V. (2020). Recognition of Microseismic and Blasting Signals in Mines Based on Convolutional Neural Network and Stockwell Transform. *IEEE Access*, 8, 45523–45530.

<https://doi.org/10.1109/ACCESS.2020.2978392>

- Sugondo, R. A., & Machbub, C. (2021). P-Wave detection using deep learning in time and frequency domain for imbalanced dataset. *Heliyon*, 7(12), e08605. <https://doi.org/10.1016/j.heliyon.2021.e08605>
- Sun, J., Wang, L., & Hou, H. (2012). Application of micro-seismic monitoring technology in mining engineering. *International Journal of Mining Science and Technology*, 22(1), 79–83. <https://doi.org/10.1016/j.ijmst.2011.06.007>
- Tang, S., Wang, J., & Tang, C. (2021). Identification of microseismic events in rock engineering by a convolutional neural network combined with an attention mechanism. *Rock Mechanics and Rock Engineering*, 54, 47–69. <https://doi.org/10.1007/s00603-020-02259-0>
- Tharwat, A. (2020). Classification assessment methods. *Applied Computing and Informatics*, 17(1), 168–192. <https://doi.org/10.1016/j.aci.2018.08.003>
- Umeaduma, L. I. (2024). Survey of image classification models for transfer learning. *World Journal of Advanced Research and Reviews*, 21(1), 373–383. <https://doi.org/10.30574/wjarr.2024.21.1.0006>
- Valero-Carreras, D., Alcaraz, J., & Landete, M. (2023). Comparing two SVM models through different metrics based on the confusion matrix. *Computers & Operations Research*, 152, 106131. <https://doi.org/10.1016/j.cor.2022.106131>
- Vallejos, J. A., & McKinnon, S. D. (2013). Logistic regression and neural network classification of seismic records. *International Journal of Rock Mechanics and Mining Sciences*, 62, 86–95. <https://doi.org/10.1016/j.ijrmms.2013.04.005>
- Vujovic, Ž. Đ. (2021). Classification Model Evaluation Metrics. *International Journal of Advanced Computer Science and Applications*, 12(6). <https://doi.org/10.14569/IJACSA.2021.0120670>
- Wamriew, D., Charara, M., & Pissarenko, D. (2022). Joint event location and velocity model update in real-time for downhole microseismic monitoring: A deep learning approach. *Computers & Geosciences*, 158, 104965. <https://doi.org/10.1016/j.cageo.2021.104965>

- Wamriew, D., Pevzner, R., Maltsev, E., & Pissarenko, D. (2021). Deep Neural Networks for Detection and Location of Microseismic Events and Velocity Model Inversion from Microseismic Data Acquired by Distributed Acoustic Sensing Array. *Sensors*, 21(19), 6627. <https://doi.org/10.3390/s21196627>
- Wang, Changbin, Si, G., Zhang, C., Cao, A., & Canbulat, I. (2023). Variation of seismicity using reinforced seismic data for coal burst risk assessment in underground mines. *International Journal of Rock Mechanics and Mining Sciences*, 165, 105363. <https://doi.org/10.1016/j.ijrmms.2023.105363>
- Wang, Cheng, Chen, D., Hao, L., Liu, X., Zeng, Y., Chen, J., & Zhang, G. (2019). Pulmonary Image Classification Based on Inception-v3 Transfer Learning Model. *IEEE Access*, 7, 146533–146541. <https://doi.org/10.1109/ACCESS.2019.2946000>
- Wang, J. Q., Prabhat, B., & Shakil, M. (2021). Review of machine learning and deep learning application in mine microseismic event classification. *Mining of Mineral Deposits*, 15(1), 19–26. <https://doi.org/10.33271/mining15.01.019>
- Wang, Jiaxu, & Tang, S. (2022). Novel Transfer Learning Framework for Microseismic Event Recognition Between Multiple Monitoring Projects. *Rock Mechanics and Rock Engineering*, 55(6), 3563–3582. <https://doi.org/10.1007/s00603-022-02790-2>
- Wang, JX, Tang, S., Heap, M., Tang, C., & Tang, L. (2021). An auto-detection network to provide an automated real-time early warning of rock engineering hazards using microseismic monitoring. *International Journal of Rock Mechanics and Mining Sciences*, 140, 104685. <https://doi.org/10.1016/j.ijrmms.2021.104685>
- Wang, X., Chen, B., Ran, Y., Zhu, X., & Wang, Q. (2022). Application of Deep Learning in Microseismic Waveform Classification: A Case Study of The Yebatan Hydropower Station Project. In *2022 8th International Conference on Hydraulic and Civil Engineering: Deep Space Intelligent Development and Utilization Forum (ICHCE)* (pp. 1292–1298). <https://doi.org/10.1109/ICHCE57331.2022.10042535>

- Wang, Yaojun, Qiu, Q., Lan, Z., Chen, K., Zhou, J., Gao, P., & Zhang, W. (2022). Identifying microseismic events using a dual-channel CNN with wavelet packets decomposition coefficients. *Computers & Geosciences*, 166, 105164. <https://doi.org/10.1016/j.cageo.2022.105164>
- Wang, Yulin, Han, Y., Wang, C., Song, S., Tian, Q., & Huang, G. (2024). Computation-efficient deep learning for computer vision: A survey. *Cybernetics and Intelligence*, 1–24. <https://doi.org/10.26599/CAI.2024.9390002>
- Wang, Z., Hong, T., & Piette, M. A. (2020). Building thermal load prediction through shallow machine learning and deep learning. *Applied Energy*, 263, 114683. <https://doi.org/10.1016/j.apenergy.2020.114683>
- Wei, H., Shu, W., Dong, L., Huang, Z., & Sun, D. (2020). A Waveform Image Method for Discriminating Micro-Seismic Events and Blasts in Underground Mines. *Sensors*, 20(15), 4322. <https://doi.org/10.3390/s20154322>
- Wilkins, A. H., Strange, A., Duan, Y., & Luo, X. (2020). Identifying microseismic events in a mining scenario using a convolutional neural network. *Computers & Geosciences*, 137, 104418. <https://doi.org/10.1016/j.cageo.2020.104418>
- Wu, S., Wang, Y., Zhan, Y., & Chang, X. (2016). Automatic microseismic event detection by band-limited phase-only correlation. *Physics of the Earth and Planetary Interiors*, 261, 3–16. <https://doi.org/10.1016/j.pepi.2016.09.005>
- Xie, A. Y., & Li, B. Q. (2024). Transfer learning framework for multi-scale crack type classification with sparse microseismic networks. *International Journal of Mining Science and Technology*, 34(2), 167–178. <https://doi.org/10.1016/j.ijmst.2024.01.003>
- Xie, Z., Yu, X., Gao, X., Li, K., & Shen, S. (2022). Recent Advances in Conventional and Deep Learning-Based Depth Completion: A Survey. *IEEE Transactions on Neural Networks and Learning Systems*, 1–21. <https://doi.org/10.1109/TNNLS.2022.3201534>
- Yacouby, R., & Axman, D. (2020). Probabilistic Extension of Precision, Recall, and F1 Score for More Thorough Evaluation of Classification Models. In S. Eger, Y. Gao,

- M. Peyrard, W. Zhao, & E. Hovy (Eds.), Proceedings of the First Workshop on Evaluation and Comparison of NLP Systems (pp. 79–91). Online: Association for Computational Linguistics. <https://doi.org/10.18653/v1/2020.eval4nlp-1.9>
- Yang, D. H., Zhou, X., Wang, X. Y., & Huang, J. P. (2021). Micro-earthquake source depth detection using machine learning techniques. *Information Sciences*, 544, 325–342. <https://doi.org/10.1016/j.ins.2020.07.045>
- Yang, Z., Li, H., Tuo, X., Li, L., & Wen, J. (2023). Unsupervised Clustering of Microseismic Signals Using a Contrastive Learning Model. *IEEE Transactions on Geoscience and Remote Sensing*, 61, 1–12. <https://doi.org/10.1109/TGRS.2023.3240728>
- Yi, Q., Cheng, T., Wu, Y., & Zhang, Z. (2020). Feature Extraction and Classification Method of Mine Microseismic Signals Based on CEEMDAN_SE. In 2020 IEEE 3rd International Conference on Electronics Technology (ICET) (pp. 602–606). <https://doi.org/10.1109/ICET49382.2020.9119585>
- Yin, H., Zhang, G., Wu, Q., Yin, S., Soltanian, M. R., Thanh, H. V., & Dai, Z. (2023). A Deep Learning-Based Data-Driven Approach for Predicting Mining Water Inrush From Coal Seam Floor Using Microseismic Monitoring Data. *IEEE Transactions on Geoscience and Remote Sensing*, 61, 1–15. <https://doi.org/10.1109/TGRS.2023.3300012>
- Yin, X., Liu, Q., Huang, X., & Pan, Y. (2021). Real-time prediction of rockburst intensity using an integrated CNN-Adam-BO algorithm based on microseismic data and its engineering application. *Tunnelling and Underground Space Technology*, 117, 104133. <https://doi.org/10.1016/j.tust.2021.104133>
- Yu, Q., Zhao, D., Xia, Y., Jin, S., Zheng, J., Meng, Q., Mu, C., & Zhao, J. (2022). Multivariate Early Warning Method for Rockburst Monitoring Based on Microseismic Activity Characteristics. *Frontiers in Earth Science*, 10. <https://doi.org/10.3389/feart.2022.837333>

- Zhang, C., Jin, G., Liu, C., Li, S., Xue, J., Cheng, R., Wang, X., & Zeng, X. (2021). Prediction of rockbursts in a typical island working face of a coal mine through microseismic monitoring technology. *Tunnelling and Underground Space Technology*, 113, 103972. <https://doi.org/10.1016/j.tust.2021.103972>
- Zhang, C., & Van Der Baan, M. (2022). Signal Processing Using Dictionaries, Atoms, and Deep Learning: A Common Analysis-Synthesis Framework. *Proceedings of the IEEE*, 110(4), 454–475. <https://doi.org/10.1109/JPROC.2022.3155904>
- Zhang, H., Zeng, J., Ma, J., Fang, Y., Ma, C., Yao, Z., & Chen, Z. (2021). Time Series Prediction of Microseismic Multi-parameter Related to Rockburst Based on Deep Learning. *Rock Mechanics and Rock Engineering*, 54(12), 6299–6321. <https://doi.org/10.1007/s00603-021-02614-9>
- Zhang, J., Jiang, R., Li, B., & Xu, N. (2019). An automatic recognition method of microseismic signals based on EEMD-SVD and ELM. *Computers & Geosciences*, 133, 104318. <https://doi.org/10.1016/j.cageo.2019.104318>
- Zhang, S., Tang, C., Wang, Y., Li, J., Ma, T., & Wang, K. (2021). Review on Early Warning Methods for Rockbursts in Tunnel Engineering Based on Microseismic Monitoring. *Applied Sciences*, 11(22), 10965. <https://doi.org/10.3390/app112210965>
- Zhang, Zhen, Liu, Y., Ye, Y., Yao, N., Hu, N., Luo, B., Fu, F., Luo, X., & Feng, J. (2024). Research on the classification of complex noise-mixed microseismic events based on machine vision. *GEOPHYSICS*, 1–51. <https://doi.org/10.1190/geo2023-0395.1>
- Zhang, Zhilu, & Sabuncu, M. (2018). Generalized Cross Entropy Loss for Training Deep Neural Networks with Noisy Labels. In *Advances in Neural Information Processing Systems* (Vol. 31). Curran Associates, Inc. Retrieved from <https://proceedings.neurips.cc/paper/2018/hash/f2925f97bc13ad2852a7a551802fee0-Abstract.html>
- Zhao, G., Ma, J., Dong, L., Li, X., Chen, G., & Zhang, C. (2015). Classification of mine blasts and microseismic events using starting-up features in seismograms.

- Transactions of Nonferrous Metals Society of China, 25(10), 3410–3420.
[https://doi.org/10.1016/S1003-6326\(15\)63976-0](https://doi.org/10.1016/S1003-6326(15)63976-0)
- Zhao, H., Chen, B., & Zhu, C. (2021). Decision Tree Model for Rockburst Prediction Based on Microseismic Monitoring. *Advances in Civil Engineering*, 2021(1), 8818052. <https://doi.org/10.1155/2021/8818052>
- Zhao, X., Wang, L., Zhang, Y., Han, X., Deveci, M., & Parmar, M. (2024). A review of convolutional neural networks in computer vision. *Artificial Intelligence Review*, 57(4), 99. <https://doi.org/10.1007/s10462-024-10721-6>
- Zhao, Yi, Zhang, X., Feng, W., & Xu, J. (2022). Deep Learning Classification by ResNet-18 Based on the Real Spectral Dataset from Multispectral Remote Sensing Images. *Remote Sensing*, 14(19). <https://doi.org/10.3390/rs14194883>
- Zhao, Yong, Xu, H., Yang, T., Wang, S., & Sun, D. (2021). A hybrid recognition model of microseismic signals for underground mining based on CNN and LSTM networks. *Geomatics, Natural Hazards and Risk*, 12(1), 2803–2834. <https://doi.org/10.1080/19475705.2021.1968043>
- Zhao, Z., & Gross, L. (2017). Using supervised machine learning to distinguish microseismic from noise events. In *SEG Technical Program Expanded Abstracts 2017* (pp. 2918–2923). Houston, Texas: Society of Exploration Geophysicists. <https://doi.org/10.1190/segam2017-17727697.1>
- Zhao, Z.-Q., Zheng, P., Xu, S.-T., & Wu, X. (2019). Object Detection With Deep Learning: A Review. *IEEE Transactions on Neural Networks and Learning Systems*, 30(11), 3212–3232. <https://doi.org/10.1109/TNNLS.2018.2876865>
- Zhu, J., Fang, L., Miao, F., Fan, L., Zhang, J., & Li, Z. (2022). Deep learning and transfer learning of earthquake and quarry-blast discrimination: Applications to southern California and eastern Kentucky. *Authorea Preprints*.
- Zhu, Q., Sui, L., Liu, Y., Yin, Y., Ouyang, Z., Chen, X., & Liu, W. (2023). Research on feature vector construction and classification recognition of typical mine microseismic waveforms. *Journal of Loss Prevention in the Process Industries*, 86, 105183. <https://doi.org/10.1016/j.jlp.2023.105183>

Zhu, W. Q., Mousavi, S. M., & Beroza, G. C. (2019). Seismic Signal Denoising and Decomposition Using Deep Neural Networks. *Ieee Transactions on Geoscience and Remote Sensing*, 57(11), 9476–9488.

<https://doi.org/10.1109/tgrs.2019.2926772>



ลิขสิทธิ์มหาวิทยาลัยเชียงใหม่
Copyright© by Chiang Mai University
All rights reserved

APPENDIX A

The topics in my dissertation are published as the followings:

Journal papers:

- 1) Shu, H., & Dawod, A. Y. (2023). Microseismic Monitoring Signal Waveform Recognition and Classification: Review of Contemporary Techniques. *Applied Sciences*, 13(23), 12739. (Published) (SCOPUS Q2)
- 2) Shu, H., Dawod, A. Y., Tepsan, W., Mu, L., & Tang, Z. Multi-channel microseismic signals classification with convolutional neural networks. *IAES International Journal of Artificial Intelligence (IJ-AI)*, 2252(8938), 1039. (Published) (SCOPUS Q2)
- 3) Shu, H., Dawod, A. Y., Dong, L. (2024) Intelligent Recognition and Classification of Microseismic Events using HOG and Shallow Machine Learning Method. (Submitted and Under Review)

International conference papers:

- 1) Shu, H., Dawod, A. Y., Mu, L., & Tepsan, W. (2023, December). A Survey of Machine Learning Applications in Microseismic Signal Recognition and Classification. In *2023 15th International Conference on Software, Knowledge, Information Management and Applications (SKIMA)* (pp. 18-23). IEEE. (Published and Presentation)

APPENDIX B

Journal paper 1

Microseismic Monitoring Signal Waveform Recognition and Classification: Review of Contemporary Techniques

Hongmei Shu, Ahmad Yahya Dawod

The original article was published in Applied Sciences (Scopus Q2).

Shu, H., & Dawod, A. Y. (2023). Microseismic Monitoring Signal Waveform Recognition and Classification: Review of Contemporary Techniques. *Applied Sciences*, 13(23), 12739. <https://doi.org/10.11591/ijai.v13.i1.pp1038-1049>



Review

Microseismic Monitoring Signal Waveform Recognition and Classification: Review of Contemporary Techniques

Hongmei Shu and Ahmad Yahya Dawod

International College of Digital Innovation, Chiang Mai University, Chiang Mai 50200, Thailand; hongmei_shu@cmu.ac.th

* Correspondence: ahmadyahyadawod.a@cmu.ac.th

Abstract: Microseismic event identification is of great significance for enhancing our understanding of underground phenomena and ensuring geological safety. This paper employs a literature review approach to summarize the research progress on microseismic signal identification methods and techniques over the past decade. The advantages and limitations of commonly used identification methods are systematically analyzed and summarized. Extensive discussions have been conducted on cutting-edge machine learning models, such as convolutional neural networks (CNNs), and their applications in waveform image processing. These models exhibit the ability to automatically extract relevant features and achieve precise event classification, surpassing traditional methods. Building upon existing research, a comprehensive analysis of the strengths, weaknesses, opportunities, and threats (SWOT) of deep learning in microseismic event analysis is presented. While emphasizing the potential of deep learning techniques in microseismic event waveform image recognition and classification, we also acknowledge the future challenges associated with data availability, resource requirements, and specialized knowledge. As machine learning continues to advance, the integration of deep learning with microseismic analysis holds promise for advancing the monitoring and early warning of geological engineering disasters.

Keywords: microseismic events; machine learning; signal processing; waveform recognition; image classification; sensor technology



Citation: Shu, H.; Dawod, A.Y. Microseismic Monitoring Signal Waveform Recognition and Classification: Review of Contemporary Techniques. *Appl. Sci.* 2023, 13, 12739. <https://doi.org/10.3390/app132312739>

Academic Editor: Gino Iannace

Received: 2 November 2023

Revised: 23 November 2023

Accepted: 24 November 2023

Published: 28 November 2023



Copyright: © 2023 by the authors. Licensee MDPI, Basel, Switzerland. This article is an open access article distributed under the terms and conditions of the Creative Commons Attribution (CC BY) license (<https://creativecommons.org/licenses/by/4.0/>).

1. Introduction

In the contemporary landscape of mining operations, a profound transformation is underway, marked by the transition to intelligent mining [1]. This paradigm shift is catalyzed by the integration of cutting-edge technologies such as the Internet of Things (IoT) [2], big data analytics [3], and artificial intelligence (AI) [4]. Central to this transformation is the unwavering commitment to enhancing mining safety [5]. As mining operations plunge deeper into the Earth's crust, the stability of rock formations is increasingly susceptible to disruptions caused by human activities [6]. These disruptions give rise to geological hazards like rock bursts and mining-induced seismic events, posing grave threats to the safety of miners and the productivity of mining endeavors [7,8]. Within this context, microseismic monitoring technology has emerged as a fundamental pillar for ensuring geological safety in mining operations (Figure 1).

Microseismic monitoring entails the continuous surveillance of minuscule seismic events during mining activities [9]. These imperceptible events provide valuable information about evolving geological conditions. They serve as early warning signals, offering crucial insights into potential hazards and enabling timely preventive measures. This not only safeguards the well-being of miners but also enhances the overall efficiency and sustainability of mining practices [10]. In addition to its practical value and significance in smart mining, microseismic monitoring technology is widely used in various fields. By searching the Web of Science database using the keyword “microseismic monitoring”, we

Multi-channel microseismic signals classification with convolutional neural networks

Hongmei Shu^{1,2}, Ahmad Yahya Dawod¹, Worawit Tepsan¹, Lei Mu^{1,3}, Zheng Tang²

¹International College of Digital Innovation, Chiang Mai University, Chiang Mai, Thailand

²School of Resources and Safety Engineering, Central South University, Changsha, China

³Office of International Collaboration and Exchange, Chengdu University, Chengdu, China

Article Info

Article history:

Received May 11, 2023

Revised Aug 16, 2023

Accepted Sep 8, 2023

Keywords:

Classification
Convolutional neural network
Microseismic events
Multi-channel waveform
Recognition
Transfer learning

ABSTRACT

Identifying and classifying microseismic signals is essential to warn of mines' dangers. Deep learning has replaced traditional methods, but labor-intensive manual identification and varying deep learning outcomes pose challenges. This paper proposes a transfer learning-based convolutional neural network (CNN) method called microseismic signals-convolutional neural network (MS-CNN) to automatically recognize and classify microseismic events and blasts. The model was instructed on a limited sample of data to obtain an optimal weight model for microseismic waveform recognition and classification. A comparative analysis was performed with an existing CNN model and classical image classification models such as AlexNet, GoogLeNet, and ResNet50. The outcomes demonstrate that the MS-CNN model achieved the best recognition and classification effect (99.6% accuracy) in the shortest time (0.31 s to identify 277 images in the test set). Thus, the MS-CNN model can efficiently recognize and classify microseismic events and blasts in practical engineering applications, improving the recognition timeliness of microseismic signals and further enhancing the accuracy of event classification.

This is an open access article under the [CC BY-SA](https://creativecommons.org/licenses/by-sa/4.0/) license.



Corresponding Author:

Ahmad Yahya Dawod
International College of Digital Innovation, Chiang Mai University
239 Huay Kaew Rd, Suthep, Mueang Chiang Mai District, Chiang Mai 50200, Thailand
Email: ahmadyahyadawod.a@cmu.ac.th

1. INTRODUCTION

Microseismic monitoring technology (MMT) has found extensive applications in underground engineering for disasters and safety monitoring [1]. Specifically, it has been utilized for location monitoring [2], [3], as well as forecasting and providing early warning systems for rock bursts [4], and mine earthquake disasters during mining operations [5], [6]. The basic principle involves identifying microseismic events by analyzing prominent features within the monitoring data [7]. Subsequently, the relevant parameters of these events are analyzed to facilitate informed decision-making [8]. Due to the complex geological environment of mines [9], many interference signals frequently mix with the recorded microseismic signals, such as blasting, rock drilling, fan vibration, and other noises generated during engineering operations [10]. Therefore, the basis of MMT is to identify microseismic events quickly and accurately, which determines the timeliness and effectiveness of mine safety early warning [11].

Earlier studies have investigated several strategies, such as conventional signal processing methods and machine learning algorithms [12], [13], to identify and classify microseismic signals [14]. However, these techniques have limitations regarding their efficiency and accuracy. Recently, convolutional neural networks (CNNs) [15], [16] have shown great promise in identifying and categorizing images. Based on this

Journal homepage: <http://ijai.iaescore.com>

Journal paper 3

Intelligent Recognition and Classification of Microseismic Events using HOG and Shallow Machine Learning Method

Hongmei Shu, Ahmad Yahya Dawod, Longjun Dong

The original article was submitted to Journal of Applied Geophysics (Scopus Q2).

This article is currently under review.



The screenshot shows the 'Submissions Being Processed for Author' page on the Journal of Applied Geophysics website. The page includes a navigation menu at the top, a table of submissions, and a 'Results per page' dropdown set to 10. The table contains one submission entry with the following details:

Action	Manuscript Number	Title	Initial Date Submitted	Status Date	Current Status
View Submission View Reference Checking Results Send E-mail	APPGEO-D-24-00219	Recognition and Classification of Microseismic Event Waveforms Based on HOG and Shallow Machine Learning Approach	Apr 22, 2024	Jun 05, 2024	Under Review



ลิขสิทธิ์มหาวิทยาลัยเชียงใหม่
Copyright© by Chiang Mai University
All rights reserved

A Survey of Machine Learning Applications in Microseismic Signal Recognition and Classification

Hongmei Shu
International College of Digital
Innovation
Chiang Mai University
Chiang Mai, Thailand
hongmei_shu@cmu.ac.th

Ahmad Yahya Dawod
International College of Digital
Innovation
Chiang Mai University
Chiang Mai, Thailand
ahmadyahyadawod.a@cmu.ac.th

Lei Mu
Office of International
Collaboration and Exchange
Chengdu University
Chengdu, China
mulei@cdu.edu.cn

Worawit Tepsan
International College of Digital
Innovation
Chiang Mai University
Chiang Mai, Thailand
worawit.tepsan@cmu.ac.th

Abstract—Effective microseismic event identification and classification form the bedrock of data analysis in microseismic monitoring systems, facilitating real-time source location, rockburst prediction, and mine safety. However, the complex mining environment necessitates preprocessing of sensor-collected microseismic signal data, plagued by noise. Traditional methods often yield inaccurate results when events exhibit similar traits. Machine learning's high precision separation proves promising, anticipating safety alerts by learning historical microseismic event patterns, and applying them to real-time data for predictive analysis. This approach mitigates inefficiencies and errors associated with manual recognition. Hence, machine learning has gained substantial traction in microseismic monitoring. This paper reviews recent machine learning applications in microseismic signal recognition and classification, addressing limitations of traditional methods, highlighting developmental disparities, presenting machine learning-based categorization, and summarizing advancements in signal recognition models. Lastly, the potential and challenges of machine learning in microseismic signal recognition are discussed.

Keywords—microseismic signals; event waveforms; classification and recognition; machine learning; image recognition

I. INTRODUCTION

In recent years, the deep integration of information technologies such as the Internet of Things, big data, and artificial intelligence with modern mining techniques and operations has propelled the evolution of smart mines from conceptualization to realization [1]. Notably, microseismic monitoring methods based on acoustic emission and seismology have emerged as pivotal components of mine safety monitoring, finding extensive utility across domains encompassing stress impact in coal mines, rockburst, mining-induced seismicity [2], slope instability [3], and other critical facets [4]. Facilitating this is the microseismic monitoring system (MMS), which includes functions such as microseismic signal acquisition, multi-channel clock synchronization, noise attenuation, automated onset detection, source localization, analysis of rock microfracture stress, and interpretation. Leveraging seismic analysis methods, allows for precise determination of seismic attributes, including time, spatial location, magnitude, frequency domain characteristics, and source mechanisms. These calculated results enable the visualization and prediction of spatiotemporal

changes in microseismic event evolution, consequently enabling continuous monitoring and early-warning systems for potential disasters [5]. The MMS usually consists of sensors, data collectors, signal processors, underground data centers, and surface monitoring facilities, as illustrated in Fig. 1.

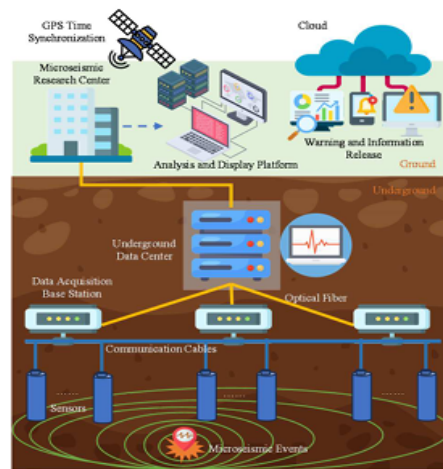


Fig. 1. The composition of a smart mine microseismic monitoring system

Due to the complex mining environment, the MMS captures a diverse range of signals from the seismic sources. A microseismic event is characterized by the generation of elastic waves that is generated when a rock breaks and is used primarily to predict earthquakes resulting from the structural instability of the rock [6]. These waves are considered valuable signals and are the primary focus of analysis in microseismic monitoring systems. Blasting is an event where rock fragmentation is induced by the shock wave from an explosive blast. Depending on the study's objective, blasting is at times treated as noise and at other times as a valuable signal. Rock drilling events involve



Certificate of Participation

This certifies that

Hongmei Shu, Ahmad Yahya Dawod, Lei Mu and Worawit Tepsan

have presented a paper entitled

A Survey of Machine Learning Applications in Microseismic Signal Recognition and Classification

at the

**15th International Conference (IEEE Technical co-Sponsored) on Software, Knowledge,
Information Management & Applications (SKIMA 2023)
on 8 - 9 December 2023**

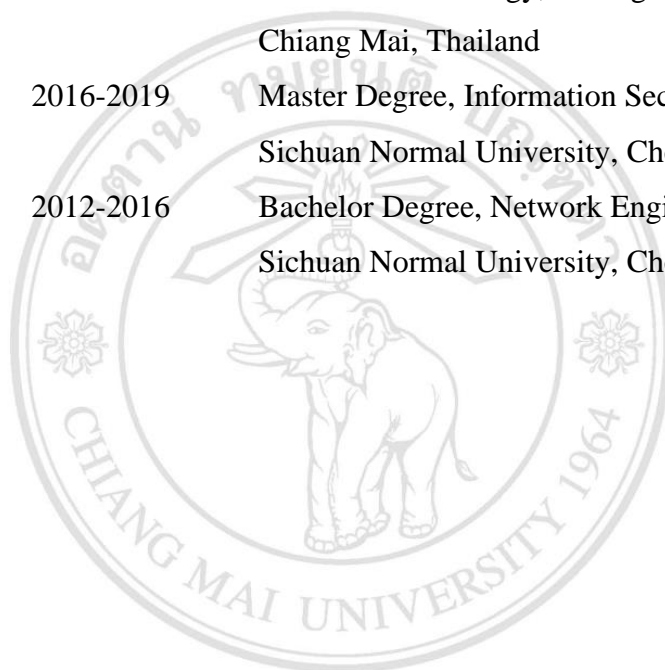
Assoc. Prof. Ir. Ts. Dr. Nurul Mu'azzah Abdul Latiff
GENERAL CHAIR
SKIMA 2023



ลิขสิทธิ์มหาวิทยาลัยเชียงใหม่
Copyright© by Chiang Mai University
All rights reserved

CURRICULUM VITAE

Author's Name	Hongmei Shu	
Place of Birth	Guangan City, Sichuan Province, China	
Education	2020-2024	Doctor of Philosophy in Digital Innovation and Financial Technology, Chiang Mai University, Chiang Mai, Thailand
	2016-2019	Master Degree, Information Security, Sichuan Normal University, Chengdu, China
	2012-2016	Bachelor Degree, Network Engineering, Sichuan Normal University, Chengdu, China



ลิขสิทธิ์มหาวิทยาลัยเชียงใหม่
Copyright© by Chiang Mai University
All rights reserved